We have submitted a revised manuscript (ms), which includes all the modifications described in our two response letters. The main differences from our ms published in BGD (referred to original ms below) are as follows:

1. The previous STD configuration is removed from the revised ms, and the QM configuration is renamed as the STD configuration in the revised ms. The new STD, RD, VIDRD and OBRD configurations are taken as the main configurations, and described and discussed in the main text. The VD, VDRD, VID and OB configurations are described briefly as sensitivity configurations in Appendix E of the revised ms. Figs. 2 and 3 (now Figs. 2 and 4) are also revised accordingly.
2. Several sentences are modified to specify the regions of results we have cited, and either from models or observations. Please see our response to Referee #1 for details.
3. Summary sentences are added to make statements more specific in order to clarify the role of each model configuration and sensitivity experiment. Please see details in our response to Referee #1.
4. A new subsection "2.5 Sensitivity experiments" is added on Page 10 of the revised ms, where we have described all model sensitivity experiments.
5. A new subsection "3.3 Model sensitivity" is added on Page 14 of the revised ms, where all model sensitivity experiment results are summarised.
6. New analyses are performed to investigate model sensitivity to uncertainties in biogeochemical model parameters. The results of these sensitivity experiments are added in the new subsections "2.5 Sensitivity experiments", and "3.3 Model sensitivity" of the revised ms.
7. The paragraph comparing model fluxes and literature results (second paragraph on Page 11109 of the original ms) is moved to Page 17 (L20–L27) of the revised ms (moved from the Results to the Discussion section). This paragraph is also modified according to our modifications to Table 6.
8. Table 3 of the original ms is improved by adding a description of each model configuration in the caption. Please see Table 5 of the revised ms.
9. Table 6 of the original ms is improved by adding more data to validate the nitrogen loss via denitrification in the oxygen minimum zone.
10. Figure 2 of the original ms is improved by reducing the number of bars and adding horizontal blue lines to indicate the WOA2009 data.
11. Figure 4 of the original ms is improved by removing two columns and enlarging the font in the legend. Details are shown in Figure 5 of the revised ms.
12. Figure 5 of the original ms has beed improved by including results of sensitivity experiments for the biogeochemical parameters and showing the absolute fluxes instead of the normalized fluxes. Figure 6 in the revised ms is the corresponding improved new figure now.
13. Figure 6 of the original ms is improved by changing the location of the x-axis. The improved figure is Figure 8 in the revised ms now.
14. We have clarified how g_U and g_S are determined in Appendix D of the revised ms.
15. The Appendices are reordered:
    - Appendix B in the original ms $\longrightarrow$ Appendix C in the revised ms.
    - Appendix C in the original ms $\longrightarrow$ Appendix D in the revised ms.
    - Appendix D in the original ms $\longrightarrow$ Appendix B in the revised ms.
    - Appendix E in the revised ms is new.
16. The sequence of the tables is changed:
    - Table 2 in the original ms $\longrightarrow$ Table 4 in the revised ms.
    - Table 3 in the original ms $\longrightarrow$ Table 5 in the revised ms.
    - Table 4 in the original ms $\longrightarrow$ Table 2 in the revised ms.
    - Table 5 in the original ms $\longrightarrow$ Table 3 in the revised ms.
17. The sequence of the figures is changed as follows:
    - Fig. 3 in the original ms $\longrightarrow$ Fig. 4 in the revised ms.
    - Fig. 4 in the original ms $\longrightarrow$ Fig. 5 in the revised ms.
    - Fig. 5 in the original ms $\longrightarrow$ Fig. 6 in the revised ms.

- Fig. 6 in the original ms $\longrightarrow$ Fig. 8 in the revised ms.
- Fig. 8 in the original ms $\longrightarrow$ Fig. 3 in the revised ms.
- Fig. 9 in the original ms is removed.

Please see our response letters for details.

The detailed differences between the original and revised ms are also shown in the marked-up PDF file processed with *latexdiff*, which we have submitted together with the revised ms. Please note that the following changes are not visible in the marked-up PDF file:

1. Linear mortality ''M'' is removed from Table 3 in the revised ms.
2. Explanation for maximum growth rate of NF (μ_{NF}) is shown in note (e) below Table 3 of the revised ms.
3. Bold text is added in Tables 2 and 5 in the revised ms to mark the main model configurations.

We have submitted two letters respectively in response to the comments from our two referees already. Here we summarise our detailed point-by-point response to referee comments and specify all changes in the revised manuscript (ms) in response to the relevant comments. A list of all relevant changes made in the revised ms is also submitted together with this response.

We will refer to the ms published in BGD as the original ms, and all figure and table numbers refer to the original ms unless otherwise noted. Please note that we plan to remove the STD configuration in our revised ms. QM will be taken as the new STD configuration in the revised ms, hence there will be no configuration designated as QM in the revised ms.

Response to Referee #1:

Comment: This paper addresses the problem of biogeochemical models simulating complete depletion of nitrate in oxygen minimum zones, while observations show that complete depletion does not take place. The problem is addressed using a box-model of the Eastern Tropical South Pacific and investigated which processes that could be responsible for the discrepancy. The authors are able to produce the wanted effect by reducing the remineralization rate and thus indicate to how global biogeochemical models can be altered to account for this process. The model is tested with a varying degree of ventilation with the surrounding ocean regions, quadratic mortality, allowing nitrogen fixers to take up NO_3^- and reduced denitrification. This is an interesting paper that also demonstrate how box-models is a powerful tool for investigation ocean processes.
Response: We thank the reviewer for the general positive evaluation and thereafter will concentrate on questions and suggestions to improve our original ms.

Comment: My main concern with this paper the lack of systematic testing of the other parameters in the model, if the model sensitivity that been tested in previous publications it should be stated clearer. As previous optimization studies has shown biogeochemical models can give similar results with different combinations of parameters and I therefore think a systematic sensitivity analysis should be performed, unless previous publications can be cited.
Response: There are 13 parameters in total for our biogeochemical model now (listed in Table 5, M is omitted since the old STD configuration is removed from the revised ms). We have mainly focused on parameters that could be significant for the nitrogen cycle in the OMZ and potentially affect our conclusions. The parameters for the stoichiometry of C, N, P and O_2 are r_a, r_c, r_{den} and r_p. μ, μ_{NF}, M_q, N_h and P_h are parameters responsible for growth of both OP and NF. The remineralisation fractions f_U, f_{UM}, f_S, and f_I determine the fractions of exported production remineralised in different boxes. We now address the sensitivity of our model to the uncertainty in these parameters as follows. We add the following paragraph at the end of the new Section 2.5 (Sensitivity experiments):
"The literature ranges in Table 3 provide only a rough guide for the biogeochemical parameters. The sensitivity of r_p, μ, μ_{NF}, N_h and P_h is tested by changing each of them in the OBRD configuration according to the literature range. Effects of changing the remineralisation fractions f_U, f_{UM}, f_S, and f_I are examined by redistributing remineralisation between the U and UM, and S and I boxes. These sensitivity experiments will be discussed in Section 3.3 below."
The following paragraph is added at the end of the new Section 3.3 (Model sensitivity). Accordingly, we will replace Fig. 5 with Fig. 1 of this response letter. :
"Varying biogeochemical parameters affects individual model predictions but not our main conclusions. The strongest effects are those of varying the N:P ratio r_p and the remineralisation fractions (f_U, f_{UM}, f_S, and f_I) (Fig. 5). Lowering r_p to 12 increases N_{UM} by about 35 %, but cannot change the strength of our model domain as a net NO_3^- source. Increasing r_p to 20 decreases N_{UM} by about 18 %, but triples the strength of our model domain as a NO_3^- source. However, observations indicate that r_p for the ETSP is more likely to be higher than lower compared to the Redfield N:P ratio of 16 [Franz et al., 2012]. Increasing the maximum growth rate of NF, μ_{NF}, to $1/2\mu$, the maximum growth rate of Phy, results in higher N_{UM} concentrations and our model domain being a larger NO_3^- source. Intuitively, decreasing μ_{NF} to $1/4\mu$ results in lower N_{UM} concentrations and our model domain becoming a smaller NO_3^- source. Varying the NO_3^- half saturation constant, N_h, results in virtually unchanged

results. N_{UM} increases when changing remineralisation fractions in the intermediate boxes (f_{UM} and f_I) from 70 % to 50 % and 30 % respectively, effectively lowering export production via lowering the export ratio. Nevertheless the qualitative behaviour of the model remains the same in these sensitivity experiments."

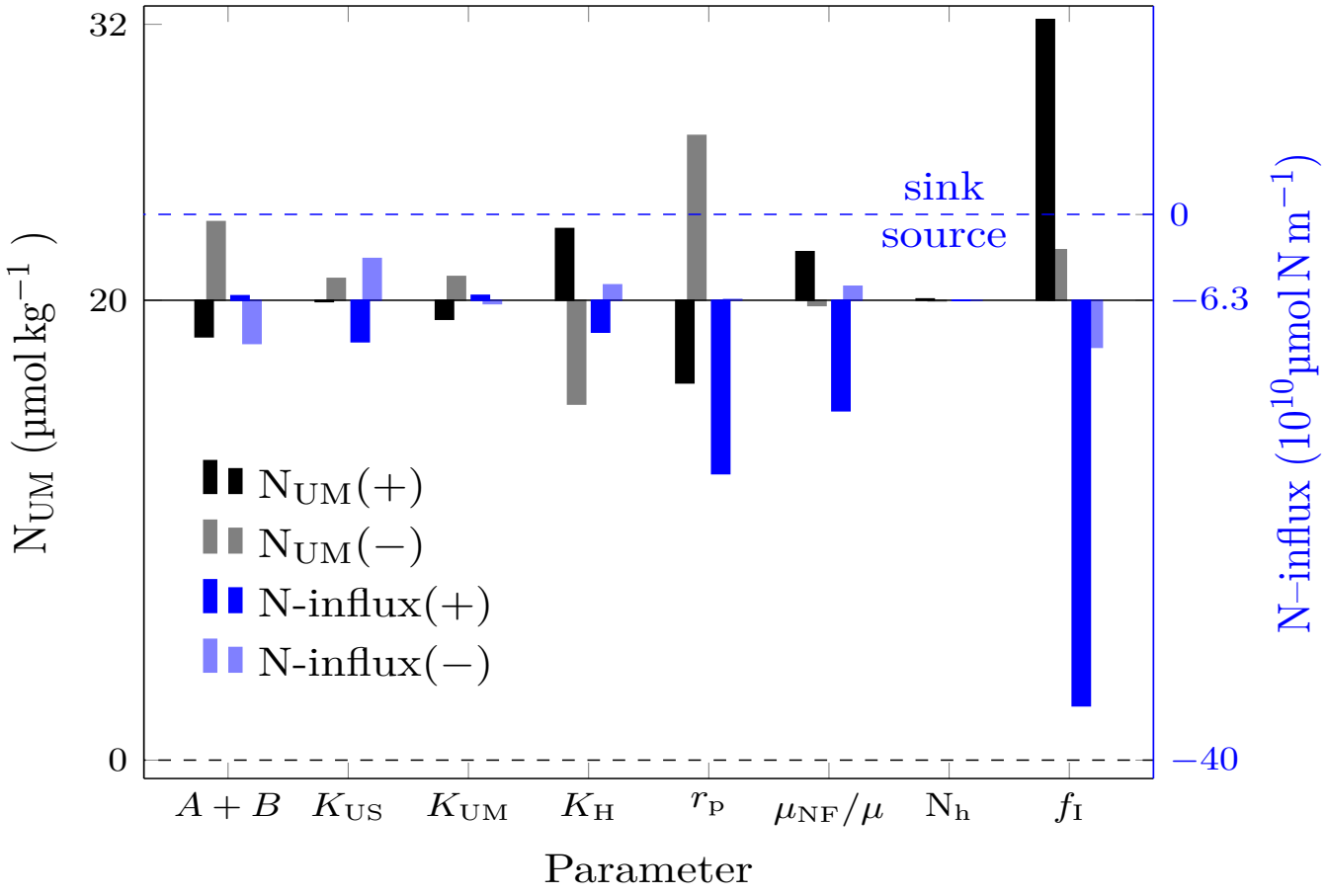

Figure 1: Sensitivity of NO_3^- concentration in the OMZ (N_{UM}) and the net NO_3^- flux out of the model domain to variations of the individual parameters describing ocean transport and biogeochemical processes (see Tables 2,5 and Fig. 1 for a description of the parameters). Black and blue bars represent changes in N_{UM} and N-influx, respectively. "+" and "−" indicate the response to increased and decreased parameters. Physical circulation parameters are varied by ±50%. r_P is varied between 12 and 20. μ_{NF}/μ is varied between 1/4 and 1/2. Nh varies between 0.3 and 0.9 µmol kg^{-1}. For f_i, "+" indicates f_U=f_S=60% and f_{UM}=f_I= 30%, and "−" means 40% and 50%, respectively.

For detailed results of these sensitivity experiments in all model configurations, see also Fig. 2 of this response and our replies to the comments about deviations from Redfield ratio, confidence about NF growing at 1/3 of OP, and confidence about the remineralisation fractions, below. Fig. 2 of this response letter indicates that our main conclusions stay virtually unchanged for different N_h.

Comments: I also find that the composition of the paper is confusing, the authors jump back and forth among different runs, the paper could be made clearer with better structure (see suggestion below). The figures show a lot of information and I think the authors could get the message of the paper better across if they are more selective with the figures, for example reduce the number of panels to show fewer model variables, but focus on the ones most discussed in the text.
Response: We thank the reviewer for pointing out the lack of clarity in our original ms, which we will address more carefully in the revised ms. We describe how we plan to change the composition of our original ms below in response to this comment "The paper presents the 7 main model configurations summarized in table 4, but in between other experiments with sensitivity to different parameters are

Figure 2: NO_3^- concentrations in the UM box for the sensitivity experiments for N_h.

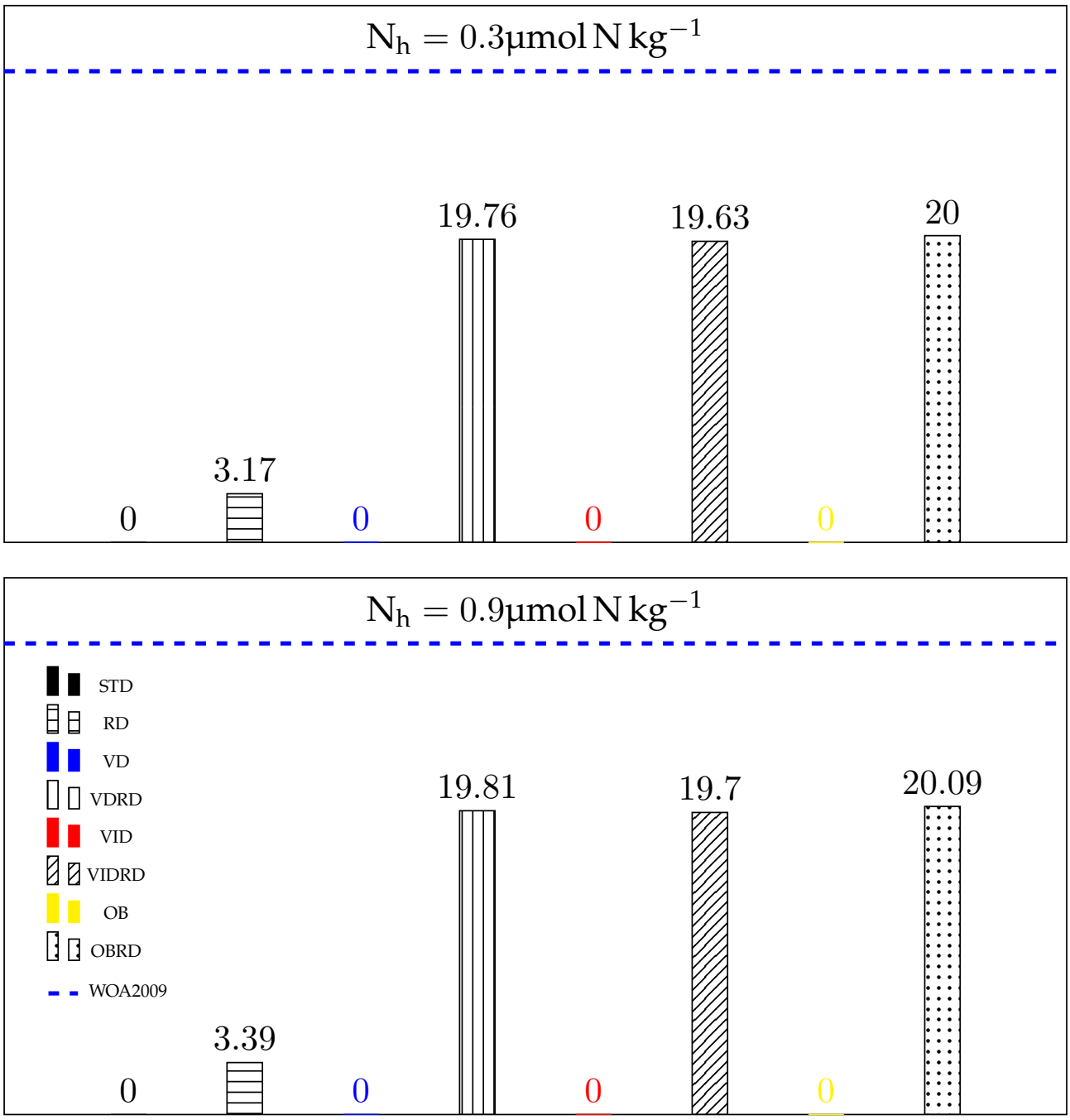

also described in the result section and a couple more appear in the discussion. The paper would be easier to read if these runs were described separately from the runs in table 4, for example under a sub-heading "3.3 Sensitivity run"., and the figures will also be changed accordingly.

Comment: In general, when results from other literature is mention it is useful to add information about how the results where obtained, was it model or observation (what kind?), was it the same OMZ-region? (For example top of p11097)

Response: Thanks for reminding us about pointing out the conclusions from either models or observations. We will **reword** these statements in the revised ms to make them clearer:

1, The top of P11097: Estimates derived from both field data and model analyses for the global oceanic fixed-N budget range from sources roughly balancing sinks [Gruber and Sarmiento, 1997, Gruber, 2004, Eugster and Gruber, 2012, DeVries et al., 2013], to a rather large net deficit between 140 and 234 $TgNyr^{-1}$ [Codispoti et al., 2001, Galloway et al., 2004, Codispoti, 2007].

2, P11097 L15-L18: OMZs currently account for only about 8% of the global ocean area but observations of intense denitrification and anammox in the OMZs indicate that they could be responsible for 30–50% of the total fixed-N loss [Gruber and Sarmiento, 1997, Codispoti et al., 2001, Dalsgaard et al., 2005, Paulmier and Ruiz-Pino, 2009].

3, P11098 L1-L2: Although alternative explanations for these nutrient patterns have been proposed in models [Mills and Arrigo, 2010], direct measurements have confirmed the occurrence of nitrogen fixation in and above the OMZ of the ETSP [Fernandez et al., 2011].

4, P11099 L2-L5: Anammox has recently been reported as another major pathway for fixed-N removal [Kuypers et al., 2005, Hamersley et al., 2007, Molina and Farás, 2009], but the relative contributions of anammox and denitrification are still a matter of debate [Ward et al., 2009, Bulow et al., 2010].

5, P11112 L16-L18: This strong control of the N cycle by phosphate is similar to the finding of previous models [e.g. Lenton and Watson, 2000, Canfield, 2006], where the occurrence and extent of oceanic anoxia was also tightly linked to phosphate supply.

6, P11113 L17-L20: Ganachaud and Wunsch [2002] estimated a net northward NO_3 transport of 270 ± 170 kmol s^{-1} (119.2 ± 75.1 Tg N yr^{-1}) across 17°S into the ETSP in a geostrophic inverse box model, which indicates that the ETSP is a net nitrogen sink, but their estimate included benthic denitrification, which is not accounted for in our current analysis.

7, P11113 L23-L25: From an ocean circulation-biogeochemical model-based analysis of nutrient concentrations and transport rates, Deutsch et al. [2007] estimated nitrogen fixation rates in the Pacific Ocean of about 95 Tg N yr^{-1}, half of which was speculated to occur in the ETSP.

8, P11113 L28-L29: More recently, Eugster and Gruber [2012] probabilistically estimated nitrogen fixation and water-column and benthic denitrification separately in their box model, which appears to be consistent with our results as their results also indicate that the water column of the IndoPacific is a large fixed-N source for that region.

Comment: Confidence about the nitrogen fixation being 1/3 of the maximum growth rate for phytoplankton.

Response: The lower maximum growth rate of nitrogen-fixation phytoplankton (NF) compared to ordinary phytoplankton (OP) has been observed in both lab cultures and physiological models. It is attributed mainly to the high energetic cost associated with fixing N_2 and also to more severe temperature limitation [LaRoche and Breitbarth, 2005, Breitbarth et al., 2007, Grimaud et al., 2014], and this will be mentioned in Section 2.2 (Biogeochemical model). But the exact ratio of maximum growth rates for NF and OP is unclear. Now we present sensitivity experiments with nitrogen fixation being 1/2 and 1/4 of the maximum growth rate for the OP in all model configurations. Still, our conclusion remains valid that NO_3^- depletion in the OMZ can be prevented only if the remineralisation rate via denitrification is slower than that via aerobic respiration (Fig. 3 of this response letter). The only problem is that NO_3^- inventory in our model domain can not reach steady-state in the VDRD and VIDRD configurations when the nitrogen fixation rate is 1/2 of the maximum growth rate for OP, but this does not happen in our most realistic configuration (OBRD). This problem can be solved by including the facultative N_2-fixation, where NF can take up NO_3^- under hight ambient NO_3^- conditions.

Currently, many global biogeochemical models include a temperature-dependent growth rate for NF [Schmittner et al., 2007, 2008, Keller et al., 2012, Landolfi et al., 2013], e.g., Schmittner et al. [2008] use a maximum growth rate for the NF of about 13.7% to 31% of that for OP for temperatures between 20 and 30°C (Fig. 4 of this response letter), which is even lower than our estimate.

Comment: Confidence about the remineralization rate in the different boxes?

Response: For our biogeochemical model, we assume a fixed remineralization rate in different boxes. A brief justification has been given in caption (b) of Table 5. According to Suess [1980] and Martin et al. [1987], about 92% and 97% of the total primary production are remineralised in the top 500m of the ocean, and we applied 90% in our model. About 20% regeneration is needed in the surface box to allow coexistence of the OP and NF. We have now performed sensitivity experiments to test the effects of different remineralization rates. Our conclusion that the reduced denitrification rate is the main

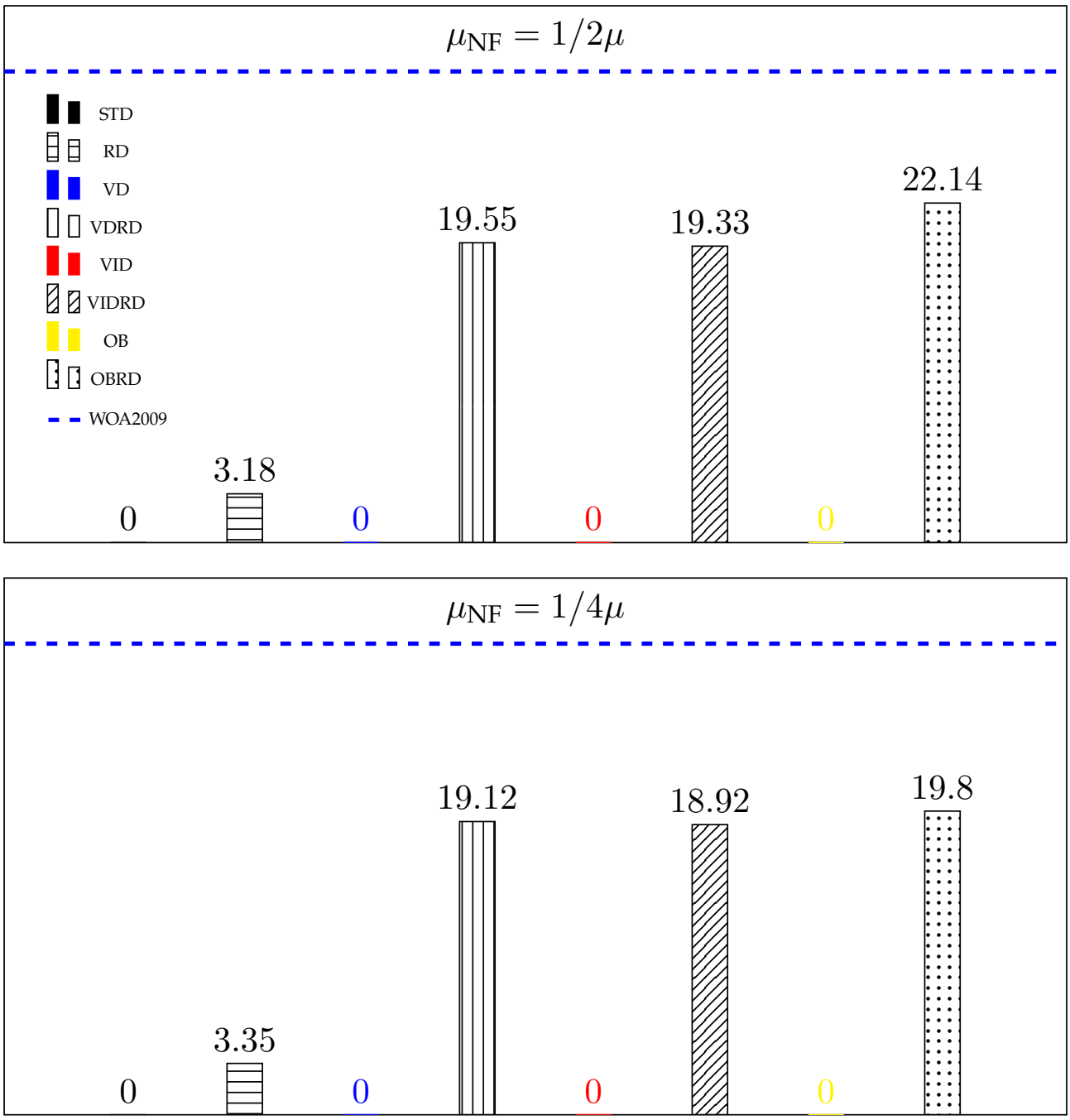

Figure 3: NO_3^- concentrations in the UM box for the sensitivity experiments for u_{NF}. The NO_3^- concentration in the OMZ in the VDRD and VIDRD configurations of the top panel is from the facultative N_2-fixation.

mechanism in preventing NO_3^- depletion in the OMZ is robust no matter whether there are 40% and 50%, 50% and 40%, or 60% and 30% primary production remineralized in the surface and intermediate boxes, respectively (Fig. 5 of this response letter). But the nitrogen inventory of our model domain can not reach steady state when the remineralisation ratios are 50% and 40%, or 60% and 30% in the VDRD and VIDRD configurations, where nitrogen fixation exceeds fixed-N loss via denitrification, leading to an ever increasing fixed-N inventory in the model domain. Still, this problem can be solved by including facultative N_2-fixation and does not occur in the most realistic configuration (OBRD).

Comment: What about deviations from the Redfield ratio in terms of nutrient uptake, the ability of some organisms to utilize organic phosphorous?
Response: We have now tested the response of our model to deviations from the Redfield Ratio in

Figure 4: Maximum growth rate estimated from the Schmittner (2008) model.

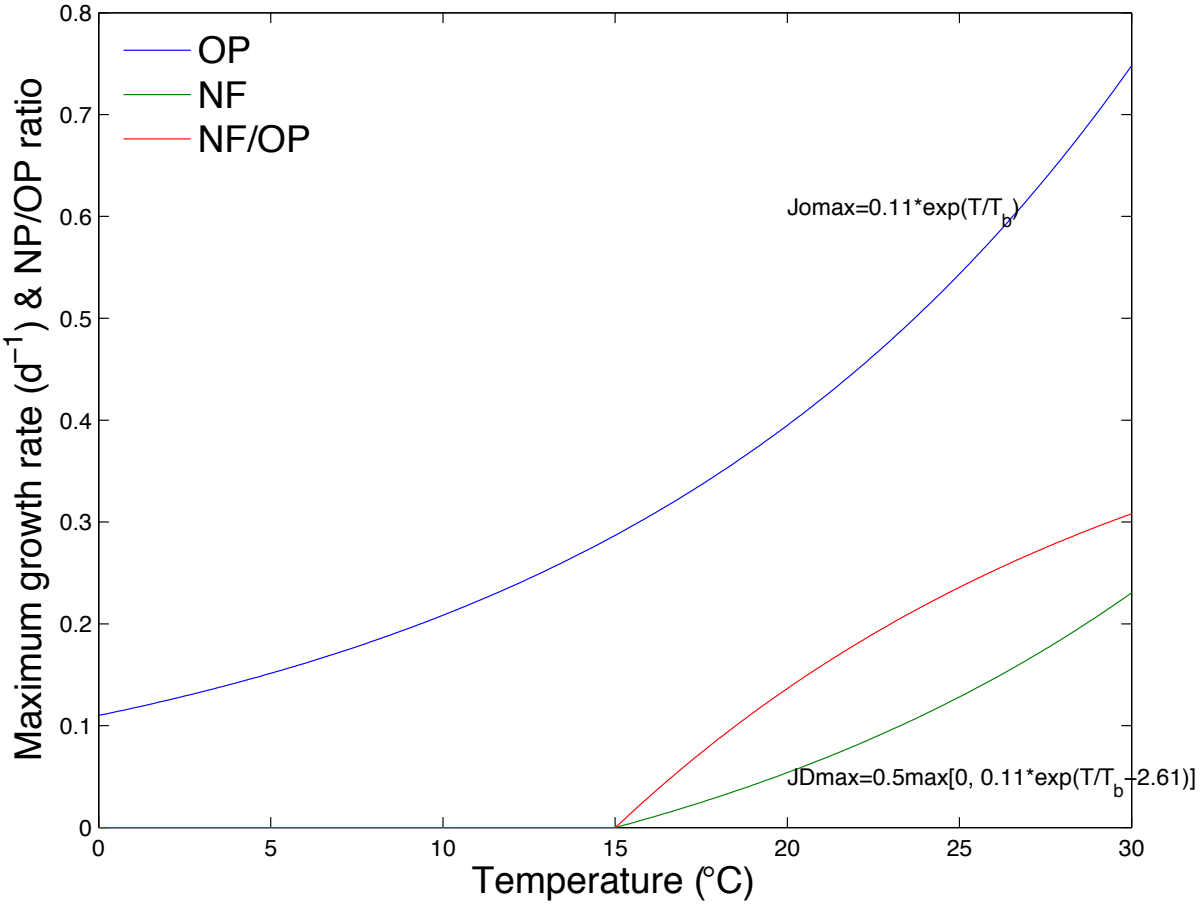

terms of nutrient uptake. Since phytoplankton can have different N:P uptake ratios in different OMZs, <16 in the Western Africa but >16 in Peru [Franz et al., 2012], we have tested N:P $= 12$ and N:P $= 20$ respectively for both OP and NF in our model. Also, because higher N:P ratios (>16) for diazotrophic phytoplankton are found to better agree with the observations both in experiments [Sañudo-Wilhelmy et al., 2004] and models [Klausmeier et al., 2004], we have made another sensitivity run with N:P $= 12$ for OP and N:P $= 25$ for NF. We are confident with our conclusion that the reduced denitrification rate is the main mechanism to prevent NO_3^- depletion in the OMZ, because this conclusion does not change (Fig. 6 of this response letter). We find that the oxygen conditions can vary slightly with different uptake ratios (figure not shown).

While the ability to utilise organic P has been proposed as an advantage of diazotrophs [Houlton et al., 2008, Ye et al., 2012], ordinary phytoplankton can also use DOP [e.g., Chu, 1946, Cotner, Jr. and Wetzel, 1992] and a clear advantage of diazotrophs over ordinary phytoplankton in the presence of DOP has never been demonstrated. Thus, we treat all available P to phytoplankton operationally as PO_4^{3-} and assume that all organic phosphate is remineralized to PO_4^{3-}. We will clarify this in Section 2.2 (Biogeochemical model) of the revised ms.

Comment: In table 5: two parameters (U_{NF} and M) have been set outside the range given in the column to the right. Could an explanation for this be added to the text?
Response: The U_{NF} range in Table 5 refers to the maximum rates obtained at the optimal temperature for each species, but the annual average temperature in our U box is only about 19°C, which is much

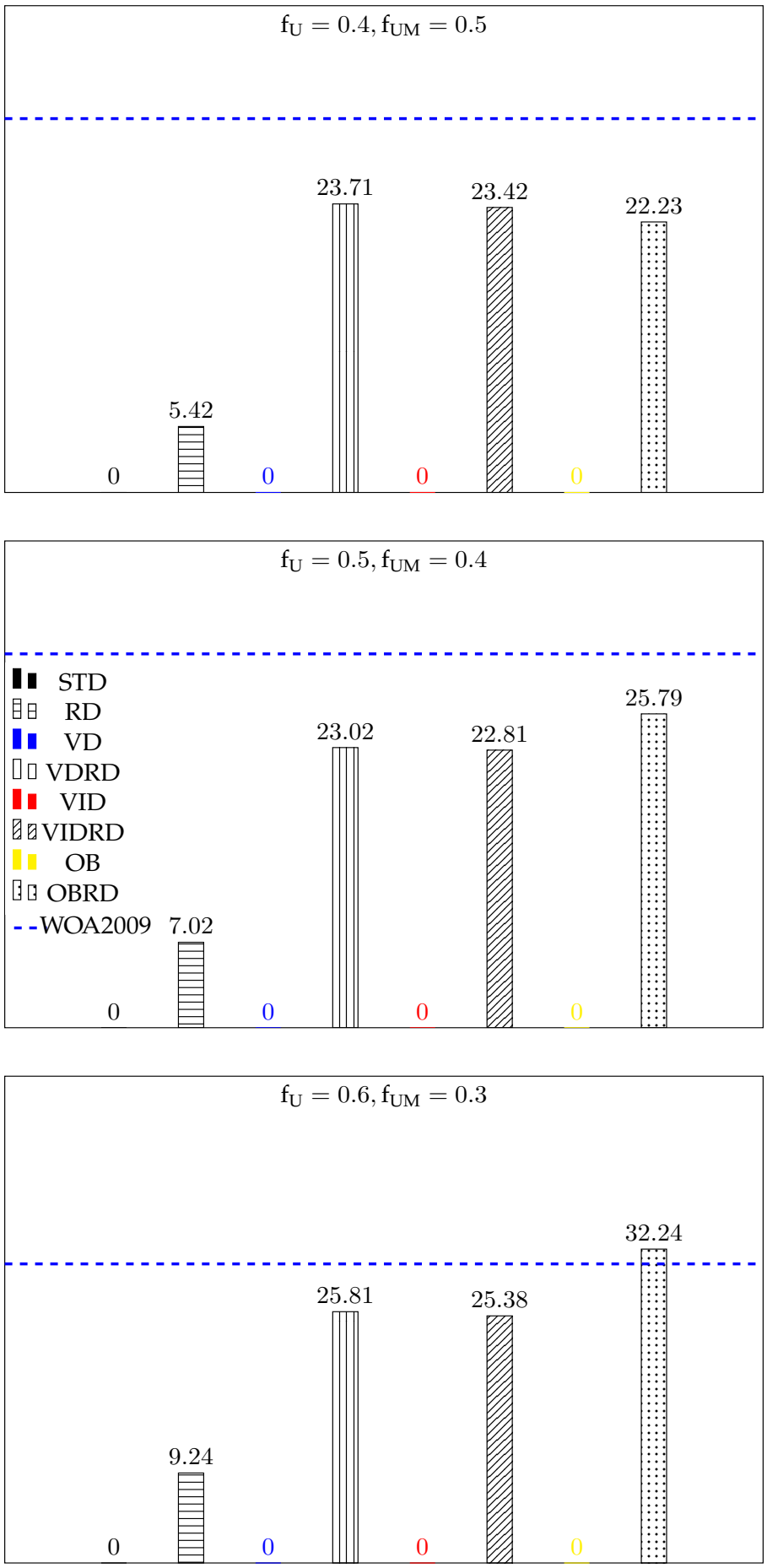

Figure 5: NO_3^- concentrations in the UM box for the sensitivity experiments for f_U, f_S, f_{UM} and f_I. The NO_3^- concentration in the VDRD and VIDRD configurations of the last two panels is from the facultative N_2-fixation, which can prevent the unsteady state problem.

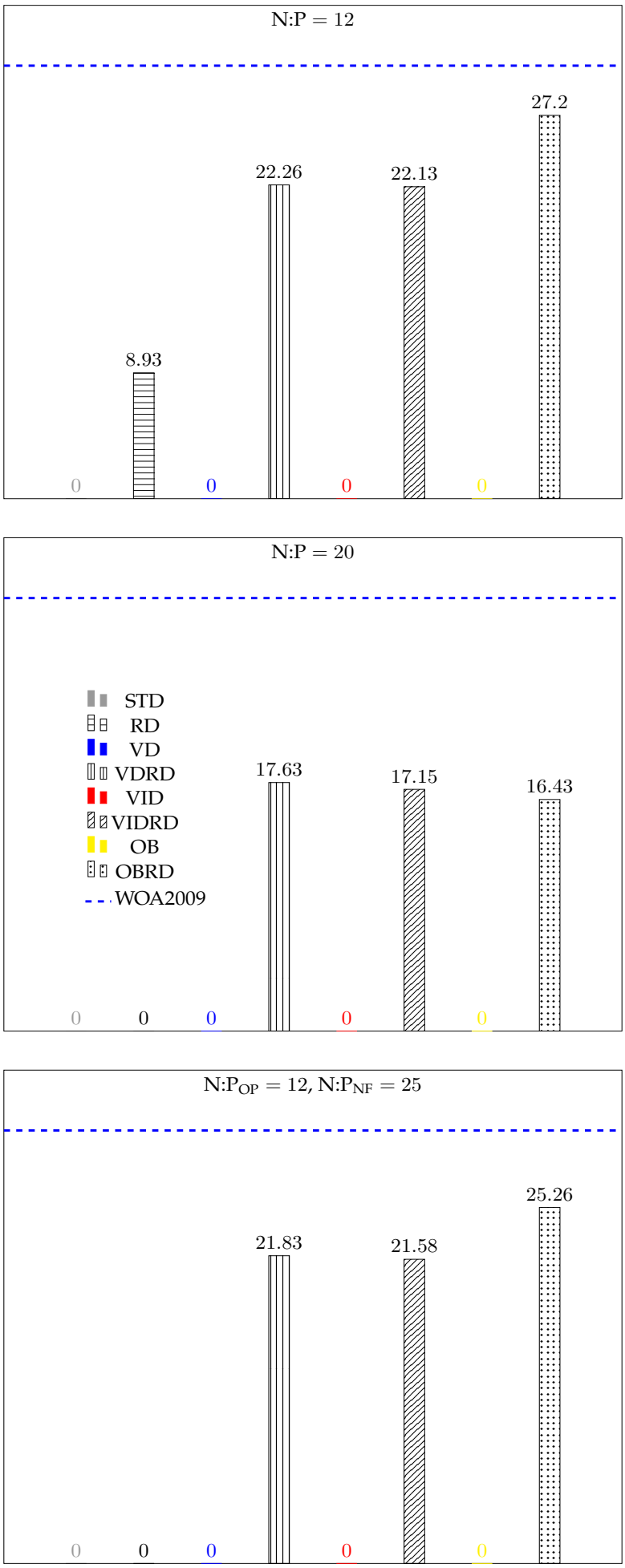

Figure 6: NO_3 concentrations in the UM box for sensitivity experiments for deviation from the Redfield ratio.

lower than the optimal temperature ($\approx$ 27°C) of diazotrophs. Considering the strong temperature sensitivity of diazotrophy [e.g., Breitbarth et al., 2007], our U_{NF} value is well within the temperature-corrected literature range. We will clarify this in the revised ms.

For simplicity, we use the same linear mortality for ordinary and diazotrophic phytoplankton in the STD configuration of the original ms. M has been removed from the model, as all configurations now employ quadratic mortality terms.

Comment: Explain how gu and gs were determined.
Response: A brief introduction about how g_U and g_S were determined was given in Appendix C of the original ms.
^{14}C data were employed to calibrate the physical parameters of our model. We have 7 parameters to be determined (listed in Table 4), but there are only 5 linear equations representing transport and SMS terms for $\widehat{^{14}C}$ (one equation for each box). We derived transport parameters A, B, K_{US}, K_{UM} and K_{H} with air-sea $\Delta^{14}C$ exchange rates g_U and g_S for the U and S boxes respectively as inputs. All possible combinations of values (with a step size of 0.01 myr^{-1}) for g_U and g_S were applied to derive the values for transport parameters A, B, K_{US}, K_{UM} and K_{H}. Subsequently, g_U and g_S were constrained in a two-step procedure. First, all combinations were determined which result in transport parameters in the literature range in Table 5. Finally, the combination giving the most realistic NO_3, PO_4, and O_2 distributions (closest to observations) was chosen for the experiments in the main text (Fig. 8). This will be clarified in Appendix D of the revised ms.

Comment: Is there any evidence that the denitrification rate is in fact slower under suboxic conditions that conventional parameterization of biogeochemical models suggest (other than it giving improved model results)? What was the justification used in Schmittner et al.
Response: We did not find the justification in the Schmittner et al. [2008] paper, but there are both observations and models indicating a slower remineralization rate under suboxic conditions [Liu and Kaplan, 1984, Devol and Hartnett, 2001, Van Mooy et al., 2002]. We had already addressed this topic in the original ms (P11106 L12–15), which will be amended in the revised ms.

Comment: The paper presents the 7 main model configurations summarized in table 4, but in between other experiments with sensitivity to different parameters are also described in the result section and a couple more appear in the discussion. The paper would be easier to read if these runs were described separately from the runs in table 4, for example under a sub-heading "3.3 Sensitivity runs".
Response: We agree that the ms structure was somewhat confusing. We will improve it in the revised ms in response to this comment together with the comments from the other reviewer.
We will remove the STD configuration from the revised ms, because it contributes nothing to our conclusion, and rename the QM configuration from the original ms as the STD configuration in the revised ms. We will choose the new STD, RD, VIDRD and OBRD configurations as the main configurations, and mainly describe and discuss their results in the main text, since these are the configurations that illustrate our conclusions. We will add a subsection "3.3 Model sensitivity", where we will summarise all model sensitivity experiments. The VD, VDRD, VID and OB configurations will now be described as sensitivity configurations briefly in Appendix E of the revised ms. Accordingly, Figure 2 and Figure 3 will also be replaced by Figures. 7 and 8 of this response letter.
We will also include several more summary sentences and make some statements more specific in order to clarify the role of each model configuration and sensitivity experiment. These are:
1, P11101 L14 "Sensitivity experiments are also performed with a configuration where N_2 fixation is inhibited by NO_3^-, but overall results are found to be virtually unchanged (Appendix D).".
will be **reworded to**: "Sensitivity experiments are also performed with a configuration where nitrogen fixers preferentially use nitrate when available and cover only the residual nitrogen demand via N_2 fixation, denoted as facultative N_2-fixation, but overall results are found to be virtually unchanged (Appendix B)."

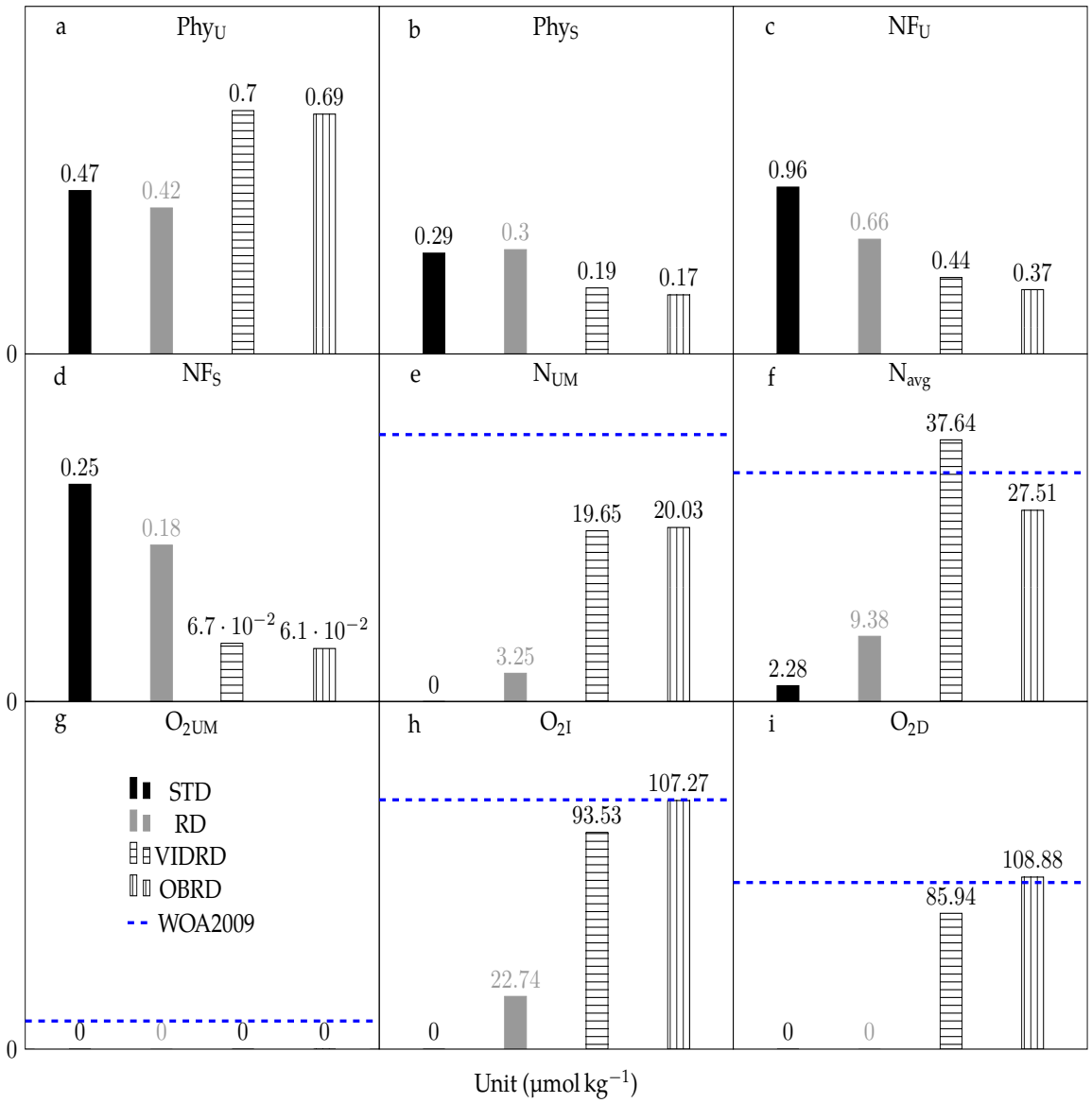

Figure 7: Simulated steady-state phytoplankton, nutrient and oxygen concentrations for the main model configurations defined in Tables 3 and 4. Each panel uses linear scale of the y-axis starting at zero. Dashed blue lines represent the average of the WOA2009 data of the corresponding boxes. There are no data for Phy_U, Phy_S, NF_U and NF_S.

2, P11103 L23:"In order to investigate the relationships between the different biotic and physical processes and the nitrogen cycle in an OMZ, we introduce eight additional model configurations (Table 5)"
will be **reworded to**: "In order to investigate the sensitivity of the nitrogen cycle in an OMZ to the different biotic and physical processes, we introduce seven additional model configurations. The main differences to the STD configuration are shown in Table 5."

3, "Two sensitivity experiments are performed for each of the VID and OB configurations to explore possibilities for preventing NO_3^- depletion in the OMZ: (a) different reduced remineralisation rates (f_{UM}) and (b) facultative N_2-fixation (see Appendix E)." will be **added** to P10L25–L27 of the revised ms.

4, P11105 L4–L11 will be **reworded to**: "For the OBRD configuration, three sensitivity experiments are performed to investigate our model sensitivity to variable physical transports and biogeochemical tracer concentrations: (1) The mixing rate with the southern boundary, K_H, is reduced for individ-

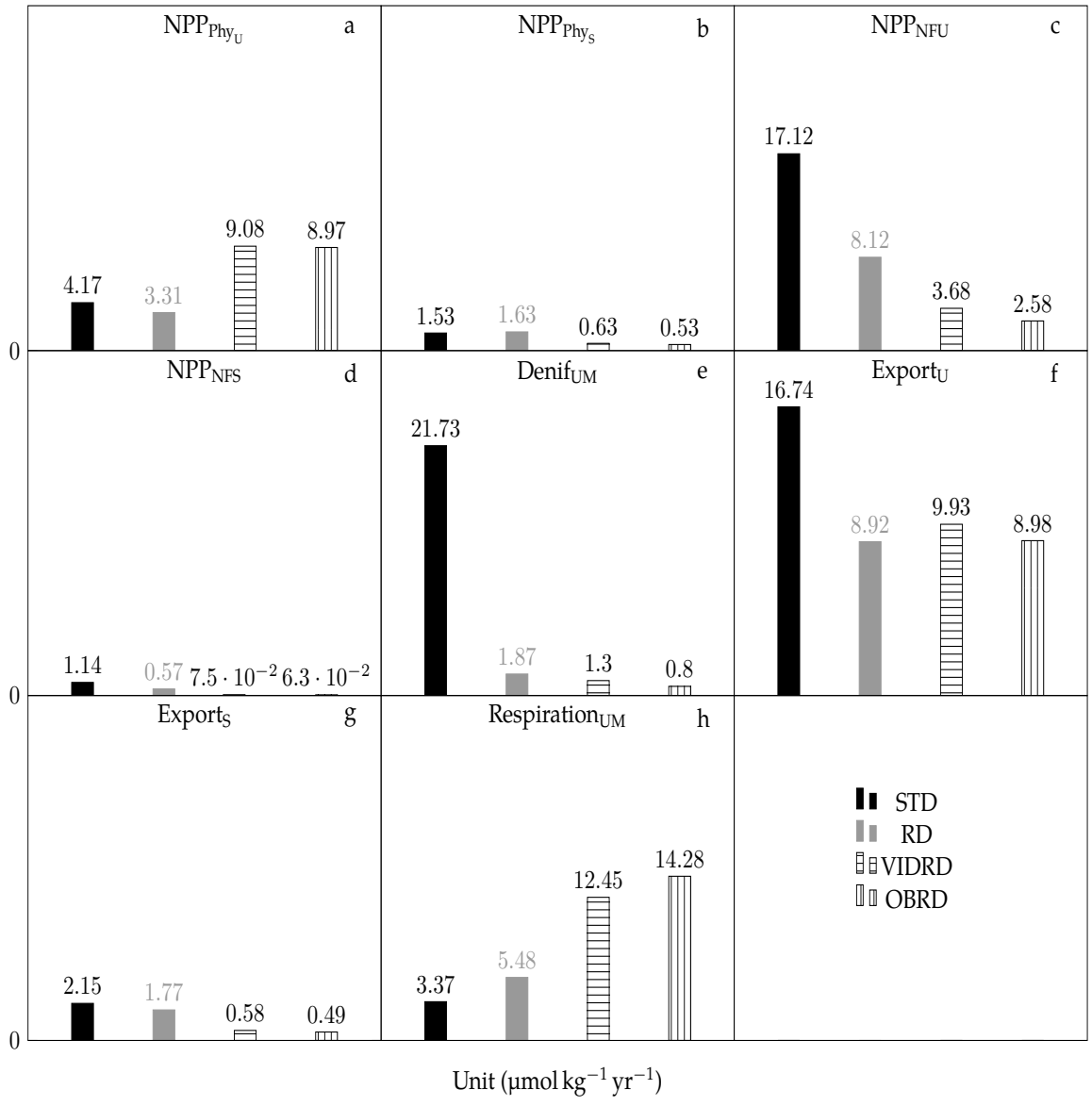

Figure 8: Simulated steady-state biogeochemical fluxes for the main model configurations.

ual tracers (nutrients, oxygen) or combinations thereof from full rates to zero. (2) Simulations are repeated with individual circulation parameters varied by ±10 %, ±20 % and ±50 %, respectively, to explore the sensitivity with respect to the circulation parameters of the box model. (3) The sensitivity of NO_3^- and O_2 concentrations in the OMZ to different physical parameters derived from variations of the $\Delta^{14}C$ data and O_2 concentrations in the U-box is also examined."

5, P11105 L20 after "...exported organic matter." We will **add**: "The results for biogeochemical tracer concentrations of the STD, RD, VIDRD and OBRD configurations are shown in Fig. 2, since they are the main configurations that illustrate our conclusions, while those for the VD, VDRD, VID and OB configurations are shown in Fig. 8 and described in Appendix E, because these sensitivity configurations do not contribute significantly to explaining the existence of high NO_3^- concentrations in the OMZ. ".
Afterwards, a new paragraph is started with "In the STD configuration,...".

6, P11107 L5:"Several sensitivity experiments..." will be **reworded to**: "Two sensitivity experiments..."

7, P11108 L3 **reworded to**: "For the biogeochemical fluxes, we focus on the STD, RD, VIDRD and OBRD configurations (configurations in bold in Table 5), since they show most clearly which mechanisms might be responsible for preventing NO_3^- exhaustion in the OMZ (Fig. 4)."

8, P23 L25–L27 and P24 L1–L5 in the revised ms, will be **added**: "Two further sensitivity experiments were performed for each of the VID and OB configurations to explore how NO_3^- depletion in the UM box can be prevented. (1) Decreasing the fraction of export production remineralized in the UM box (f_{UM}) from 70 % to 56 % makes NO_3^- persist in the UM box. Together with the 20 % remineralization in the U box, this implies that 76 % of the export production is remineralized in the upper 500 m of the ocean. However, the resulting NO_3^- concentration in the UM box is far below the literature range of about 15 to 40 μmol L^{-1}. (2) Facultative N_2-fixation inhibits nitrogen fixation in an environment with high NO_3^- concentrations, but fails to prevent NO_3^- depletion in the UM box. ".

Comment: Comparing model results to existing literature should be done in the discussion section (second paragraph p11109).
Response: We will move this paragraph to the discussion section of the revised ms and also modify it according to Table 6 **to**:
The NO_3^- loss by denitrification in the OMZ of the OBRD configuration is compared with that of other model-based and observational estimates in Table 6. Our simulated denitrification is consistent with the results of Somes et al. [2010] and DeVries et al. [2013] for the ETSP, lower than the estimate of Bianchi et al. [2012] and Kalvelage et al. [2013], but higher than that of Mills and Arrigo [2010]. However, the estimated denitrification byBianchi et al. [2012] represents the denitrification of the entire South Pacific but not only the ETSP. The Kalvelage et al. (2013) model has much higher fixed-N influx into the OMZ via physical transport than our model, which could compensate for their more intense NO_3^- loss by denitrification.

Comment: It wasn't immediately clear to me that 'ventilation' meant that only oxygen would be exchanged with the SO, so it took me a while to figure out the difference between VID and OB, please state this clearer.
Response: The differences between the configurations are shown in Table 3. We will address it more clearly in the revised ms.

Comment: Show how the model phosphate compare to WOA2009.
Response: The comparison of model and WOA2009 phosphate concentrations is shown in Table 1 of this response letter. The surface phosphate concentrations for all the model configurations are much lower than those for the WOA2009 data, because the top 100m is assumed to be the euphotic zone

Table 1: Phosphate concentration of each box for both models and WOA2009 data.

Box \ Configurations	STD	QM	RD	VDRD	VIDRD	OBRD	WOA2009
U	0.15	0.044	0.021	0.0096	0.012	0.0093	1.27
UM	3.22	3.22	1.73	1.80	1.92	1.73	2.53
S	0.13	0.0055	0.0037	0.0012	0.0012	0.0011	0.51
I	1.62	1.58	1.30	0.97	1.03	0.86	1.65
D	2.77	2.79	2.88	2.96	2.95	2.29	2.76

Table 2: Denitrification comparison with model-based and observational estimates.

Data/Models	Denitrificaition ($Tg\,N\,yr^{-1}$)
OBRD configuration	5.0^{c}
Kalvelage et al. [2013][a]	10.2^{c}
DeVries et al. [2013, pers. comm.][b]	7.0 ± 2.0^{c}
Bianchi et al. [2012][a]	17.6^{d}
Somes et al. [2010, pers. comm.][b]	5.8^{c}
Mills and Arrigo [2010][b]	$1.9^{c,*}$

[a]observational estimate; [b]model results; [c] ETSP; [d]entire South Pacific; *OMZ value extrapolated to UM box of out model.

in our model, but the depth of the euphotic zone is usually shallower than 100m in the ocean. The reason of our phosphate inventory of the model domain being lower than the WOA data in the OBRD configuration is that ${PO_4}^{3-}$ is lost by mixing through the boundary with the southern subtropical ocean. However, the simulated surface phosphate concentration being lower than the observations seems to be a general problem of box models (see, for example, Panel (b) of Fig. 4 in Tyrrell [1999]).

Comment: P11108, L4 mention which runs that are studied rather than refer the reader to figure 3.
Response: We will **reword** this **to**: "For the biogeochemical fluxes, we focus on the STD, RD, VIDRD and OBRD configurations (configurations in bold in Table 5), since they show most clearly the mechanisms responsible for preventing NO_3^- depletion in the OMZ (Fig. 4).".

Comment: Table 4: add a short description of each parameter.
Response: We have explained each parameter in Table 5 already. We will **add** the following note to the caption of Table 4 : "The detailed explanations for these parameters are given in Table 5."

Comment: Table 6: Are the models that are being compared also box models and are they configured for the same OMZ region?
Response: Mills and Arrigo [2010] is a box model for the OMZ of Eastern Tropical South Pacific. Kalvelage et al. [2013] is a reaction–diffusion model to estimate the nitrogen fluxes of the OMZ of Eastern Tropical South Pacific. We will replace Table 6 with Table 2 of this response letter to compare only the denitrification with other data and models, since there are many information unavailable in the original Table 6.

Comment: Figure 2: I suggest indicating the WOA2009 level by a horizontal line rather than an extra bar.
Response: We agree with this suggestion and the new figure is shown here (Fig. 7 of this response letter).

Comment: Figure 4: This figure has too many panels, the text is so small it is almost unreadable. I do not understand the significance of the separate columns from the figure labels.
Response: We now enlarge the font in the legend and modify the caption for this figure (Fig. 9 of this response letter). We will separate the figure and caption into 2 pages, which will make the figure

larger and more readable in the revised ms. We also remove the two columns named "O_2 and NO_3^-" and "O_2 and PO_4^{3-} ", since they produce quite similar results with the other two columns. The caption of this figure will be **reworded** as shown in Fig. 9 of this response letter.

Comment: Figure 5 - label: suggest to change "for different" to "to".
Response: Thanks! It will be changed in the revised ms.

Comment: Figure 6: It is hard to see the '*' on top of the x-axis.
Response: We have changed the location of the x-axis and then the '*' are more visible now (Fig. 10 of this response letter).

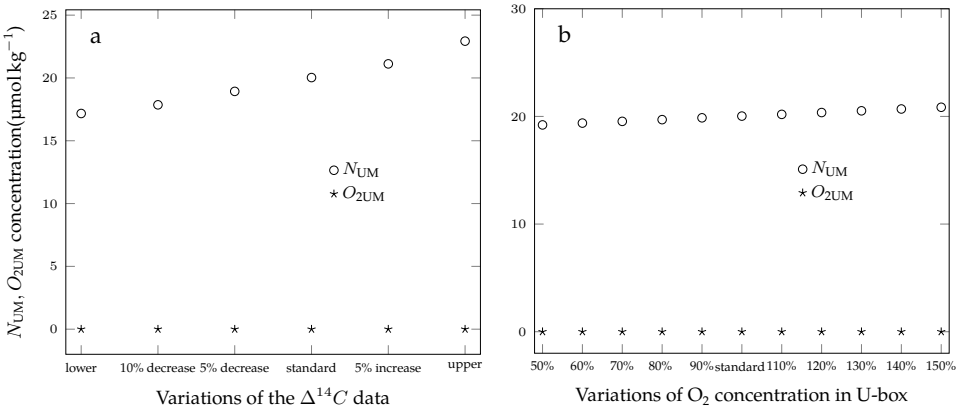

Figure 10: NO_3^- and O_2 concentrations in the OBRD configuration for different physical parameters derived from variations of the Δ^{14}C data (panel a) and O_2 concentration in the U-box (panel b). a: Decrease and increase mean that Δ^{14}C values in all boxes are reduced or increased simultaneously. b: Values of the x-axis denote the variations of O_2 concentration in the U-box relative to the standard. Standard run in each figure is the OBRD configuration with physical parameters defined in Table 4.

Comment: Figure 7- label. Add "as a function of the oxygen concentration in the D box" to the end of the first sentence.
Response: This will be included in the revised ms.

Comment: Figure 8 - what is meant by "all combinations of physical transport parameters in the literature range" (this is also mentioned in the text, but it is still unclear), perhaps I missed it, is this range indicated anywhere in the paper?
Response: This is related to how we have determined the physical transport parameters. As we have described in Appendix C of the original ms and the above answer to 'how to determine g_U and g_S', we have tried all combinations of values for g_U and g_S, each of which defines one set of physical transport parameters. Then, g_U and g_S were constrained in a two-step procedure. First, all combinations are determined which result in transport parameters within the literature range, which are shown in Table 5. Secondly, the combination giving the most realistic NO_3^-, PO_4^{3-}, and oxygen distributions is chosen for the experiments (Table 4).
We will **reword** "all combinations of physical transport parameters in the literature range" **to** "all combinations of g_U and g_S resulting in all transport parameters being inside the literature range as given in Table 5" to clarify this point in the revised ms. In Fig. 8 we show the set of parameters that we have chosen for all the model configurations, which is the second step to determine our physical parameters.

Comment: Figure 9: with only small differences between this and the original run, perhaps this figure can be omitted?
Response: Yes, only small differences can be identified after including the Schmittner formulation for

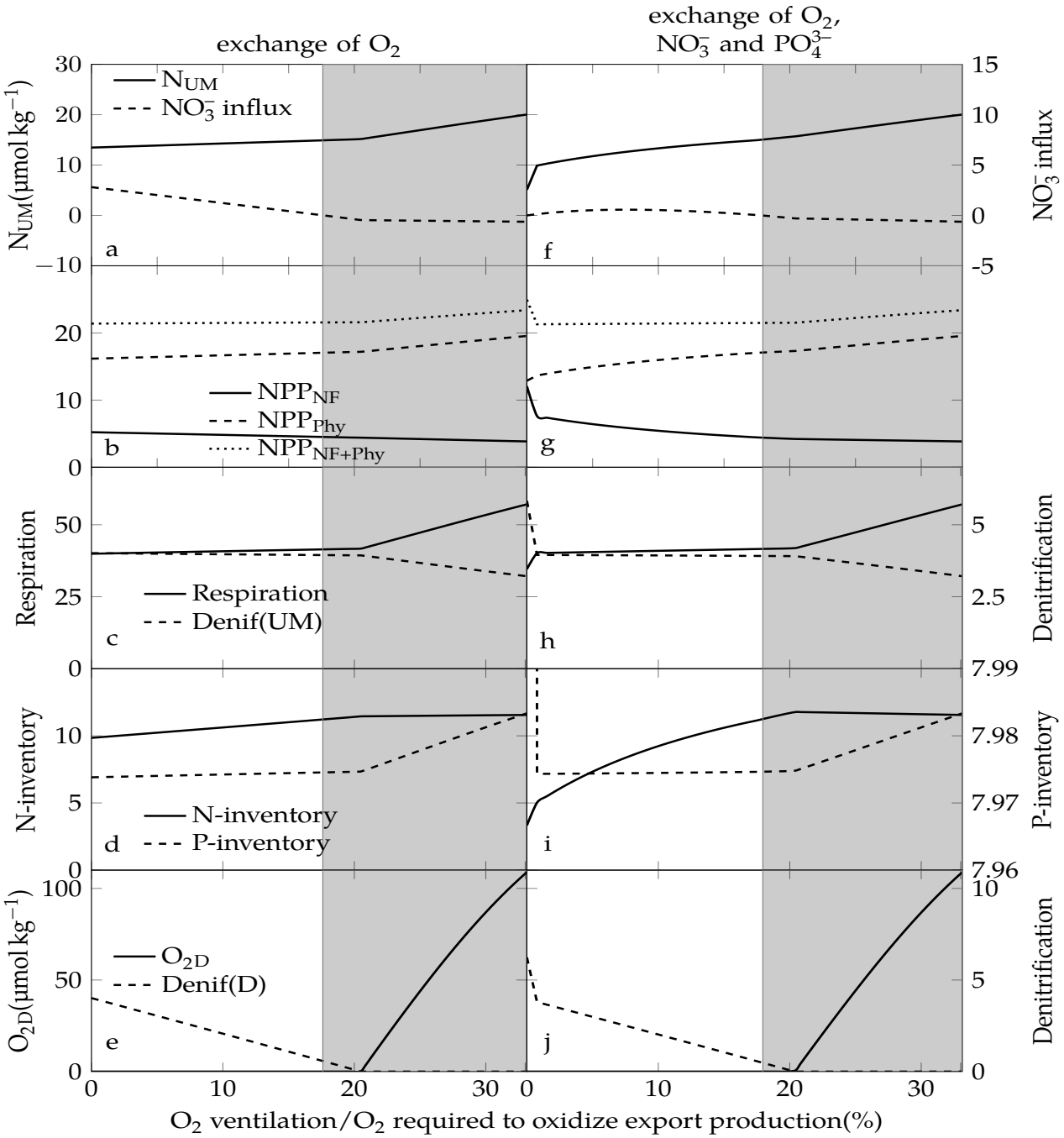

Figure 9: Dependence of biogeochemical processes on the exchange of O_2, NO_3^-, and PO_4^{3-} with the subtropical ocean through the southern boundaries of the I and D boxes. The x-axes indicate the contribution of O_2 supplied from the subtropical ocean relative to that required to oxidize all export production from the surface ocean (boxes U and S). (a–e) only O_2 exchanged through the southern boundaries is reduced; (f–j) exchange of O_2, NO_3^-, and PO_4^{3-} is reduced. N_{UM} is NO_3^- concentration in the UM box and NO_3^- influx is the NO_3^- flux through the southern boundary (positive into model domain). NPP_{Phy}, NPP_{NF} and NPP_{NF+Phy} are net primary production by ordinary phytoplankton, nitrogen fixers, and the sum of both in the surface ocean. Respiration and Denif (UM) represent O_2 consumption by aerobic remineralization and NO_3^- removal by anaerobic remineralization, respectively, in the UM box. N-inventory and P-inventory are the total nitrogen and phosphorus inventories in the model domain, including all organic and inorganic species. O_{2D} and Denif (D) represent O_2 concentration and NO_3^- removal by anaerobic remineralization in the D box. Units of all variables are 10^{11} μmol yr^{-1} m^{-1} except for N_{UM} and O_{2D}, which are given in μmol kg^{-1}. The shaded area denotes the parameter range for which the model domain is a net source of NO_3^-.

NF. We will remove it from our ms.

Response to Referee #2:

Comments: General comments: The authors use a 5-box model in order to explore controls on nutrient and oxygen dynamics in the ETSP OMZ. This work is complementary to a previous study by Canfield et al. (2006) that used a similar approach. Canfield et al. (2006) found that fixed N will persist in the OMZ provided that there is no N2 fixation in the overlying water. The addition of N2 fixation to Canfield's model drove the system to sulfate reduction. Recent work has shown that N2 fixation is in fact closely coupled to zones of N loss (OMZs), however NO3- is not observed to be exhausted as Canfield's model predicted. The current work by Su et al. explores the mechanisms by which NO3- is maintained at non-zero values in the OMZ even while there is N2 fixation in the overlying waters. They find that this condition is fulfilled when the remineralization rate by denitrification is substantially reduced relative to aerobic respiration. By also adding lateral ventilation and nutrient exchange with the subtropical ocean, the model produces realistic values of O2.
Response: We thank the reviewer for the positive evaluation and for pointing out the scientific significance of our work, which is also the information that we want to convey to our readers. Thereafter, we will concentrate on questions and suggestions from this reviewer to improve our ms.

Comment: It is an interesting topic given the discrepancy of Canfield's model results compared to observations in the OMZs. My main criticism with this work is that the results are not discussed in a way that is easy for the reader to understand. The authors present numerous model configurations although the physical significance of each configuration is not clear, nor do they all appear to be required to reach the conclusions of this work. The results of QM are similar to STD. It does not seem physically relevant to exchange O2 and 14C but not NO3- and PO4- (VD, VDRD, VI, VIRD). If those configurations were to test the importance of nutrient vs. O2 exchange, then I think that is sufficiently accomplished by the sensitivity experiments. Also, numerous sensitivity experiments were carried out but it is unclear on which model configuration and/or the relevance of all of the tests (Fig. 4-7). It may improve the reader's understanding if only the minimum number of model configurations needed to illustrate the conclusions of this work were presented. The rest of the model configurations could be placed in an appendix.
Response: We thank the reviewer for the generally positive comments and pointing out structural problems that could confuse our readers. Below we describe how we plan to modify the original ms in response to these suggestions and the comments of the other reviewer:
We will remove the STD configuration from the revised ms, because it contributes nothing to our conclusion, and rename the QM configuration from the original ms as the STD configuration in the revised ms. We will choose the new STD, RD, VIDRD and OBRD configurations as the main configurations, and mainly describe and discuss their results in the main text, since these are the configurations that illustrate our conclusions best. We will add a subsection "3.3 Model sensitivity experiments", where we will summarise all model sensitivity experiments. The VD, VDRD, VID and OB configurations will now be described briefly as sensitivity configurations in Appendix E of the revised ms. Accordingly, Fig. 2 and Fig. 3 will also be replaced by Figures. 7 and 8 in this response.
We will also include several more summary sentences and make some statements more specific in order to clarify the role of each model configuration and sensitivity experiment. These are:
1, P11101 L14 "Sensitivity experiments are also performed with a configuration where N_2 fixation is inhibited by NO_3^-, but overall results are found to be virtually unchanged (Appendix D).".
will be **reworded to**: "Sensitivity experiments are also performed with a configuration where nitrogen fixers preferentially use nitrate when available and cover only the residual nitrogen demand via N_2 fixation, denoted as facultative N_2-fixation, but overall results are found to be virtually unchanged (Appendix B)."
2, P11103 L23:"In order to investigate the relationships between the different biotic and physical processes and the nitrogen cycle in an OMZ, we introduce eight additional model configurations (Table 3)"

will be **reworded to**: "In order to investigate the sensitivity of the nitrogen cycle in an OMZ to the different biotic and physical processes, we introduce seven additional model configurations. The main differences to the STD configuration are shown in Table 3."
3, "Two sensitivity experiments are performed for each of the VID and OB configurations to explore possibilities for preventing NO_3^- depletion in the OMZ: (a) different reduced remineralisation rates (f_{UM}) and (b) facultative N_2-fixation (see Appendix E)." will be **added** to P10L25–L27 of the revised ms.
4, P11105 L4–L11 will be **reworded to**: "For the OBRD configuration, three sensitivity experiments are performed to investigate our model sensitivity to variable physical transports and biogeochemical tracer concentrations: (1) The mixing rate with the southern boundary, K_H, is reduced for individual tracers (nutrients, oxygen) or combinations thereof from full rates to zero. (2) Simulations are repeated with individual circulation parameters varied by $\pm 10\,\%$, $\pm 20\,\%$ and $\pm 50\,\%$, respectively, to explore the sensitivity with respect to the circulation parameters of the box model. (3) The sensitivity of NO_3^- and O_2 concentrations in the OMZ to different physical parameters derived from variations of the $\Delta^{14}C$ data and O_2 concentrations in the U-box is also examined."
5, P11105 L20 after "...exported organic matter." We will **add**: "The results for biogeochemical tracer concentrations of the STD, RD, VIDRD and OBRD configurations are shown in Fig. 2, since they are the main configurations that illustrate our conclusions, while those for the VD, VDRD, VID and OB configurations are shown in Fig. 8 and described in Appendix E, because these sensitivity configurations do not contribute significantly to explaining the existence of high NO_3^- concentrations in the OMZ. ".
Afterwards, a new paragraph is started with "In the STD configuration,...".
6, P11107 L5:"Several sensitivity experiments..." will be **reworded to**: "Two sensitivity experiments..."
7, P11108 L3 will be **reworded to**: "For the biogeochemical fluxes, we focus on the STD, RD, VIDRD and OBRD configurations (configurations in bold in Table 3), since they show most clearly which mechanisms might be responsible for preventing NO_3^- exhaustion in the OMZ (Fig. 4)."
8, P23 L25–L27 and P24 L1–L5 in the revised ms, will be **added**: "Two further sensitivity experiments were performed for each of the VID and OB configurations to explore how NO_3^- depletion in the UM box can be prevented. (1) Decreasing the fraction of export production remineralized in the UM box (f_{UM}) from 70 % to 56 % makes NO_3^- persist in the UM box. Together with the 20 % remineralization in the U box, this implies that 76 % of the export production is remineralized in the upper 500 m of the ocean. However, the resulting NO_3^- concentration in the UM box is far below the literature range of about 15 to 40 μmol L^{-1}. (2) Facultative N_2-fixation inhibits nitrogen fixation in an environment with high NO_3^- concentrations, but fails to prevent NO_3^- depletion in the UM box. ".

Comment: Please number all tables, figures, and appendices sequentially as they appear in the text. Some, but not all, examples: p. 11100, ln. 14. "Table 4 and 5" should be "Tables 2 and 3". p. 11101, ln. 15-16. "Appendix D" should be "B". p. 11102, ln. 9. "Appendix B" should be "C". p. 11102, ln. 13. "Table 2" should be "4". Et cetera.
Response: We will correct this problem in the revised ms.

Comment: In the "Biogeochemical tracer concentrations" section, most of the configurations where denitrification was not reduced were discussed though not shown in Figs. 2 or 3. There is a large amount of data presented in the figures for the reader to sort through and so it would be helpful if the authors could be more explicit in the text about what data can be found in the figures and what cannot.
Response: In the revised ms, we will only present the STD, RD, VIDRD and OBRD configurations in the "Biogeochemical tracer concentrations" section, and only the results of these four configurations are described in this section. Figs. 2 and 3 will also be replaced by Figures. 7 and 8 of this response letter, in which only the results of the STD, RD, VIDRD and OBRD configurations are shown. We hope that this improves the clarity sufficiently.

Comment: p. 11107, ln. 11-15. "Next, a model of nitrogen fixation: : :" Why is this mentioned

Table 3: Phosphate concentration of each box for both models and WOA2009 data.

Box \ Configurations	STD	QM	RD	VDRD	VIDRD	OBRD	WOA2009
U	0.15	0.044	0.021	0.0096	0.012	0.0093	1.27
UM	3.22	3.22	1.73	1.80	1.92	1.73	2.53
S	0.13	0.0055	0.0037	0.0012	0.0012	0.0011	0.51
I	1.62	1.58	1.30	0.97	1.03	0.86	1.65
D	2.77	2.79	2.88	2.96	2.95	2.29	2.76

only here in the paragraph that discussed the VID configuration? Was this not addressed for all of the model configurations in Appendix D and Fig. 9?
Response: The model with an inverse relationship between NO_3^- concentration and the fraction of fixed nitrogen from nitrogen fixation was applied into all model configurations presented in the original ms (please see Fig. 9). NO_3^- depletion cannot be prevented in the VID configuration, even though there is O_2 ventilation into both the I and D boxes. In P11107 L3-L15 of the original ms, we have described two sensitivity experiments targeting to prevent NO_3^- depletion in the VID configuration, one of which is applying the Schmittner model for NF. That is why we have addressed it there rather than anywhere else. We will explain this better in our revised ms.

Comment: p. 11108, ln. 26-. "Compared with VIDRD configuration, total PO43-: : :" There is much discussion of PO43-. Please add panels to Fig. 2 to show PO43-.
Response: Table 3 in this response indicates the phosphate distributions in all our configurations. The reason of our phosphate inventory of the model domain being lower than in the WOA data in the OBRD configuration is that PO_4 is lost by mixing through the boundary with the southern subtropical ocean, which is shown in Fig. 4 (better shown in Fig. 9 of this response letter). We hope that this should be sufficient for phosphate, since (1) our study is primarily concerned with the N cycle, (2) no substantial changes in phosphorus inventory occur between the different model configurations except the OB and OBRD configurations.

Comment: 11109, ln. 13. "The fluxes associated with the fixed-N: : :" The authors refer to the "OB" configuration, however according to Table 6 it is the "OBRD" configuration being discussed. Please clarify.
Response: Yes, it is the "OBRD" configuration and we will correct it in the revised ms.

Comments: p. 11109, ln. 21-. "In sensitivity experiments: : :" For which model configuration?
Response: It is the sensitivity experiment for the "OBRD" configuration, which is the most realistic configuration (NO_3^- and O_2 concentrations closest to observations). We will address it better in the revised ms as "In sensitivity experiments of the OBRD configuration, designed to elucidate the importance of the influence of the subtropical ocean on the model domain,".

Comment: p. 11110, ln. 20. "The behaviour of the model domain as a small pelagic net NO3-source: : :" Is it a source of NO3- or fixed-N (as the caption for Fig. 4 indicates)? They are close but not the same especially since we are discussing N2-fixation and assimilatory uptake of N by phytoplankton. Also, I do see that the OBRD configuration results in the model domain consistently being a net source of NO3-. Fig. 4 shows that whether or not the model domain is a net source depends on the ventilation of O2 from the subtropical ocean. Or do the authors mean that WHEN it is a source, it is insensitive to physical transport parameters? How could it be insensitive when increased ventilation involves an increase in physical transport of O2? These seem to be contradictory statements. Please clarify.
Response: Our model domain is a source of fixed-N, which in the model exists only in the form of NO_3^-. We neglect other forms of fixed-N such as NO_2^- and NH_4^- for simplicity since NO_3^- is the most abundant species. To make the statements consistent, we will use NO_3^- throughout our revised ms.

In Fig. 4, our model domain switches from a NO_3^- sink to a NO_3^- source with increasing O_2 ventilation from the southern boundary (sink: white area; source: grey area). We have indicated in Fig. 4 that whether or not the model domain is a net source depends on the ventilation of O_2 from the southern boundary, and the switching point is when the lateral mixing K_H is about 24% of the original value defined in Table 4 for the OBRD configuration (Fig. 11 of this response letter).
In Fig. 5, we have varied individual physical parameters by up to ±50%, whereby K_H represents the mixing rate between the southern boundary and I and D boxes, and also the mixing rate between the I and UM boxes. The maximum variations for K_H in Fig. 5 are ±50%, in which range our model domain is still a NO_3^- source. Our model domain can turn into a NO_3^- sink only when lateral O_2 supply (K_H for O_2) is less than about 24% of the original value.
We will **reword** "The behaviour of the model domain as a small pelagic net NO3- source: : :" **to** "The conclusion that the model domain is a small pelagic net NO_3^- source in the OBRD configuration does not change when individual physical transport parameters vary by up to ±50%. Varying biogeochemical parameters also does not affect this conclusion.".

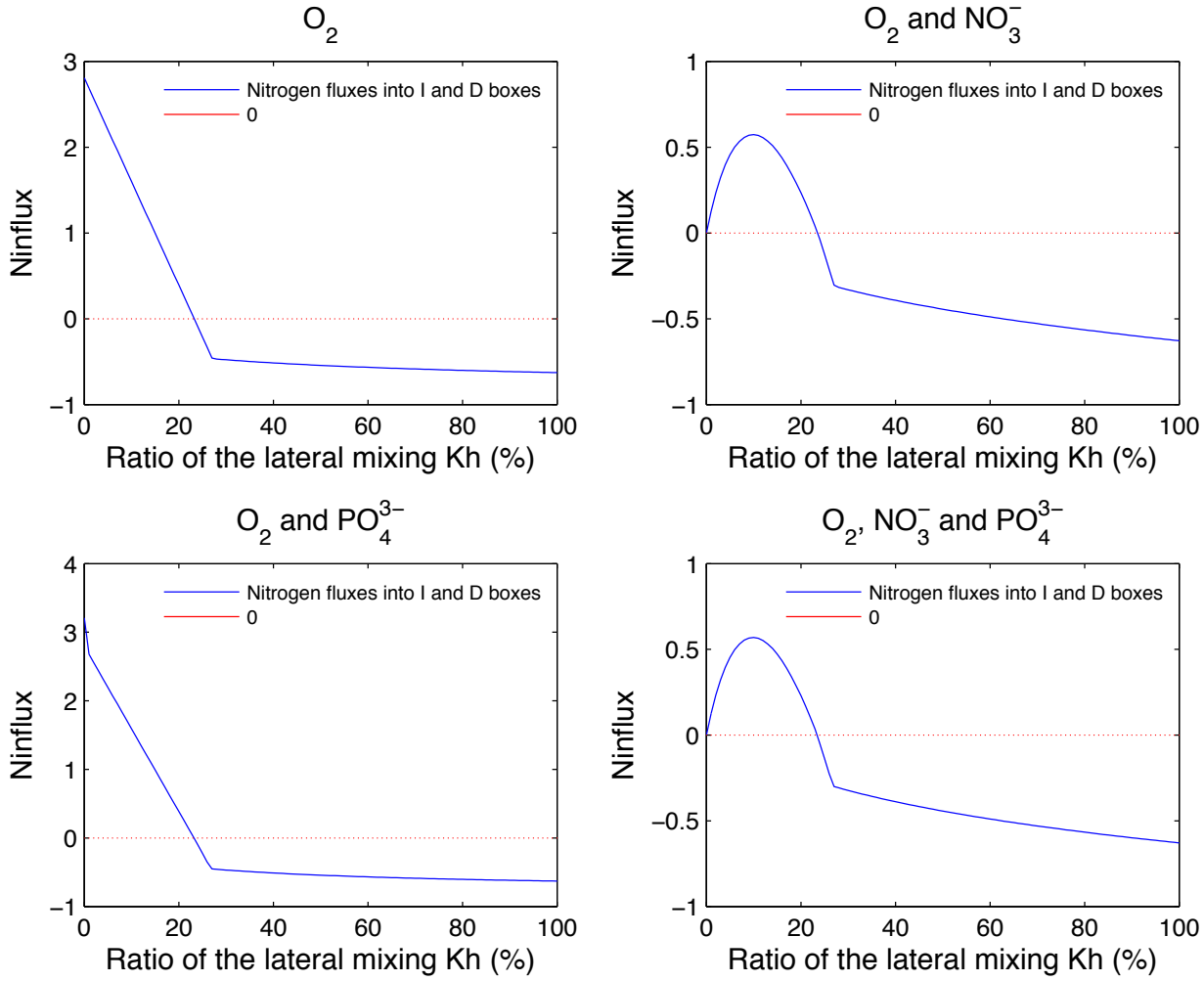

Figure 11: Positive values indicate that our model domain is a NO_3^- sink, and negative values represent a source.

Comment: p. 11110, ln. 23-25. "The finding that the model domain: : :D-box is oxic (Fig. 7)." The text implies that the entire model domain is a source of NO3- yet N-influx for only I and D boxes are presented in Fig. 7. Please show all boxes or at least the net of all of the boxes in Fig. 7.
Response: In our model only the I and D boxes are open to allow for nutrient and O_2 exchange with the southern boundary in the OB and OBRD configurations. Thus, I and D are the only boxes

through which nitrate can flow into or out of the model domain and the fluxes into/out of boxes I and D represent the total budget of the 5-box model. We will add a clarifying statement to the caption of Fig. 7.
We will also correct the unit mistake of Fig. 7 by replacing it with a new figure (Fig. 12 of this response letter).

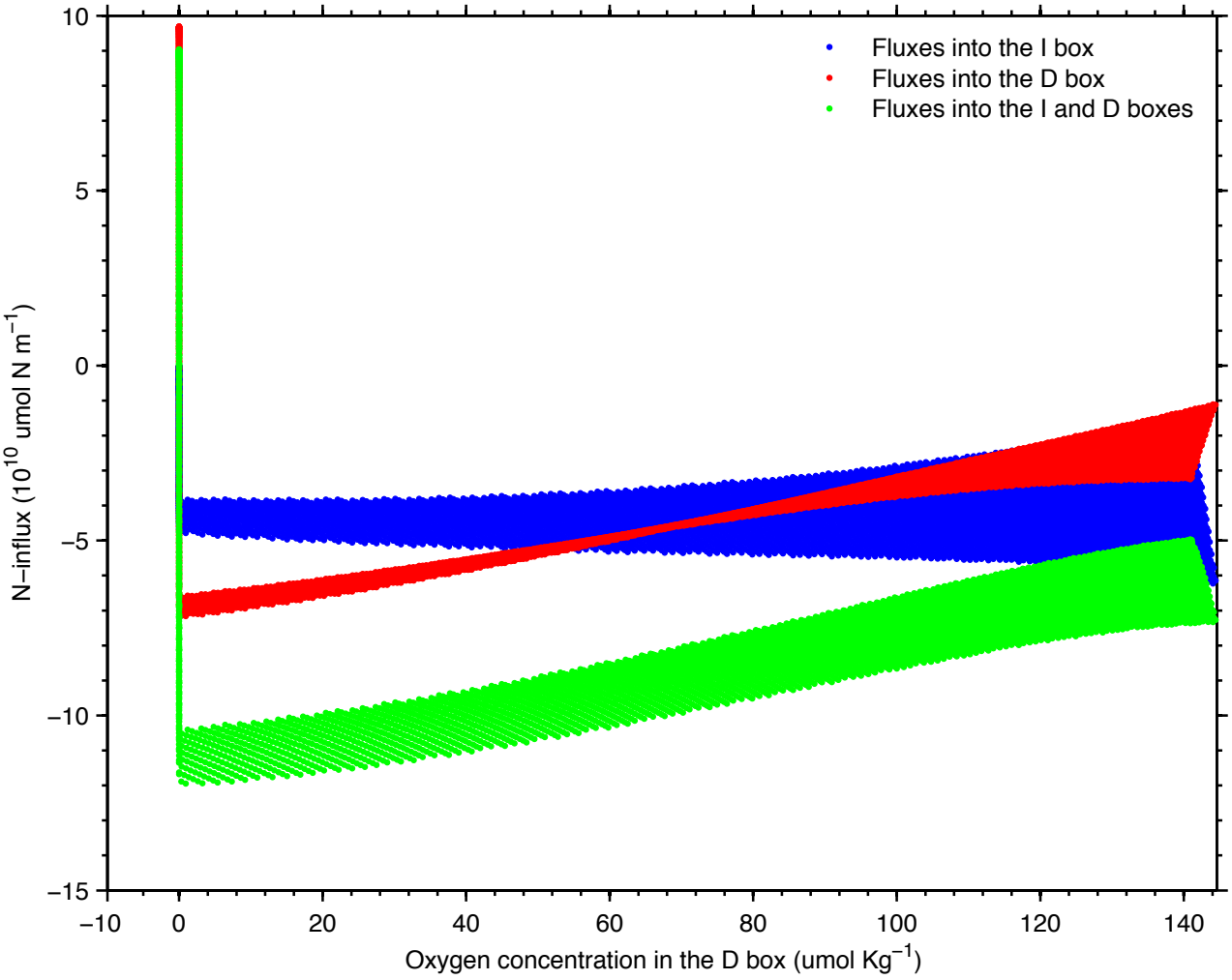

Figure 12

Comment: p. 11110, ln. 25-28 and Fig. 6. "The oxygen concentrations: : :increase in sensitivity model runs: : :" This is not what Fig. 6 shows. O2 in UM remains zero across variations in 14C. p. 11111, ln. 1-. "The UM box remains anoxic: : :" This statement appears to contradict the first sentence in this paragraph although is consistent with Fig. 6. Please clarify.
Response: We will **reword** p. 11110, ln. 25-28 **to**: "The oxygen concentrations in the I and D boxes increase in sensitivity model runs with physical parameters calibrated with increased ^{14}C concentrations (lower water mass age, not shown).". The O_2 concentrations in the I and D boxes provide the O_2 boundary conditions for the OMZ in our model. Higher concentrations can also be a result of lower water mass ages (more intense ventilation). In the sensitivity experiments for the OBRD configuration, we observed that the O_2 concentrations in the I and D boxes increase for physical parameters calibrated with increased ^{14}C concentrations (Fig. 13 of this response letter).

Comments: p. 11113, ln. 29 and p. 11114, ln. 1. "we" The authors must mean "they", referring to Eugster and Gruber (2012).
Response: When we estimated the nitrogen budget of that region from their box model results, we found that the water column of the IndoPacific is a large fixed-N source. This conclusion is not stated

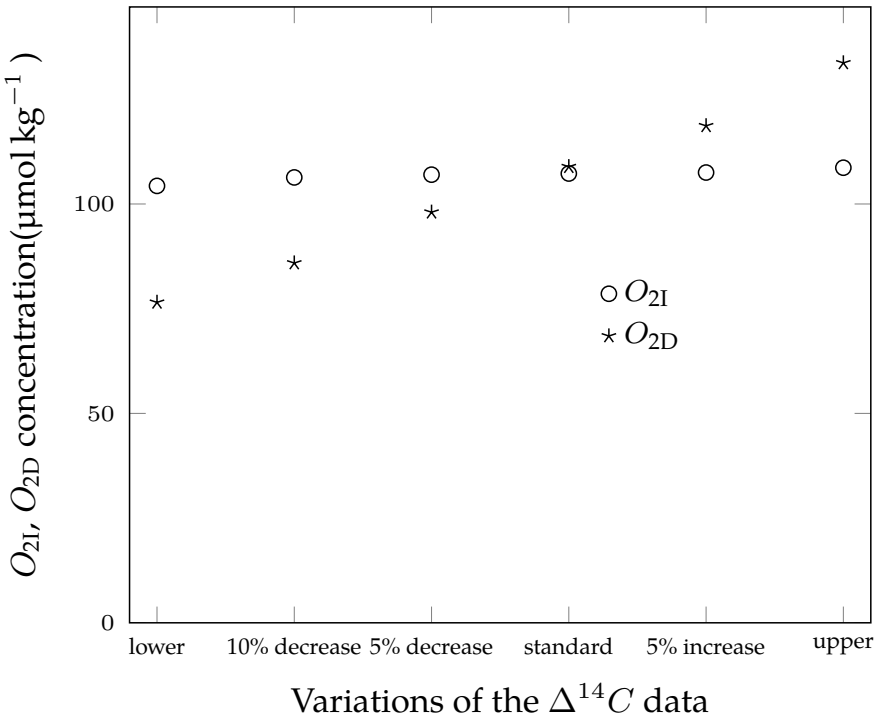

Figure 13: NO_3^- and O_2 concentrations in the I and D boxes for the OBRD configuration for different physical parameters derived from variations of the Δ^{14}C data.

directly in their paper. We will **reword** "We find" **to** "Their results indicate".

Comment: Table 3. Please add a short description of each model configuration so the reader does not have to keep flipping back to the text.
Response: Table 3 is the summary of section 2.4 (Model configurations), which is to help the readers understand the main differences among different model configurations. We will include the following text in the caption of Table. 3:
"+" means that the modification applies to this configuration. The configurations in bold are the main configurations, and the others are sensitivity configurations described in Appendix E. STD is the standard configuration defined in sections 2.2 and 2.3; in RD, a reduced denitrification rate is applied; VD indicates that the southern boundary of the model domain is partially opened to allow ventilation of O_2 and ^{14}C (but not NO_3^- and PO_4^{3-}) to the D box; VDRD is the configuration when a reduced denitrification rate is applied in VD; VID differs from VD only in that the partially open southern boundary is extended to allow ventilation of O_2 and ^{14}C also into the I box; VIDRD is the configuration when a reduced denitrification rate is applied in VID; in OB, nutrient (NO_3^- and PO_4^{3-}) mixing is added to VID; OBRD is the configuration in which the reduced denitrification rate is added to OB.".

Comment: Table 5 and Fig. 1. Please be consistent with variable names. "DS" or "SD" for the southern boundary of the deep box? Same for the intermediate box.
Response: Thanks! We will use "SD" and "SI" for all variables.

Comment: Figure 1. Define "SO" in the caption.
Response: We will **reword** the second to last sentence in the caption of Fig. 1 **to** "The model can be configured to exchange nutrients and oxygen with the southern subtropical ocean (right, denoted as "SO")".

Comment: Figure 2. Add panels to present phosphate.
Response: We only discuss the total phosphate inventory of the whole model domain rather than the individual boxes, as shown in Fig. 4 for the OBRD configuration. We hope that this should be suffi-

cient for phosphate, since (1) our study is primarily concerned with the N cycle, and (2) no substantial changes in P inventory occur between the different model configurations, except OB and OBRD.

Comment: Figure 4. Hard to read. Text is too small.
Response: We now enlarge the font in the legend and modify the caption for this figure (Fig. 9 of this response letter). We will separate the figure and caption into 2 pages, which will make the figure larger and more readable in the revised ms. We also remove the two columns named "O_2 and NO_3^-" and "O_2 and PO_4^{3-} ", since they produce quite similar results with the other two columns. The caption of this figure will be **reworded** as shown in Fig. 9 of this response.

Comment: Figure 5. "N source" and "N sink" w/arrows. It is ambiguous what these mean if OBRD is always a net source of NO3- (as the text states). Is the position of these text and arrows on the graph arbitrary?
Response: We agree that the position of the two arrows was confusing. To rectify this problem, we will replace Figure 5 with Fig. 14 of this response. We have included model sensitivity experiment results for the biogeochemical parameters in Fig. 14 and shown the absolute fluxes instead of the normalized fluxes. In Fig. 14, negative flux values indicate our model domain being a net NO_3^- source. This will be clearly stated in the caption of Fig. 14.

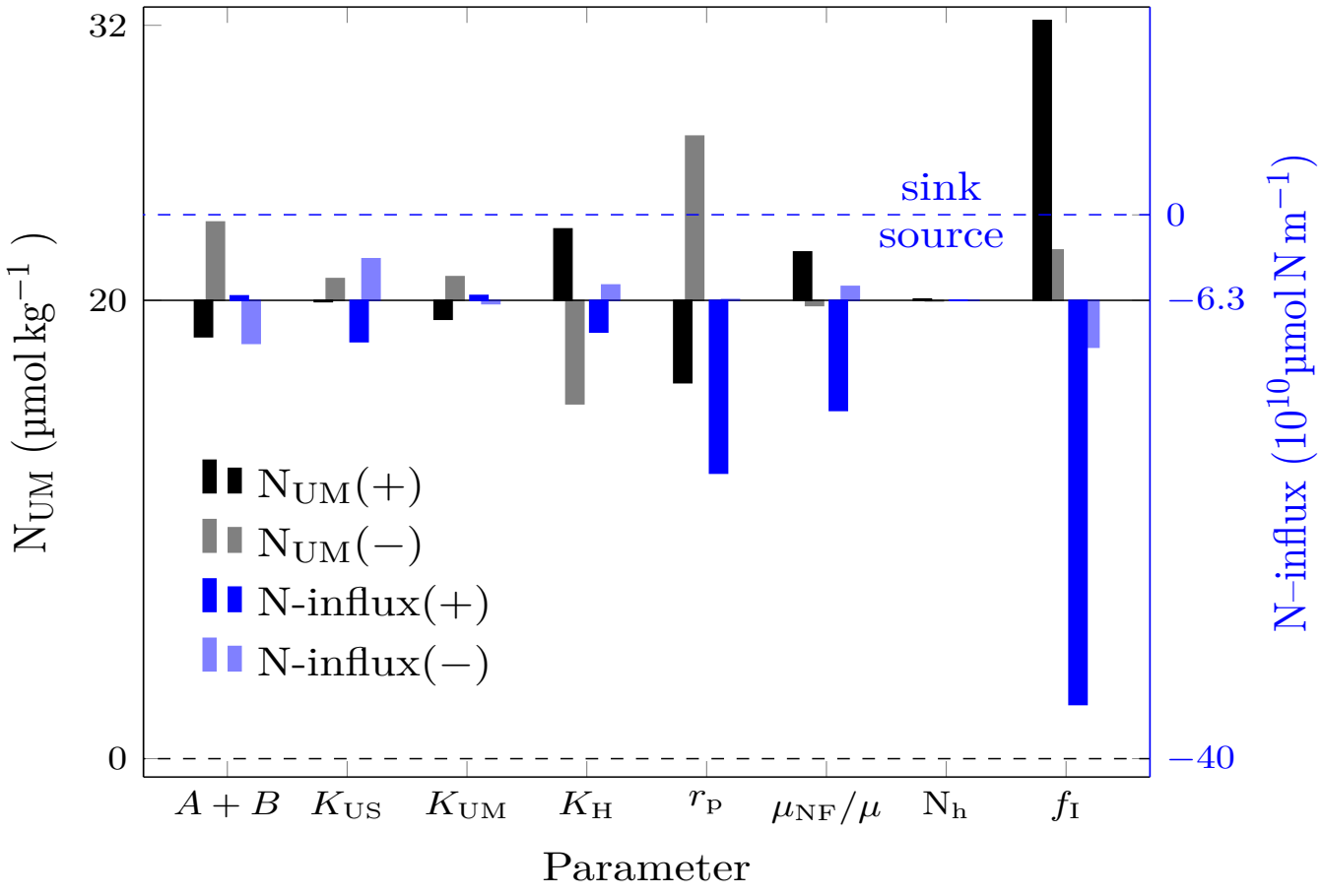

Figure 14: Sensitivity of NO_3^- concentration in the OMZ (N_{UM}) and the net NO_3^- flux out of the model domain to variations of the individual parameters describing ocean transport and biogeochemical processes (see Tables 2,5 and Fig. 1 for a description of the parameters). Black and blue bars represent changes in N_{UM} and N-influx, respectively. "+" and "−" indicate the response to increased and decreased parameters. Physical circulation parameters are varied by ±50%. r_P is varied between 12 and 20. μ_{NF}/μ is varied between 1/4 and 1/2. Nh varies between 0.3 and 0.9 μmol kg^{-1}. For f_i, "+" indicates f_U=f_S=60% and f_{UM}=f_I= 30%, and "−" means 40% and 50%, respectively.

Comment: Figures 9. Since this is only referred to in the appendices, should this also be appended?
Response: We will remove this figure from our original ms, because it does not show significant differences from Fig. 2.

Comment: Technical corrections: p. 11110, ln. 6. Second to last word in line should be "high" not "hight".
Response: We will correct it in the revised ms.

Comment: Table 5. Last 2 lines should be "Southern boundary OXYGEN concentration....." not "phosphate".
Response: We will correct it in the revised ms.

References

D. Bianchi, J. P. Dunne, J. L. Sarmiento, and E. D. Galbraith. Data-based estimates of suboxia, denitrification, and N_2O production in the ocean and their sensitivities to dissolved O_2. *Global Biogeochem. Cycles*, 26(GB2009), May 2012.

E. Breitbarth, A. Oschlies, and J. LaRoche. Physiological constrains on the global distribution of *Trichodesmium*-effect of temperature on diazotropy. *Biogeosciences*, 4:53–61, Jan. 2007.

S. E. Bulow, J. J. Rich, H. S. Naik, A. K. Pratihary, and B. B. Ward. Denitrification exceeds anammox as a nitrogen loss pathway in the Arabian Sea oxygen minimum zone. *Deep-Sea Res. I*, 57(3):384–393, 2010. doi: 10.1016/j.dsr.2009.10.014.

D. E. Canfield. Models of oxic respiration, denitrification and sulfate reduction in zones of coastal upwelling. *Geochimica et Cosmochimica Acta*, 70(23):5753 – 5765, 2006. doi: 10.1016/j.gca.2006.07.023.

S. P. Chu. The utilization of organic phosphorus by phytoplankton. *J. Mar. Biol. Assoc. U. K.*, 26(3): 285–295, July 1946.

L. A. Codispoti. An oceanic fixed nitrogen sink exceeding 400 Tg N a^{-1} vs the concept of homeostasis in the fixed-nitrogen inventory a^{-1} vs the concept of homeostasis in the fixed-nitrogen inventory. *Biogeosciences*, 4:233–253, May 2007. doi: 10.5194/bg-4-233-2007.

L. A. Codispoti, J. Brandes, J. Christensen, A. Devol, S. W. Naqvi, H. Paerl, and T. Yoshinari. The oceanic fixed nitrogen and nitrous oxide budgets: Moving targets as we enter the anthropocene? *Sci. Mar.*, 65(S2), 2001. doi: 10.3989/scimar.2001.65s285.

J. B. Cotner, Jr. and R. G. Wetzel. Uptake of dissolved inorganic and organic bphosphorus compounds by phytoplankton and bacterioplankton. *Limnol. Oceanogr.*, 37(2):232–243, 1992. doi: 10.4319/lo.1992.37.2.0232.

T. Dalsgaard, B. Thamdrup, and D. E. Canfield. Anaerobic ammonium oxidation (anammox) in the marine environment. *Res. Microbiol.*, 156(4):457 – 464, 2005. doi: 10.1016/j.resmic.2005.01.011.

C. Deutsch, J. L. Sarmiento, D. M. Sigman, N. Gruber, and J. P. Dunne. Spatial coupling of nitrogen inputs and losses in the ocean. *Nature*, 445(05392):163–167, Jan. 2007. doi: 10.1038/nature05392.

A. H. Devol and H. E. Hartnett. Role of the oxygen-deficient zone in transfer of organic carbon to the deep ocean. *Limnol. Oceanogr.*, 46(7):1684–1690, 2001. doi: 10.4319/lo.2001.46.7.1684.

T. DeVries, C. Deutsch, P. A. Rafter, and F. Primeau. Marine denitrification rates determined from a global 3-d inverse model. *Biogeosciences*, 10:2481–2496, Apr. 2013. doi: 10.5194/bg-10-2481-2013.

O. Eugster and N. Gruber. A probabilistic estimate of global marine N-fixation and denitrification. *Global Biogeochem. Cycles*, 26(GB4013):1–15, Nov. 2012. doi: 10.1029/2012GB004300.

C. Fernandez, L. Farías, and O. Ulloa. Nitrogen fixation in denitrified marine waters. *PLoS ONE*, 6 (6):e20539, June 2011. doi: 10.1371/journal.pone.0020539.

J. M. S. Franz, H. Hauss, U. Sommer, T. Dittmar, and U. Riebesell. Production, partitioning and stoichiometry of organic matter under variable nutrient supply during mesocosm experiments in the tropical Pacific and Atlantic Ocean. *Biogeosciences*, 9:4629–4643, Nov. 2012. doi: 10.5194/bg-9-4629-2012.

J. N. Galloway, F. J. Dentener, D. G. Capone, E. W. Boyer, R. W. Howarth, S. P. Seitzinger, G. P. Asner, C. C. Cleveland, P. A. Green, E. A. Holland, D. M. Karl, A. F. Michaels, J. H. Porter, A. R. Townsend, and C. J. Vörösmarty. Nitrogen cycles: past, present and future. *Biogeochem.*, 70:153–226, 2004. doi: 10.1007/s10533-004-0370-0.

A. Ganachaud and C. Wunsch. Oceanic nutrients and oxygen transports and bounds on export production during the world ocean circulation experiment. *Global Biogeochem. Cycles*, 16(4):1–14, Oct. 2002. doi: 10.1029/2000GB001333.

G. M. Grimaud, S. Rabouille, A. Dron, A. Sciandra, and O. Bernard. Modelling the dynamics of carbon–nitrogen metabolism in the unicellular diazotrophic cyanobacterium crocosphaera watsonii wh8501, under variable light regimes. *Ecol. Model.*, 291:121–133, 2014. doi: 10.1016/j.ecolmodel.2014.07.016.

N. Gruber. The dynamics of the marine nitrogen cycle and its influence on atmospheric CO_2 variations. In M. Follows and T. Oguz, editors, *The Ocean Carbon Cycle and Climate*, volume 40 of *NATO Science Series*, chapter 4, pages 97–148. Kluwer Academic, P.O.Box 17,3300 AA Dordrecht, The Netherlands, 2004.

N. Gruber and J. L. Sarmiento. Global patterns of marine nitrogen fixation and denitrification. *Global Biogeochem. Cycles*, 11:235–266, 1997. doi: 10.1029/97GB00077.

M. R. Hamersley, G. Lavik, D. Woebken, J. E. Rattray, P. Lam, E. C. Hopmans, J. S. S. Damsté, S. Krüger, M. Graco, D. Gutiérrez, and M. M. M. Kuypers. Anaerobic ammonium oxidation in the Peruvian oxygen minimum zone. *Limnol. Oceanogr.*, 52(3):923–933, May 2007. doi: 10.4319/lo.2007.52.3.0923.

B. Z. Houlton, Y.-P. Wang, P. M. Vitousek, and C. B. Field. A unifying framework for dinitrogen fixation in the terrestrial biosphere. *Nature*, 454:327–331, July 2008. doi: doi:10.1038/nature07028.

T. Kalvelage, G. Lavik, P. Lam, S. Contreras, L. Arteaga, C. R. Löscher, A. Oschlies, A. Paulmier, L. Stramma, and M. M. M. Kuypers. Nitrogen cycling driven by organic matter export in the South Pacific oxygen minimum zone. *Nature Geosci.*, 6:228–234, Mar. 2013. doi: 10.1038/NGEO1739.

D. P. Keller, A. Oschlies, and M. Eby. A new marine ecosystem model for the University of Victoria Earth System Climate Model. *Geosci. Model Dev.*, 5:1195–1220, Sep. 2012. doi: 10.5194/gmd-5-1195-2012.

C. A. Klausmeier, E. Litchman, T. Daufresne, and S. A. Levin. Optimal nitrogen-to-phosphorus stoichiometry of phytoplankton. *Nature*, 429:171–174, May 2004. doi: 10.1038/nature02454.

M. M. M. Kuypers, G. Lavik, D. Woebken, M. Schmid, B. M. Fuchs, R. Amann, B. B. Jørgensen, and M. S. M. Jetten. Massive nitrogen loss from the Benguela upwelling system through anaerobic ammonium oxidation. *Proc. Natl. Acad. Sci. USA*, 102(18):6478–6483, May 2005. doi: 10.1073/pnas.0502088102.

A. Landolfi, H. Dietze, W. Koeve, and A. Oschlies. Overlooked runaway feedback in the marine nitrogen cycle: the vicious cycle. *Biogeosciences*, 10:1351–1363, Mar. 2013. doi: 10.5194/bg-10-1351-2013.

J. LaRoche and E. Breitbarth. Importance of the diazotrophs as a source of new nitrogen in the ocean. *J. Sea Res.*, 53:67–91, 2005. doi: 10.1016/j.seares.2004.05.005.

T. M. Lenton and A. J. Watson. Redfield revisited 1. Regulation of nitrate, phosphate, and oxygen in the ocean. *Global Biogeochem. Cycles*, 14(1):225–248, March 2000. doi: 10.1029/1999GB900065.

K.-K. Liu and I. R. Kaplan. Denitrification rates and availability of organic matter in marine environments. *Earth Planet. Sci. Lett.*, 68:88–100, 1984. doi: 10.1016/0012-821X(84)90142-0.

J. H. Martin, G. A. Knauer, D. M. Karl, and W. W. Broenkow. VERTEX: carbon cycling in the northeast pacific. *Deep-Sea Res.*, 34(2):267–285, 1987.

M. M. Mills and K. R. Arrigo. Magnitude of oceanic nitrogen fixation influenced by the nutrient uptake ratio of phytoplankton. *Nature Geosci.*, 3:412–416, June 2010. doi: 10.1038/NGEO856.

V. Molina and L. Farás. Aerobic ammonium oxidation in the oxycline and oxygen minimum zone of the eastern tropical South Pacific off northern Chile ($\sim$20 °S). *Deep-Sea Res. II*, 56(16):1032–1041, 2009. doi: 10.1016/j.dsr2.2008.09.006.

A. Paulmier and D. Ruiz-Pino. Oxygen minimum zones (OMZs) in the modern ocean. *Prog. Oceanogr.*, 80:113–128, 2009. doi: 10.1016/j.pocean.2008.08.001.

S. A. Sańudo-Wilhelmy, A. Tovar-Sanchez, F.-X. F. andDouglas G. Capone, E. J. Carpenter, and D. A. Hutchins. The impact of surface-adsorbed phosphorus on phytoplankton Redfield stoichiometry. *Nature*, 432:897–901, Dec. 2004. doi: 10.1038/nature03125.

A. Schmittner, E. D. Galbraith, S. W. Hostetler, T. F. Pedersen, and R. Zhang. Large fluctuations of dissolved oxygen in the indian and Pacific oceans during Dansgaard-Oeschger oscillations caused by variations of North Atlantic Deep Water subduction. *Paleoceanography*, 22(PA3207):1–17, Aug. 2007. doi: 10.1029/2006PA001384.

A. Schmittner, A. Oschlies, H. D. Matthews, and E. D. Galbraith. Future changes in climate, ocean circulation, ecosystems, and biogeochemical cycling simulated for a business-as-usual CO_2 emission scenario until year 4000 AD. *Global Biogeochem. Cycles*, 21(GB1013), 2008. doi: 10.1029/2007GB002953.

C. J. Somes, A. Schmittner, E. D. Galbraith, M. F. Lehmann, M. A. Altabet, J. P. Montoya, R. M. Letelier, A. C. Mix, A. Bourbonnais, and M. Eby. Simulating the global distribution of nitrogen isotopes in the ocean. *Global Biogeochem. Cycles*, 24(GB4019):1–16, Nov. 2010.

E. Suess. Particulate organic carbon flux in the oceanssurface productivity and oxygen utilization. *Nature*, 288:260–263, Nov. 1980. doi: 10.1038/288260a0.

T. Tyrrell. The relative influences of nitrogen and phosphorus on oceanic primary production. *Nature*, 400:525–531, Aug. 1999.

B. A. S. Van Mooy, R. G. Keil, and A. H. Devol. Impact of suboxia on sinking particulate organic carbon: Enhanced carbon flux and preferential degradation of amino acids via denitrification. *Geochim. Cosmochim. Acta*, 66(3):457–467, 2002. doi: 10.1016/S0016-7037(01)00787-6.

B. B. Ward, A. H. Devol, J. J. Rich, B. X. Chang, S. E. Bulow, H. Naik, A. Pratihary, and A. Jayakumar. Denitrification as the dominant nitrogen loss process in the Arabian Sea. *Nature*, 461:78–81, 2009. doi: 10.1038/nature08276.

Y. Ye, C. Völker, A. Bracher, BettinaTaylor, and D. A.Wolf-Gladrow. Environmental controls on N_2 fixation by Trichodesmium in thetropical eastern North Atlantic Ocean—A model-based study. *Deep-Sea Res. I*, 64:104–117, Jan. 2012. doi: 10.1016/j.dsr.2012.01.004.

Manuscript prepared for Biogeosciences Discuss.
with version 4.1 of the LaTeX class copernicus_discussions.cls.
Date: 19 December 2014

What prevents nitrogen depletion in the OMZ of the Eastern Tropical South Pacific?

B. Su, M. Pahlow, H. Wagner, and A. Oschlies

GEOMAR Helmholtz Centre for Ocean Research Kiel, Marine Biogeochemical Modelling, Düsternbrooker Weg 20, 24105 Kiel, Germany

Correspondence to: B. Su (bsu@geomar.de)

Abstract

Local coupling between nitrogen fixation and denitrification in current biogeochemical models could result in a run-away feedback in open-ocean oxygen minimum zones (OMZs), eventually stripping OMZ waters of all fixed nitrogen. This feedback does not seem to operate at full strength in the ocean, as nitrate does not generally become depleted in open-ocean OMZs. To explore in detail ~~the mechanism that prevents~~ possible mechanisms that prevent nitrogen depletion in the OMZ of the Eastern Tropical South Pacific (ETSP), we develop a box model with fully prognostic cycles of carbon, nutrients, and oxygen in the upwelling region and its adjacent open ocean. Ocean circulation is calibrated with $\Delta^{14}C$ data of the ETSP. The sensitivity of the simulated nitrogen cycle to nutrient and oxygen exchange and ventilation from outside the model domain and to remineralization scales inside an OMZ is analysed. For the entire range of model configurations explored, we find that the fixed-N inventory can be stabilized at non-zero levels in the ETSP OMZ only if the remineralization rate via denitrification is slower than that via aerobic respiration. In our optimum model configuration, lateral oxygen supply ~~to~~ into the model domain is required at rates sufficient to oxidize at least about ~~a~~ one fifth of the export production in the model domain to prevent anoxia in the deep ocean. Under these conditions, our model is in line with the view of phosphate as the ultimate limiting nutrient for phytoplankton, and implies that for the current notion of nitrogen fixation being favored in N-deficit waters, the water column of the ETSP could even be a small net source of ~~fixed-N~~nitrate.

1 Introduction

The oceanic fixed nitrogen (fixed-N) budget is an essential control on the potential of the ocean to sequester atmospheric CO_2 via the marine biological pump. Denitrification is generally recognized as a major loss of fixed nitrogen, whereas the balance of the global oceanic nitrogen budget remains controversial. Accordingly, estimates derived from both field data and model analyses for the global oceanic fixed-N budget range from sources roughly balancing sinks ~~(Gruber and Sarmiento, 1997; Gruber, 2004; Eugster and Gruber, 2012)~~

(Gruber and Sarmiento, 1997; Gruber, 2004; Eugster and Gruber, 2012; DeVries et al., 2013) to a rather large net deficit between 140 and 234 $\mathrm{Tg\,N\,yr^{-1}}$ (Codispoti et al., 2001; Galloway et al., 2004; Codispoti, 2007).

One of the main uncertainties in the global marine nitrogen budget is the extent of nitrogen loss via denitrification and anaerobic ammonium oxidation (anammox) in oxygen minimum zones (OMZs), located in tropical coastal upwelling regions. Coastal upwelling zones are often associated with very high primary production. Subsequent decomposition of sinking organic matter leads to high levels of oxygen consumption in subsurface waters. Under conditions of sluggish circulation, oxygen-poor source waters, or lack of exchange with oxygenated surface waters, OMZs can develop, usually at intermediate depths of about 200–700 m (Bethoux, 1989; Capone and Knapp, 2007). An OMZ is commonly defined as a water body with an O_2 concentration below 20 $\mu\mathrm{mol\,L^{-1}}$ (Paulmier and Ruiz-Pino, 2009). The four major open-ocean OMZs are in the Eastern North Pacific (ENP), the Eastern Tropical South Pacific (ETSP), the Arabian Sea, and the Bay of Bengal. OMZs currently account for only about 8 % of the global ocean area but ~~are thought to~~ observations of intense denitrification and anammox in the OMZs indicate that they could be responsible for 30–50 % of the total fixed-N loss (Gruber and Sarmiento, 1997; Codispoti et al., 2001; Dalsgaard et al., 2005; Paulmier and Ruiz-Pino, 2009).

Canfield (2006) used a simple steady-state box model of a coastal OMZ to show that a positive feedback between N_2 fixation and denitrification could strip the OMZ of all fixed nitrogen when N_2 fixation was permitted to restore the nitrate : phosphate ratio to Redfield proportions in the surface ocean. Observed concentrations of fixed-N (nitrate plus nitrite) in OMZ waters, however, typically range from about 15 to 40 $\mu\mathrm{mol\,L^{-1}}$ (Codispoti and Richards, 1976; Codispoti and Packard, 1980; Morrison et al., 1998; Voss et al., 2001). A possible explanation for the relatively high nitrate concentrations even in the suboxic core of open-ocean OMZs could be low levels of nitrogen fixation in the overlying surface waters (Landolfi et al., 2013). However, recent interpretations of observed fixed-N deficits relative to the Redfield equivalent of phosphorus point to high rates of nitrogen fixation closely related to the upwelling of nitrogen-deficit waters along the South American coast (Deutsch et al., 2007). Although alternative explanations for these nutrient patterns have been proposed in models (Mills and Arrigo, 2010), direct mea-

surements have confirmed the occurrence of nitrogen fixation in and above the OMZ of the ETSP (Fernandez et al., 2011). Global biogeochemical models also generally predict substantial rates of N_2 fixation in the nitrate-deficit waters of the upwelling region of the ETSP that, if not compensated by some ad-hoc slow-down of remineralization in suboxic conditions, lead to a complete draw-down of nitrate in the OMZ (Moore and Doney, 2007; Schmittner et al., 2008). The question of how non-zero nitrate concentrations can be maintained in the OMZ thus still awaits a mechanistic answer.

The computational efficiency of box models makes them suitable for sensitivity ~~analysis~~ analyses requiring thousands of model evaluations. In spite of its simplicity, Canfield's (2006) box model is also able to capture the most important first-order interactions among ocean circulation, nitrogen fixation, denitrification, and OMZs. However, Canfield's model was limited in its power to investigate the influence of open ocean nutrients and oxygen conditions on the upwelling region, because its dynamics were restricted to the OMZ, where all biogeochemical tracers were prescribed in the surrounding waters. Based on Canfield's (2006) steady-state formulation with prescribed oxygen and nutrient concentrations at all depths outside the OMZ, we here present a fully prognostic box model of NO_3^-, PO_4^{3-} and O_2 cycles in a coastal upwelling region and an adjacent ocean basin. We employ this model to examine under which conditions the observed situation of an essentially complete drawdown of subsurface oxygen and an incomplete drawdown of nitrate can be reproduced for the case of the ETSP. Sensitivity experiments explore how nutrient exchange and oxygen ventilation from the southern boundary influence the nitrogen budget within the model domain.

By including a prognostic description not only of conditions within the OMZ, but also in the water surrounding it, we aim to represent local as well as spatially-separated feedbacks between the relatively small OMZ and the much larger open-ocean basin. The model describes net primary and export production by ordinary and N_2-fixing phytoplankton, as well as aerobic and anaerobic remineralization. The latter is generally associated with nitrogen loss, commonly attributed to denitrification (Codispoti, 1995). Anammox has recently been ~~suggested~~ reported as another major pathway for fixed-N removal (Kuypers et al., 2005; Hamersley et al., 2007; Molina and Farías, 2009), but the relative contributions of anammox and denitrification are still

a matter of debate (Ward et al., 2009; Bulow et al., 2010). In our model, we do not explicitly resolve the different inorganic nitrogen species and pragmatically consider all loss of fixed-N via anaerobic remineralization as denitrification. In Canfield's (2006) model, most of the physical model parameters were constrained by observations from suboxic upwelling zones in the Arabian Sea and the Eastern Tropical North and South Pacific. The physical dynamics of our model system is governed by vertical and horizontal mixing and advection, which are calibrated with $\Delta^{14}C$ data of the ETSP from GLODAP (Global Ocean Data Analysis Project, Key et al., 2004).

2 Model description

Figure 1 shows the model structure, consisting of five boxes representing an upwelling region and an adjacent ocean basin. The U box represents the upper upwelling region. The UM box is the underlying OMZ, where suboxia is expected to develop. The S box represents the surface ocean away from the upwelling zone. Below the S box sits the I box, which represents water of intermediate depth and exchanges water with UM. D is the deep box, which represents water deeper than 500 m. When the UM, I, or D boxes become suboxic, denitrification (Denif) will ensue to remineralize the exported organic matter, causing a loss of ~~fixed nitrogen (Denif~~nitrate (the only form of fixed inorganic nitrogen in our model) .

Prognostic tracers represent NO_3^-, PO_4^{3-}, O_2, ^{14}C and the biomass of ordinary and N_2-fixing phytoplankton, respectively (Table 1). The rate of concentration change of a tracer~~(~~, X_i~~)~~, in box i is composed of physical transport, Transport(X_i), and a sources-minus-sinks term, SMS(X_i), which represents the effects of biotic processes, air–sea gas exchange and, in the case of ^{14}C, radioactive decay on the tracer concentration (Eq. 1).

$$\frac{\mathrm{d}X_i}{\mathrm{d}t} = \frac{\mathrm{Transport}(X_i) + \mathrm{SMS}(X_i)}{V_i} \quad i \in [\mathrm{U, S, UM, I, D}] \tag{1}$$

where U, S, UM, I and D refer to the model boxes defined above and V_i to the corresponding volumes (Fig. 1).

2.1 Transport model

Advection represents the large-scale circulation and is indicated in Fig. 1 by wide grey lines. L_{U} and L_{S} are the horizontal scales of the upwelling region and the open ocean, and H_{U}, H_{UM} and H_{D} refer to the thickness of the respective boxes. The volumes V_i of the boxes are defined in this 2-D model by $V_i = H_i \cdot L_i$. K_{US}, K_{UM} and K_{H} are the coefficients of mixing between different boxes. A and B represent the deep and shallow large-scale circulation. The upwelling intensity into box U is given by $A + B$. The tracer transport equations for the standard configuration are given in Appendix A (Eqs. A1–A5). All parameters are defined in Tables 2 and 3.

2.2 Biogeochemical model

The ecological model is composed of two phytoplankton types, ordinary phytoplankton, Phy, and nitrogen fixers, NF. The SMS terms for phytoplankton are ~~then~~ obtained as the difference between net primary production (NPP) and mortality (~~M):~~ M):

$$\mathrm{SMS}(\mathrm{Phy}_i) = (\mathrm{NPP}^{\mathrm{Phy}_i} - M\mathrm{M}^{\mathrm{Phy}_i} \cdot \mathrm{Phy}_i) \cdot V_i \quad i \in [\mathrm{U}, \mathrm{S}] \tag{2}$$

$$\mathrm{SMS}(\mathrm{NF}_i) = (\mathrm{NPP}^{\mathrm{NF}_i} - M\mathrm{M}^{\mathrm{NF}_i} \cdot \mathrm{NF}_i) \cdot V_i \quad i \in [\mathrm{U}, \mathrm{S}] \tag{3}$$

~~Both types require phosphate, whereas nitrate is required in addition to phosphate only by Phy, and NF can fix as long as is available.~~

Growth of ordinary phytoplankton is described by a Liebig-type dependence on the nitrate and phosphate limitation terms (Eq. 4),

$$\mathrm{NPP}^{\mathrm{Phy}_i} = \mu \cdot \min\left(\frac{\mathrm{N}_i}{\mathrm{N}_i + \mathrm{N}_{\mathrm{h}}}, \frac{\mathrm{P}_i}{\mathrm{P}_i + \mathrm{P}_{\mathrm{h}}}\right) \cdot \mathrm{Phy}_i \quad i \in [\mathrm{U}, \mathrm{S}] \tag{4}$$

$$\mathrm{NPP}^{\mathrm{NF}_i} = \mu_{\mathrm{NF}} \cdot \frac{\mathrm{P}_i}{\mathrm{P}_i + \mathrm{P}_{\mathrm{h}}} \cdot \mathrm{NF}_i \quad i \in [\mathrm{U}, \mathrm{S}] \tag{5}$$

where i is the model box, μ and μ_{NF} are the maximum growth rates of Phy_i and NF_i respectively. N_i and P_i are nitrate and phosphate concentrations, and N_{h} and P_{h} are half-saturation concen-

trations for nitrate and phosphate. Considering possible viral lysis, phytoplankton aggregation, or a feedback between zooplankton grazing and phytoplankton concentration, a quadratic mortality term is adopted for both Phy and NF in all model configurations (Eq. 6).

$$\mathrm{M}^{\mathrm{Phy}_i} = M_\mathrm{q} \cdot \mathrm{Phy}_i^2 \qquad \mathrm{M}^{\mathrm{NF}_i} = M_\mathrm{q} \cdot \mathrm{NF}_i^2 \tag{6}$$

Both Phy and NF require phosphate, whereas nitrate is required in addition to phosphate only by Phy, and NF can fix $\mathrm{N_2}$ as long as $\mathrm{PO_4^{3-}}$ is available (Eq. 4, 5). While the ability to utilise organic P has been proposed as an advantage of diazotrophs (Houlton et al., 2008; Ye et al., 2012) , ordinary phytoplankton can also use DOP (e.g., Chu, 1946; Cotner, Jr. and Wetzel, 1992) and a clear advantage of diazotrophs over ordinary phytoplankton in the presence of DOP has never been demonstrated. Thus, we treat all available P to phytoplankton operationally as $\mathrm{PO_4^{3-}}$ and assume that all organic phosphate is remineralized to $\mathrm{PO_4^{3-}}$ directly. $\mathrm{N_2}$ fixers are given a lower maximum growth rate (μ_NF, Eq. 5), which is $1/3$ of the maximum growth rate of ordinary phytoplankton (μ), to account for the high cost of nitrogen fixation (La Roche and Breitbarth, 2005). The dependence of NF on iron is not explicitly considered in this model (Mills et al., 2004). Both ~~Phy and NF~~ types use nitrogen and phosphorus in the Redfield ratio of $16:1$ (Redfield et al., 1963). ~~Phytoplankton mortality can be linear or quadratic in Phy and NF depending on the model configuration.~~

Sensitivity experiments are also performed with a configuration where ~~fixationis inhibited by~~ , nitrogen fixers preferentially use nitrate when available and cover only the residual nitrogen demand via $\mathrm{N_2}$ fixation, denoted as facultative $\mathrm{N_2}$-fixation, but overall results are found to be virtually unchanged (Appendix ~~D).~~ B).

Dead phytoplankton is immediately remineralized in the surface layer and underlying boxes according to the respective remineralization fraction f_i of box i. Remineralization occurs preferentially via aerobic respiration, with anaerobic remineralization and the associated nitrogen loss setting in only when all $\mathrm{O_2}$ has been consumed by aerobic respiration. Phytoplankton growth and aerobic remineralization together with denitrification and, once all inorganic nitrogen is consumed, remineralization via sulfate reduction define the SMS terms of the nitrogen and

phosphorus cycles:

$$\mathrm{SMS}(\mathrm{N}_i) = -\mathrm{NPP}^{\mathrm{Phy}_i} \cdot V_i + \mathrm{Rem}_i^{\mathrm{N}} - \mathrm{Denif}_i \tag{7}$$

$$\mathrm{SMS}(\mathrm{P}_i) = -\frac{(\mathrm{NPP}^{\mathrm{Phy}_i} + \mathrm{NPP}^{\mathrm{NF}_i}) \cdot V_i}{r_{\mathrm{p}}} + \mathrm{Rem}_i^{\mathrm{P}} \tag{8}$$

where the remineralization (Rem) and denitrification (Denif) terms are defined in Appendix ~~B~~C.

O_2 is set constant in the surface ocean boxes U and S, which are in immediate contact with the atmosphere, but varies as a function of transport and respiration in the UM, I and D boxes. Thus, the aerobic respiration terms (Res_i) are only needed in the interior boxes UM, I and D:

$$\mathrm{SMS}(\mathrm{O}_{2i}) = -\mathrm{Res}_i \quad i \in [\mathrm{UM, I, D}] \tag{9}$$

where Res is defined in Appendix ~~B~~ C (Eq. C10). Note that aerobic respiration will, in general, also take place in anoxic model boxes, where it utilizes the O_2 transported from adjacent boxes, before anaerobic respiration starts. All model runs are initialized with O_2, NO_3^- and PO_4^{3-} annual data from the World Ocean Atlas 2009 (Garcia et al., 2010a,b), averaged over the regions indicated in Table 4.

2.3 Model calibration

In the present work, the prescribed transport among the different boxes in terms of advection and mixing was calibrated by fitting the modeled $\Delta^{14}C$ distribution to the GLODAP "pre-bomb" $\Delta^{14}C$ distribution of the Eastern Tropical South Pacific (Key et al., 2004; Table 4). The ^{13}C fractionation-corrected ratio of $^{14}C/^{12}C$, $\Delta^{14}C$, is commonly used in ocean modeling to evaluate and calibrate model physics (Toggweiler et al., 1989; Shaffer and Sarmiento, 1995), because it tends to cancel the effect of the biotic downward transport of ^{14}C with the rain of organic particles produced by marine organisms. ~~The distribution in our model is simulated with the help of a water-mass tracer,~~ For practical reasons, we employ the arbitrary scale introduced by Shaffer and Sarmiento (1995) to represent $\Delta^{14}C$, and define $\widehat{\Delta^{14}C}$~~, which is~~. $\widehat{\Delta^{14}C}$ can be

converted to $\Delta^{14}\mathrm{C}$ units as follows:

$$\Delta^{14}\mathrm{C} = 1000(\widehat{\Delta^{14}\mathrm{C}} - 1)\,‰ \tag{10}$$

The $^{14}\mathrm{C}$ dynamics in the model includes input from the atmosphere at the sea surface and radioactive decay with decay rate $\lambda = 1.21 \times 10^{-4}\,\mathrm{yr}^{-1}$ within the model domain. The SMS term for $\widehat{\Delta^{14}\mathrm{C}}$ is thus given by:

$$\mathrm{SMS}(\widehat{\Delta^{14}\mathrm{C}_i}) = (\frac{g_i(\widehat{\Delta^{14}\mathrm{C}_\mathrm{a}} - \widehat{\Delta^{14}\mathrm{C}_i})}{H_i} - \lambda\widehat{\Delta^{14}\mathrm{C}_i}) \cdot V_i \quad i \in [\mathrm{U, UM, S, I, D}] \tag{11}$$

where $\widehat{\Delta^{14}\mathrm{C}_i}$ is the value of $\widehat{\Delta^{14}\mathrm{C}}$ in box i, $\widehat{\Delta^{14}\mathrm{C}_\mathrm{a}}$ is the atmospheric $\widehat{\Delta^{14}\mathrm{C}}$, and g_i is the gas exchange rate~~$g_i = 0$ for~~. For $i \in [\mathrm{UM, I, D}]$, $g_i = 0$. We assume that the $\Delta^{14}\mathrm{C}$ of the preindustrial atmosphere, $\Delta^{14}\mathrm{C}_\mathrm{a}$, is $0\,‰$~~; therefore, the atmospheric $\widehat{\Delta^{14}\mathrm{C}_\mathrm{a}}$~~. Therefore, $\widehat{\Delta^{14}\mathrm{C}_\mathrm{a}}$ is 1. Model configurations with an open southern boundary also include $^{14}\mathrm{C}$ exchange with the adjacent subtropical ocean. We also investigate how sensitive our main conclusions are to the uncertainty in the $\Delta^{14}\mathrm{C}$ data. Table 4 shows the $\Delta^{14}\mathrm{C}$ values used for the calibrations of the different model configurations. Transport and SMS terms for $\widehat{^{14}\mathrm{C}}$ constitute a system of 5 linear equations ~~in~~ with 7 parameters, including ~~the transport parameters~~5 transport parameters, A, B, K_{US}, K_{UM}, K_{H}~~and the~~ , and 2 air–sea $\widehat{^{14}\mathrm{C}}$ exchange coefficients~~for~~ , g_{U} and g_{S}. After setting g_{U} and g_{S}, the 5 equations can be inverted to solve for the transport parameters. A detailed description of the inversion scheme is provided in Appendix ~~C~~D.

2.4 Model configurations

Above transport and biogeochemical formulations define the standard (STD) configuration, where ~~phytoplankton mortality is formulated by a linear term with constant coefficient ($M^{\mathrm{Phy}_i} = M^{\mathrm{NF}_i} = M$). In the STD configuration, the above~~ the transport and biogeochemical models are applied without exchange with the southern boundary ~~.~~ (“SO” in Fig. 1). Fixed fractions f_i of net primary production in U and S are remineralized in the U, UM, S and I boxes,

with the remainder being remineralized in D (Fig. 1). Nutrient regeneration is assumed to be instantaneous.

In order to investigate the relationships between the different biotic and physical processes and the nitrogen cycle in an OMZ, we introduce ~~eight~~ seven additional model configurations~~(Table 5): (~~. The main differences to the STD configuration are shown in Table 5. (1~~) In the QM configuration , a quadratic form is adopted for the mortality of both ordinary phytoplankton and nitrogen fixers:~~

$$M^{\mathrm{Phy}_i} = M_{\mathrm{q}}\mathrm{Phy}_i \qquad M^{\mathrm{NF}_i} = M_{\mathrm{q}}\mathrm{NF}_i$$

~~Possible mechanisms represented by a quadratic mortality term are viral lysis, phytoplankton aggregation, or a feedback between zooplankton grazing and phytoplankton concentration. (2~~) In the Reduced-denitrification (RD) configuration, denitrification in the OMZ is reduced to $1/5$ of the rate of the STD configuration following the procedure applied in the global biogeochemical circulation model by Schmittner et al. (2008). When oxygen is exhausted in the OMZ, denitrification within the UM box will ~~then~~ be responsible for only $1/5$ of the remaining organic matter remineralization and the remainder will be remineralized in the D box (Eqs. C7 and C8). (~~3~~2) The Ventilation-D (VD) configuration modifies the ~~QM~~ STD configuration in that the southern boundary of the model domain is partially opened to allow ventilation of O_2 and ^{14}C (but not NO_3^- and PO_4^{3-}) to the D box from the southern subtropical ocean (Eq. A7). The circulation parameters were recalibrated to account for ventilation of ^{14}C from the south. Ventilation is simulated by applying lateral mixing with the subtropical oligotrophic ocean tracer ~~reservoir~~ reservoirs with prescribed ^{14}C and O_2 concentrations inferred from observations. All other biogeochemical processes within the model domain are kept the same as in the ~~QM~~ STD configuration. (~~4~~3) In the Ventilation-D + Reduced-denitrification (VDRD) configuration, the reduced denitrification rate is applied in the VD configuration. (~~5~~4) In the Ventilation-ID (VID) configuration, the partially open southern boundary is extended to allow ventilation of O_2 and ^{14}C also into the I box from the subtropical ocean (Eq. A6). Again, circulation parameters are recalibrated against observed $\Delta^{14}C$ taking into account the ^{14}C exchange between the subtropical ocean and the I and D boxes. (~~6~~5) In the Ventilation-ID + Reduced-denitrification

(VIDRD) configuration, the reduced denitrification rate is also applied in the VID configuration. (~~7~~6) In the Open-boundary (OB) configuration, nutrient mixing is added to the VID configuration to allow for exchange of nutrients between the I and D boxes and the subtropical ocean. (~~8~~7) In the Open-boundary + Reduced-denitrification (OBRD) configuration, the reduced-denitrification rate is again added to the OB configuration. The physical transports of NO_3^- and PO_4^{3-} for the I and D boxes in the last six configurations are represented by Eqs. (A6) and (A7) in Appendix A.

2.5 Sensitivity experiments

Two sensitivity experiments are performed for each of the VID and OB configurations to explore possibilities for preventing NO_3^- depletion in the OMZ: (a) different reduced remineralisation rates (f_{UM}) and (b) facultative N_2-fixation (see Appendix E).

For the OBRD configuration, three sensitivity experiments are performed ~~in which the mixing rates~~ to investigate our model sensitivity to variable physical transports and biogeochemical tracer concentrations: (1) The mixing rate with the southern boundary, K_H, is reduced for individual tracers (nutrients, oxygen) or combinations thereof from full rates to zero. ~~To~~ (2) Simulations are repeated with individual circulation parameters varied by ± 50 % to explore the sensitivity with respect to the circulation parameters of the box model~~, simulations of the OBRD configuration were repeated with individual circulation parameters varied by ± 10, $\pm 20$and ± 50, respectively.~~. (3) The sensitivity of NO_3^- and O_2 concentrations in the OMZ to different physical parameters derived from variations of the $\Delta^{14}C$ data and O_2 concentrations in the U-box is also examined.

The literature ranges in Table 3 provide only a rough guide for the biogeochemical parameters. The sensitivity of r_p, μ, μ_{NF}, N_h and P_h is tested in the OBRD configuration by changing each of them according to the literature range. Effects of changing the remineralisation fractions f_U, f_{UM}, f_S, and f_I are examined by redistributing remineralisation between the U and UM, and S and I boxes. These sensitivity experiments will be discussed in Section 3.3 below.

3 Results

The physical circulation parameters calibrated with $\Delta^{14}C$ are given in Table 2. The resulting circulation is comparable with our expectations for the upwelling region of the Eastern Tropical South Pacific. The parameters of the biogeochemical model are shown in Table 3.

3.1 Biogeochemical tracer concentrations

Nutrient and oxygen concentrations in the upwelling region (boxes U and UM) are influenced by physical exchange with regions outside the upwelling zone (boxes I and D) and subsequent remineralization of exported organic matter. The results for biogeochemical tracer concentrations of the STD, RD, VIDRD and OBRD configurations are shown in Fig. 2 and will be used to develop our main conclusions, whereas those of the VD, VDRD, VID and OB configurations are also included in Fig. 3 and described in Appendix E.

In the STD configuration, NO_3^- levels in the UM box are quickly exhausted by denitrification in the UM box (black bars in Fig. 2), where decomposition of exported organic matter consumes all O_2 entering the UM box via advection and diffusion, and all NO_3^- entering via physical transport and remineralization of exported organic matter. In the STD configuration, O_2 is also depleted in the D box, owing to weak ventilation. This results in over 90 % of the initial nitrate being lost from the model domain by denitrification once the model has reached steady state. The large nitrate deficit with respect to phosphate in the upwelling waters results in nitrogen fixers becoming dominant in the U box despite having a lower maximum growth rate than ordinary phytoplankton . Ordinary phytoplankton and nitrogen fixers become almost extinct in the S box because of severe nutrient limitation.

In the QM configuration, ordinary phytoplankton and nitrogen fixers persist in box S (grey (black bars in Fig. 2). The quadratic mortality reduces mortality at low phytoplankton concentrations and thereby prevents extinction of ordinary phytoplankton in the open ocean. Still, the main problems remain, i.e., nitrate vanishes in the UM box, the D box becomes anoxic, and more than 90of the initial is lost. a, c).

In the RD configuration, complete NO_3^- exhaustion in the UM box is prevented (~~bars with horizontal lines~~ grey bars in Fig. 2). There is some observational evidence for the efficiency of decomposition of organic matter driven by denitrification in some high-productivity areas being lower than for respiratory processes in the presence of sufficient dissolved oxygen ~~(Liu and Kaplan, 1984; Van Mooy et al., 2002)~~ (Liu and Kaplan, 1984; Devol and Hartnett, 2001; Van Mooy et al., 2002). In our model, this mechanism helps preventing NO_3^- depletion in the OMZ because less nitrate is consumed by denitrification during the passage of the particles through the OMZ. However, the NO_3^- concentration in the UM box is only 3.25 $\mu mol\,kg^{-1}$, far less than the literature range from about 15 to 40 $\mu mol\,L^{-1}$. The additional organic matter now passing through the OMZ must be remineralized in the D box, which still becomes anoxic in this configuration.

~~The VD configuration, which supplies additional from the subtropical ocean into the D box, avoids anoxic deep waters, but fails to prevent nitrate exhaustion in the UM box (Fig. 3). The I and D boxes are oxic at steady state, but~~ Even though the RD configuration fails to simulate the realistic biogeochemical tracer concentrations in the OMZ and its adjacent ocean, it reveals a possible mechanism for preventing NO_3^- ~~is still exhausted by denitrification in the UM box. Comparing the oxygen concentrations of the RD configuration and VD configuration, we conclude that ventilation helps to prevent oxygen~~ depletion in the ~~D box, but this mechanism alone cannot prevent eventual run-away denitrification in the UM box. After incorporating reduced denitrification rate in the VDRD configuration, nitrate depletion is prevented and the I and D boxes are oxic (bars with vertical lines in~~ OMZ.

While a reduced remineralisation rate under suboxic conditions appears to be a prerequisite for maintaining non-zero nitrate in the OMZ (Fig. ~~2). But the concentration in the I box is about 28lower than that of~~ 3), we find that ventilation of O_2 from the lateral subtropical ocean into the model domain is essential for preventing anoxic condition in the ~~WOA2009 data, which indicates that supply into the D box only may not be enough to ventilate the model domain .~~

~~The VID configuration, in which ventilation into the I box is also incorporated in addition to the~~ D box~~, fails in preventing~~. But even ventilation of O_2 into both I and D boxes fails to prevent NO_3^- ~~depletion by denitrification in the OMZ (Fig. 3). Several sensitivity~~

experiments were performed to explore how depletion in the UM box can be prevented in the VID configuration . Decreasing the fraction for export production remineralized in the UM box (f_{UM}) from 70to 56makes persist in the UM box.Together with the 20remineralization in the U box, this implies that 76of the export production is remineralized in the upper 500of the ocean. However, the concentration in the UM box is only 3.8, far away from the literature range from about 15 to 40. Next, a model of nitrogen fixation with an inverse relationship between concentration and the fraction of fixed nitrogen from nitrogen fixation (Holl and Montoya, 2005; Mills and Arrigo, 2010) was implemented. This approach inhibits nitrogen fixation in an environment with high concentrations, but fails to prevent depletion in the UM box.

(Fig. 3i). After reducing the denitrification rate in the OMZ, which is the configuration denoted as VIDRD, NO_3^- depletion is prevented (bars with oblique horizontal lines in Fig. 2). Compared with the VDRD configuration, concentrations in the I box increase by about 21, to the RD configuration, NO_3^- concentration in the UM box is in a realistic range (15-40 $\mu mol\,kg^{-1}$) for the OMZ, and O_2 concentrations in the I and D boxes are also closer to the WOA2009 data, however, concentration in the D box decreases due to a higher upwelling rate $A + B$ and slightly lower ventilation rate K_H (Table 2but still about 15.0% and 22.7% lower than the observations (blue dashed lines in Fig. 2).

In the OB In the OBRD configuration, nutrients are exchanged in addition to O_2 between the subtropical ocean and the I and D boxes. In this configuration, nitrate exhaustion in the OMZ is still not prevented even though there are lower phytoplankton and nitrogen fixer concentrations in the surface U and S boxes (Fig. 3). Again, after , together with reducing the denitrification rate under suboxic conditionsin the OBRD configuration, , N_{UM} depletion is prevented and N_{UM} approaches a concentration of 20 $\mu mol\,kg^{-1}$ at steady state (bars with dots horizontal lines in Fig. 2). The UM box is suboxic and the O_2 concentrations in the I and D boxes agree very well with the WOA2009 data (gridded bars blue dashed lines in Fig. 2). Overall, tracer distributions simulated by the OBRD configuration agree best with the observationscompared with other configurations. . In the sensitivity configuration OB, where only nutrients are exchanged in

addition to O_2 between the subtropical ocean and the I and D boxes, nitrate is still exhausted in the OMZ (Fig. 3m).

3.2 Biogeochemical fluxes

For the biogeochemical fluxes, we ~~will~~ focus on the ~~model configurations in Fig. 4~~STD, RD, VIDRD and OBRD configurations (configurations in bold in Table 5), since they ~~represent the most important mechanisms in preventing exhaustion~~ show most clearly the mechanisms responsible for preventing NO_3^- depletion in the OMZ ~~. The STD and QM configurations display very similar biogeochemical fluxes because the physical parameters in the two configurations are the same (black and grey bars in~~ (Fig. 4~~respectively). However, denitrification rates are~~). Denitrification rates are much higher in the STD ~~and QM configurations~~ than in the RD configuration (~~bars with horizontal lines~~ black and grey bars in Fig. 4 respectively), even though the physical parameters are the same in ~~all three~~ the two configurations, leading to nitrate exhaustion in the UM box of the STD ~~and QM configurations~~ but not in the RD configuration. In ~~the VDRD configuration,~~ both VIDRD and OBRD configurations, NO_3^- depletion is prevented (bars with horizontal and vertical lines in ~~panel E of~~ Fig. 2~~). Compared with the VDRD configuration, the VIDRD configuration has a slightly higher denitrification rate and aerobic respiration rate in the OMZ because the altered transport parameters allow for a somewhat higher export production into the OMZ.~~ e). Denitrification is weaker in the OBRD ~~configuration~~ than in the VIDRD configuration (bars with ~~oblique~~ horizontal lines in Fig. 4), even though the physical parameters are the same in both~~configurations~~, keeping more NO_3^- in the UM-box in the OBRD configuration~~(bars with dots in Fig. 4).~~ . Aerobic respiration in the UM box continues even when the UM box is anoxic. It consumes all O_2 entering the UM box via the various physical transport processes and thereby oxidizes ~~respectively about 9.9,~~ about 8.7 %, 64 %, ~~87,~~ 85 % and 92 % of the organic matter remineralized (denitrification+ aerobic respiration) in the UM box in all ~~six configurations~~four configurations, STD, RD, VIDRD and OBRD, respectively. Aerobic respiration is increased in the OBRD configuration compared with the VIDRD configuration (92 % vs. 85 %) at the expense of denitrification.

Compared with the VIDRD configuration, total PO_4^{3-} in the model domain decreases by about 28 % in the OBRD configuration at steady state, and the net PO_4^{3-} flux out of the I box and the corresponding net flux of PO_4^{3-} from the subtropical ocean into the D box causes a 9.6 % decrease in organic matter exported into the UM box. This explains why NO_3^- concentrations in the OMZ and O_2 concentrations in the I and D boxes are slightly higher (bars with ~~oblique lines and bars with dots~~ vertical lines in Fig. 2). Restricting, in a hypothetical sensitivity experiment, exchange with the subtropical oligotrophic ocean to NO_3^- and O_2 ~~cannot~~ does not result in higher O_2 concentrations in the I and D boxes, because ~~it does not reduce the export production to be decomposed there. Restricting~~PO_4^{3-} is conserved and export production dose not change substantially. Restricting, on the other hand, exchange to PO_4^{3-} and O_2 depresses production and organic matter decomposition by almost the same amount as in the model run that exchanges NO_3^-, PO_4^{3-} and O_2, and succeeds in driving O_{2I} and O_{2D} concentrations closer to the observations (not shown). Thus, opening the model boundary to PO_4^{3-} and O_2 helps to improve the ~~behaviour of VIDRD configuration by depressing biological production in the upwelling region.~~ model results with respect to those of the VIDRD configuration that does not exchange PO_4^{3-} across the southern boundary.

~~The fluxes associated with the fixed-N cycle in the OMZ of the OB configuration are compared with those of other models in Table 6. Our simulated export production and aerobic remineralization are mostly consistent with the results of Kalvelage et al. (2013) , but our simulated anaerobic remineralization and fixed-N loss in the OMZ are much lower. However, our model's fixed-N loss due to denitrification is between the values reported by Mills and Arrigo (2010) and Kalvelage et al. (2013) . The Kalvelage et al. (2013) model has much higher fixed-N influx into the OMZ via physical transport, which could compensate for their more intense loss in the OMZ.~~

3.3 Model sensitivity

In sensitivity experiments of the OBRD configurations, designed to elucidate the importance of the influence of the subtropical ocean on the model domain, we reduce the mixing rates (K_H) of O_2, NO_3^- and PO_4^{3-} across the southern boundary in different combinations (two of them

are shown in Fig. 5). Total net primary production (NPP) is the same when varying the mixing rate of either only O_2 or O_2 together with NO_3^-, as long as the PO_4^{3-} exchange rate with the subtropical ocean remains unchanged (dotted lines in Fig. 5b~~and g~~). The reason is that changes in nitrate exchange with the subtropical ocean are compensated by changes in denitrification and nitrogen fixation. This implies that NPP is, at steady state, determined only by phosphate availability. Once the total NPP of NF and Phy is determined by PO_4^{3-} supply, aerobic respiration will increase with increasing O_2 supply, while anaerobic remineralization will decrease (solid and dashed lines in Fig. 5c~~and h~~). Comparing simulations that vary the mixing rate of O_2 together with that of PO_4^{3-}, with simulations that vary the mixing rate of O_2 together with that of NO_3^- and PO_4^{3-} (dotted lines in Fig. 5~~l and q~~g) reveals that the combined NPP of Phy and NF decreases with decreasing PO_4^{3-} inventory at low mixing rates and increases with increasing PO_4^{3-} inventory at ~~hight~~ high mixing rates, irrespective of NO_3^- mixing rate.

It turns out that NO_3^- depletion in the OMZ is prevented in the four sensitivity experiments of Fig. 5 no matter how much O_2 is supplied from the subtropical ocean into the model domain. But anoxia in the D box can only be prevented if the external O_2 supply can oxidise more than about 20 % export production in the model domain (solid lines in Fig. 5e, j~~, o and t~~). This ratio can vary according to the size of S box. It increases for a smaller S box, because a smaller S box leads to less downward O_2 supply from the surface box into the lower model domain and more lateral ventilation is needed, and vice versa (not shown). These experiments also reveal an interesting link among the O_2 supply from the subtropical ocean, the nitrate concentration in the OMZ, and the NO_3^- flux between the model domain and surrounding ocean. As soon as the O_2 supply from the subtropical ocean accounts for about 17.5 % of the respiratory O_2 consumption, the model domain turns into a small net source of ~~fixed N~~ NO_3^- (dashed lines in the first row of Fig. 5). Once anoxia is prevented in the D box, the nitrate concentration in the OMZ (UM box) increases quite strongly from about 15 $\mu mol\,kg^{-1}$ to reach about 20 $\mu mol\,kg^{-1}$ at full mixing strength.

The ~~behaviour of~~ conclusion that the model domain ~~as~~ is a small pelagic net NO_3^- source in the OBRD configuration ~~is rather insensitive to the~~ does not change when individual physical transport parameters vary by up to $\pm$50% (Fig. 6). ~~The model domain remains a net source~~

even when the physical transport parameters are varied by up to ±50Varying biogeochemical parameters also does not affect this conclusion. The finding that the model domain is a net NO_3^- source is also tenable for all suites of physical transport parameters in the literature range for which the D-box is oxic (Fig. 7).

The oxygen concentrations in the UM, I and D boxes increase in sensitivity model runs with physical parameters calibrated from increased ^{14}C concentrations (lower water mass age, figure not shown). NO_3^- depletion is prevented in the OMZ in the OBRD configuration within the range of about ±10 % around the default ventilation intensity (Fig. 8a). The UM box remains anoxic when $\Delta^{14}C$ is varied within this range, which indicates that this mechanism for preventing NO_3^- depletion in the OMZ may be robust against modest changes in the regional ocean circulation patterns. Meanwhile, NO_3^- and O_2 in the UM box are quite insensitive to the O_2 concentration in the U-box for this configuration (Fig. 8b).

Varying biogeochemical parameters affects individual model predictions but not our main conclusions. The strongest effects are those of varying the N:P ratio r_p and the remineralisation fractions (f_U, f_{UM}, f_S, and f_I) (Fig. 6). Lowering r_p to 12 increases N_{UM} by about 35 %, but cannot change the strength of our model domain as a net NO_3^- source. Increasing r_p to 20 decreases N_{UM} by about 18 %, but triples the strength of our model domain as a NO_3^- source. However, observations indicate that r_p for the ETSP is more likely to be higher than lower compared to the Redfield N:P ratio of 16 (Franz et al., 2012) . Increasing the maximum growth rate of NF, μ_{NF}, to 1/2μ, the maximum growth rate of Phy, results in higher N_{UM} concentrations and our model domain being a larger NO_3^- source. Intuitively, decreasing μ_{NF} to 1/4μ results in lower N_{UM} concentrations and our model domain becoming a smaller NO_3^- source. Varying the NO_3^- half saturation constant, N_h, results in virtually unchanged results. N_{UM} increases when changing remineralisation fractions in the intermediate boxes (f_{UM} and f_I) from 70 % to 50 % and 30 % respectively, effectively lowering export production via lowering the export ratio. Nevertheless the qualitative behaviour of the model remains the same in these sensitivity experiments.

4 Discussion and conclusions

Nitrogen is often considered to be the primary limiting nutrient in marine upwelling regions with OMZs (Cline and Richards, 1972; Codispoti and Christensen, 1985; Morrison et al., 1998; Voss et al., 2001), where denitrification rates can be high and are generally thought to cause a major loss of ~~fixed N~~ NO_3^- from the world ocean. The nitrogen deficit is commonly assumed to stimulate N_2 fixation, both in observational estimates of N_2 fixation (Deutsch et al., 2007; Monteiro et al., 2010) and in current descriptions of N_2 fixation in biogeochemical models (Moore and Doney, 2007; Schmittner et al., 2008). However, if N_2 fixation is tightly linked to nitrogen loss processes, denitrification of organic matter derived from N_2 fixation can consume more nitrogen than was fixed via N_2 fixation and thereby lead to a vicious cycle of run-away nitrogen loss (Landolfi et al., 2013). This has been found to lead to total depletion of NO_3^- in the OMZ of box models (Canfield, 2006) and global biogeochemical circulation models (Moore and Doney, 2007; Schmittner et al., 2008). For our fully prognostic 5-box model, we have identified the mechanisms capable of arresting the run-away nitrogen loss that can result from a close coupling of nitrogen fixation and denitrification (Landolfi et al., 2013) and maintaining realistic non-zero NO_3^- concentrations in open-ocean OMZs of the ETSP: reduced NO_3^- consumption by denitrification owing to slower remineralization under suboxic compared to oxic conditions, coupled with lateral ventilation ~~between the model domain and an ocean basin outside of the model domain (the subtropical ocean in this case)~~of oxygen and, to some extent, nutrients with the subtropics.

In this work, the model configuration with reduced denitrification rate and lateral ventilation and nutrient exchange (OBRD configuration) ~~behaves most reasonable~~performs best with respect to the observations, whereas reduced rates of denitrification alone ~~leads~~ lead to unrealistic O_2 depletion in the deep waters, and reduced rates of denitrification combined with only O_2 ventilation in the D or both I and D boxes ~~configurations do worse in fitting~~ still underestimate the WOA2009 data for O_2 in the I and D boxes. By allowing for exchange of O_2 and nutrients with the subtropical ocean in the OBRD configuration, the delicate balance between sufficient O_2 supply required for maintaining high levels of aerobic respiration and sufficient PO_4^{3-} loss

through the open boundary appears fulfilled. Compared with other box models (Shaffer and Sarmiento, 1995; Tyrrell, 1999; Deutsch et al., 2004; Canfield, 2006; Mills and Arrigo, 2010; Eugster and Gruber, 2012; DeVries et al., 2012), the box model we use here explicitly employs both a reduced-denitrification rate and an open boundary condition, which seems to be a prerequisite for the ability to simulate realistic nitrate conditions in the OMZ and oxygen concentrations in the adjacent ocean.

The NO_3^- loss by denitrification in the OMZ of the OBRD configuration is compared with that of other model-based and observational estimates in Table 6. Our simulated denitrification is consistent with the results of Somes et al. (2010) and DeVries et al. (2013) for the ETSP, lower than the estimate of Bianchi et al. (2012) and Kalvelage et al. (2013) , but higher than that of Mills and Arrigo (2010) . However, the estimated denitrification by Bianchi et al. (2012) represents that of the entire South Pacific but not only the ETSP. The Kalvelage et al. (2013) model has much higher fixed-N influx into the OMZ via physical transport than our model, which could compensate for their more intense NO_3^- loss by denitrification.

Phosphate turns out as the ultimate limiting nutrient in our model (~~second and forth rows of~~ Fig. 5), and hence determines the nitrogen content of the OMZ. This strong control of ~~phosphate on~~ the N cycle by phosphate is similar to the finding of previous ~~studies~~ models (e.g. Lenton and Watson, 2000; Canfield, 2006), where the occurrence and extent of oceanic anoxia was also tightly linked to phosphate supply. These studies explicitly assumed that N_2 fixation acts to restore surface-oceanic dissolved inorganic N : P ratio towards the Redfield ratio. By contrast, we do not prescribe the effect of nitrogen fixation on surface inorganic nutrients, and the finding of phosphate as the ultimate limiting nutrient is obtained regardless of whether NF responds directly to the N : P ratio in the surface ocean or whether NF is inhibited by the presence of NO_3^- (see Appendix ~~D~~B).

Even though our model indicates only a weak dependence of simulated NO_3^- concentrations in the OMZ on the lateral O_2 supply from the subtropical ocean, O_2 depletion in the adjacent ocean can be prevented only when the O_2 supply from the subtropical ocean accounts for more than 20 % of the O_2 required to oxidize export production from the surface ocean of our model

domain (U and S boxes). This value only varies ~~from~~ between about 17 % ~~to~~ and 23 %, when the size of the S box varies by ±50 %, indicating that our above conclusion is rather insensitive to our choice for the model domain. The O_2 supply from the subtropical ocean might be also linked to the balance of the regional fixed-N cycle. In the most realistic (OBRD) configuration, the balance of water-column denitrification and nitrogen fixation is tightly linked to the nitrate concentration in the OMZ: if the model domain acts as a sink for ~~fixed-N~~NO_3^-, nitrate concentrations in the OMZ do not exceed about 15 $\mu mol\,kg^{-1}$, i.e., the lower limit of current observations, 15 to 40 $\mu mol\,kg^{-1}$ (Codispoti and Richards, 1976; Codispoti and Packard, 1980; Morrison et al., 1998; Voss et al., 2001). Nitrate concentrations close to those commonly found in OMZs are predicted only when nitrogen fixation exceeds water-column denitrification and the ocean basin containing the OMZ becomes a net source of ~~fixed-N (first row of~~ NO_3^- (Fig. 5a, f).

There are no specific data or model results focusing on the water-column nitrogen balance of the ETSP. Our simulations using a parameterisation where nitrogen fixation is inhibited by the presence of nitrate yield very similar results, only with slightly reduced nitrogen fixation resulting in a somewhat reduced (by ≤ 15 %) nitrogen source for strong enough lateral oxygen supply. Ganachaud and Wunsch (2002) estimated a net northward NO_3 transport of $270 \pm 170\,kmol\,s^{-1}$ ($119.2 \pm 75.1\,Tg\,N\,yr^{-1}$) across 17° S into the ETSP ~~indicating~~ in a geostrophic inverse box model, which indicates that the ETSP is a net nitrogen sink, but their estimate included benthic denitrification, which is not accounted for in our current analysis. In a model-guided analysis, DeVries et al. (2012) predicted water-column denitrification rates of 21–33 $Tg\,N\,yr^{-1}$ by simulating the distribution of observed dissolved N_2 gas produced by denitrifying bacteria. From an ocean circulation-biogeochemical model-based analysis of nutrient concentrations and transport rates, Deutsch et al. (2007) estimated nitrogen fixation rates in the Pacific Ocean of about 95 $Tg\,N\,yr^{-1}$, half of which was speculated to occur in the ETSP. From these estimates, we cannot rule out that the water column of the ETSP is a net source of ~~fixed-N~~NO_3^-, which would be consistent with our results obtained in the OBRD configuration. More recently, Eugster and Gruber (2012) probabilistically estimated nitrogen fixation and water-column and benthic denitrification separately ~~, and we find~~ in their box model, which appears to be consistent with our

results as their results also indicate that the water column of the IndoPacific is a large fixed-N source~~when we estimated the fixed-N budget for that regions, which appears to be consistent with our results~~.

Based on our model results, we conclude that reduced NO_3^- consumption by denitrification owing to slower remineralization under suboxic conditions together with lateral transport is essential to arrest the vicious cycle of run-away fixed-N loss in the OMZ. More research is needed to better constrain the model parameters, in particular the upwelling transport and the difference between the organic matter remineralisation rate via aerobic respiration and anaerobic denitrification.

Appendix A

Physical transports of a tracer X among the boxes U, UM, S, I, and D are defined for the STD configuration as follows:

$$\text{Transport}(X_\text{U}) = (X_\text{UM} - X_\text{U})(A + B + K_\text{US}) \cdot L_\text{U} \tag{A1}$$

$$\begin{aligned}\text{Transport}(X_\text{UM}) = {} & [AX_\text{D} + BX_\text{I} - X_\text{UM}(A + B) + K_\text{US}(X_\text{U} - X_\text{UM})] \cdot L_\text{U} \\ & + K_\text{UM}(X_\text{D} - X_\text{UM}) \cdot L_\text{U} + K_\text{H}(X_\text{I} - X_\text{UM}) \cdot H_\text{UM}\end{aligned} \tag{A2}$$

$$\text{Transport}(X_\text{S}) = (A + B)(X_\text{U} - X_\text{S}) \cdot L_\text{U} + K_\text{US}(X_\text{I} - X_\text{S}) \cdot L_\text{S} \tag{A3}$$

$$\begin{aligned}\text{Transport}(X_\text{I}) = {} & (A + B)(X_\text{S} - X_\text{I}) \cdot L_\text{U} + K_\text{H}(X_\text{UM} - X_\text{I}) \cdot H_\text{UM} \\ & + K_\text{US}(X_\text{S} - X_\text{I}) \cdot L_\text{S} + K_\text{UM}(X_\text{D} - X_\text{I}) \cdot L_\text{S}\end{aligned} \tag{A4}$$

$$\text{Transport}(X_\text{D}) = A\ (X_\text{I} - X_\text{D}) \cdot L_\text{U} + K_\text{UM}(X_\text{UM} - X_\text{D}) \cdot L_\text{U} + K_\text{UM}(X_\text{I} - X_\text{D}) \cdot L_\text{S} \tag{A5}$$

For the VD, VDRD, VID, VIDRD, OB and OBRD configurations, Eqs. (A4) and (A5) are modified to read:

$$\text{Transport}(X_\text{I}) = (A + B)(X_\text{S} - X_\text{I}) \cdot L_\text{U} + K_\text{H}(X_\text{UM} - X_\text{I}) \cdot H_\text{UM}$$

$$+ K_{\mathrm{US}}(X_{\mathrm{S}} - X_{\mathrm{I}}) \cdot L_{\mathrm{S}} + K_{\mathrm{UM}}(X_{\mathrm{D}} - X_{\mathrm{I}}) \cdot L_{\mathrm{S}}$$
$$+ K_{\mathrm{H}}(X_{\mathrm{SI}} - X_{\mathrm{I}}) \cdot H_{\mathrm{UM}} \tag{A6}$$

$$\mathrm{Transport}(X_{\mathrm{D}}) = A\,(X_{\mathrm{I}} - X_{\mathrm{D}}) \cdot L_{\mathrm{U}} + K_{\mathrm{UM}}(X_{\mathrm{UM}} - X_{\mathrm{D}}) \cdot L_{\mathrm{U}} + K_{\mathrm{UM}}(X_{\mathrm{I}} - X_{\mathrm{D}}) \cdot L_{\mathrm{S}}$$
$$+ K_{\mathrm{H}}(X_{\mathrm{SD}} - X_{\mathrm{D}}) \cdot H_{\mathrm{D}} \tag{A7}$$

The transport equations (Eqs. A1 and A3) are modified for Phy and NF because Phy and NF are assumed to be capable of regulating their buoyancy and exist only in U and S without being transported vertically between the U and UM or the S and I boxes.

Appendix B

It is well known from laboratory studies that diazotrophic phytoplankton can also utilize nitrate for growth, denoted as facultative N_2-fixation (e.g., Holl and Montoya, 2005) . Schmittner et al. (2008) introduced a formulation where nitrogen fixers preferentially use nitrate when available and cover only the residual nitrogen demand via N_2 fixation. In order to examine the behavior of our model when nitrogen fixers (NF) preferentially use nitrate, nitrogen fixation is separated from diazotroph growth, as in Schmittner et al. (2008) :

$$\mathrm{Nitrogen\text{-}fixation}_i = \left(1 - \frac{\mathrm{N}}{\mathrm{N} + \mathrm{N_h}}\right) \cdot \mathrm{NPP}^{\mathrm{NF}_i} \qquad i \in [\mathrm{U,\ S}] \tag{B1}$$

and Eq. (7) was modified to accomodate the additional nitrate uptake by NF as follows:

$$\mathrm{SMS}(\mathrm{N}_i) = \left(-\mathrm{NPP}^{\mathrm{Phy}_i} - \left(\mathrm{NPP}^{\mathrm{NF}_i} - \mathrm{Nitrogen\text{-}fixation}_i\right)\right) \cdot V_i + \mathrm{Rem}_i^{\mathrm{N}} - \mathrm{Denif}_i$$
$$i \in [\mathrm{U,\ UM,\ S,\ I,\ D}] \tag{B2}$$

After incorporating Eqs. B1 and B2 in our all configurations described in Section 2.2, they behave very similarly compared to Fig. 2, except that $\mathrm{Phy_U}$ and $\mathrm{Phy_S}$ concentrations are somewhat lower because nitrogen fixers take up $\mathrm{NO_3^-}$ as well. Thus, we conclude that our results are robust with respect to assumptions about facultative $\mathrm{N_2}$-fixation by diazotrophs.

Appendix C

The nitrogen cycle in this model includes nitrogen fixation, denitrification, inorganic nitrogen regeneration by remineralization, ~~and~~ physical transport of ~~nitrogen~~$\mathrm{NO_3^-}$, and transport of Phy and NF between the U and S boxes. The physical transport process of $\mathrm{NO_3^-}$ is the same as for other tracers. $\mathrm{Rem}_i^{\mathrm{N}}$ represents nitrogen remineralization in box i with fixed fractions f_i of the net primary production in the overlaying surface boxes.

$$\mathrm{Rem}_{\mathrm{U}}^{\mathrm{N}} = f_{\mathrm{U}} M(\mathrm{Phy_U} + \mathrm{NF_U}) \cdot H_{\mathrm{U}} \cdot L_{\mathrm{U}} \tag{C1}$$

$$\mathrm{Rem}_{\mathrm{UM}}^{\mathrm{N}} = f_{\mathrm{UM}} M(\mathrm{Phy_U} + \mathrm{NF_U}) \cdot H_{\mathrm{U}} \cdot L_{\mathrm{U}} \tag{C2}$$

$$\mathrm{Rem}_{\mathrm{S}}^{\mathrm{N}} = f_{\mathrm{S}} M(\mathrm{Phy_S} + \mathrm{NF_S}) \cdot H_{\mathrm{U}} \cdot L_{\mathrm{S}} \tag{C3}$$

$$\mathrm{Rem}_{\mathrm{I}}^{\mathrm{N}} = f_{\mathrm{I}} M(\mathrm{Phy_S} + \mathrm{NF_S}) \cdot H_{\mathrm{U}} \cdot L_{\mathrm{S}} \tag{C4}$$

$$\begin{aligned}\mathrm{Rem}_{\mathrm{D}}^{\mathrm{N}} = M\big[&(1 - f_{\mathrm{U}} - f_{\mathrm{UM}})(\mathrm{Phy_U} + \mathrm{NF_U}) \cdot L_{\mathrm{U}} \\ &+ (1 - f_{\mathrm{S}} - f_{\mathrm{I}})(\mathrm{Phy_S} + \mathrm{NF_S}) \cdot L_{\mathrm{S}}\big] \cdot H_{\mathrm{U}}\end{aligned} \tag{C5}$$

Denitrification (Denif) is the nitrogen loss to $\mathrm{N_2}$ when UM, I and D are anoxic. It is defined as:

$$\mathrm{Denif}_i = \max(\mathrm{Rem}_i^{\mathrm{N}} - \frac{\mathrm{Res}_i}{r_{\mathrm{a}}}, 0) \cdot \frac{r_{\mathrm{c}}}{r_{\mathrm{den}}} \quad i \in [\mathrm{UM, I, D}] \tag{C6}$$

with the aerobic respiration term Res_i given below (Eq. C10). In the RD, VDRD, VIDRD and OBRD configuration, the equations for denitrification in the i box and remineralization in D are

given by:

$$\mathrm{Denif}_i = \frac{1}{5} \cdot \max(\mathrm{Rem}_i^{\mathrm{N}} - \frac{\mathrm{Res}_i}{r_{\mathrm{a}}}, 0) \cdot \frac{r_{\mathrm{c}}}{r_{\mathrm{den}}} \quad i \in [\mathrm{UM, I}] \tag{C7}$$

$$\mathrm{Rem}_{\mathrm{D}}^{\mathrm{N}} = M\left[(1 - f_{\mathrm{U}} - f_{\mathrm{UM}})(\mathrm{Phy_U} + \mathrm{NF_U}) \cdot L_{\mathrm{U}} + (1 - f_{\mathrm{S}} - f_{\mathrm{I}})(\mathrm{Phy_S} + \mathrm{NF_S}) \cdot L_{\mathrm{S}}\right] \cdot H_{\mathrm{U}} + 4 \cdot \frac{\mathrm{Denif}_i \cdot r_{\mathrm{den}}}{r_{\mathrm{c}}} \quad i \in [\mathrm{UM, I}] \tag{C8}$$

All the organic matter is composed according to the Redfield Ratio, i.e., $\mathrm{C:N:P} = 106:16:1$. $\mathrm{Rem}_i^{\mathrm{P}}$ represents phosphate remineralization in box i, which is obtained by dividing $\mathrm{Rem}_i^{\mathrm{N}}$ by the Redfield N : P ratio, r_{p}:

$$\mathrm{Rem}_i^{\mathrm{P}} = \frac{\mathrm{Rem}_i^{\mathrm{N}}}{r_{\mathrm{p}}} \quad i \in [\mathrm{U, S, UM, I, D}] \tag{C9}$$

Respiration (Res_i) is considered in the intermediate and deep ocean. In the presence of sufficient oxygen or when oceanic circulation supplies enough $\mathrm{O_2}$, organic matter will be preferentially oxidized by respiration. We use a ratio of $-\mathrm{O_2:N} = 170:16$ during oxic remineralization of organic matter (Anderson and Sarmiento, 1994).

$$\mathrm{Res}_i = \begin{cases} r_{\mathrm{a}} \cdot \mathrm{Rem}_i^{\mathrm{N}} & \text{if} \quad \mathrm{O}_{2i} > 0 \\ \min\left(\mathrm{Transport}(\mathrm{O}_{2i}), r_{\mathrm{a}} \cdot \mathrm{Rem}_i^{\mathrm{N}}\right) & \text{if} \quad \mathrm{O}_{2i} = 0 \end{cases} \qquad i \in [\mathrm{UM, I, D}] \tag{C10}$$

Appendix D

Transport and SMS terms for $\widehat{^{14}\mathrm{C}}$ constitute a system of 5 linear equations including transport parameters A, B, K_{US}, K_{UM} and K_{H}, which are inverted from the $\Delta^{14}\mathrm{C}$ values with air–sea $\Delta^{14}\mathrm{C}$ exchange rates g_{U} and g_{S} for the U and S boxes respectively as inputs. All possible

combinations of values (with a step size of 0.01 $\mathrm{m\,yr^{-1}}$) for g_U and g_S are applied to derive the values for transport parameters A, B, K_{US}, K_{UM} and K_H. g_U and g_S ~~were~~ are constrained in a two-step procedure. First, all combinations are determined which result in transport parameters in the literature range in Table 3. Finally, the combination giving the most realistic biogeochemical tracer concentrations (closest to observations) is chosen for the experiments in the main text (Fig. 3). This approach for determining the physical transport parameters is applied to obtain the ones in Table 2.

Appendix E

~~It is well known from laboratory studies that diazotrophic phytoplankton can also utilize nitrate for growth (e.g., Holl and Montoya, 2005) . Schmittner et al. (2008) introduced a formulation where nitrogen fixers preferentially use nitrate when available and cover only the residual nitrogen demand via fixation. In order to examine the behavior of our model when nitrogen fixers (NF) preferentially use nitrate, nitrogen fixation is separated from diazotroph growth, as in Schmittner et al. (2008) :~~

$$\text{Nitrogen-fixation}_i = \left(1 - \frac{\mathrm{N}}{\mathrm{N} + \mathrm{N_h}}\right) \cdot \mathrm{NPP}^{\mathrm{NF}_i} \qquad i \in [\mathrm{U, S}]$$

~~and Eq. (7)was modified to accomodate the additional nitrate uptake by NF as follows:~~

$$\mathrm{SMS}(\mathrm{N}_i) = \left(-\mathrm{NPP}^{\mathrm{Phy}_i} - \left(\mathrm{NPP}^{\mathrm{NF}_i} - \text{Nitrogen-fixation}_i\right)\right) \cdot V_i + \mathrm{Rem}_i^{\mathrm{N}} - \mathrm{Denif}_i$$

$$i \in [\mathrm{U, UM, S, I, D}]$$

~~Model results for all configurationswith Eqs. (E1) and (E1) are presented in~~ The VD, VDRD, VID and OB configurations are sensitivity configurations that we employ to explore the ability of several mechanisms for preventing nitrogen exhaustion in the OMZ. Even though all of them

fail in simulating realistic biogeochemical tracer concentrations compared with observations, they reveal insights into the effects of the respective mechanisms.

The VD configuration, which differs from the STD configuration in supplying additional O_2 from the subtropical ocean into the D box, avoids anoxic deep waters, but fails to prevent nitrate exhaustion in the UM box (Fig. 3e, f). The I and D boxes are oxic at steady state, but NO_3^- is still exhausted by denitrification in the UM box. Comparing the oxygen concentrations of the RD and VD configurations, we conclude that ventilation helps to prevent oxygen depletion in the D box, but this mechanism alone cannot prevent eventual run-away denitrification in the UM box.

After incorporating reduced denitrification in the VDRD configuration, nitrate depletion is prevented and the I and D boxes are oxic (Fig. ~~9. Compared to~~ 3g, h). But the O_2 concentration in the I box is about 28 % lower than that of the WOA2009 data, which indicates that O_2 supply into the D-box only may not suffice to ventilate the model domain.

The VID configuration, which is modified from the VD configuration by including O_2 ventilation into the I box, fails in preventing NO_3^- depletion by denitrification in the OMZ (Fig. ~~2, this configuration behaves very similarly, except that Phy_U and Phy_S concentrations are somewhat lower because nitrogen fixers take up~~ 3i, j).

In the OB configuration, nutrients are exchanged in addition to O_2 between the subtropical ocean and the I and D boxes. In this configuration, nitrate exhaustion in the OMZ is still not prevented, even though phytoplankton and nitrogen fixer concentrations are lower in the surface U and S boxes (Fig. 3m, n).

Two further sensitivity experiments were performed for each of the VID and OB configurations to explore how NO_3^- ~~as well. Thus, we conclude that our results are robust with respect~~ depletion in the UM box can be prevented. (1) Decreasing the fraction of export production remineralized in the UM box (f_{UM}) from 70 % to ~~assumptions about~~ 56 % makes NO_3^- persist in the UM box. Together with the 20 % remineralization in the U box, this implies that 76 % of the export production is remineralized in the upper 500 m of the ocean. However, the resulting NO_3^- concentration in the UM box is far below the literature range of about 15 to

40 μmol L^{-1}. (2) Facultative N_2-fixation inhibits nitrogen fixation in an environment with high NO_3^- concentrations, but fails to prevent NO_3^- depletion in the UM box.

The sensitivity with respect to the biogeochemical parameters (Section 2.5) is examined for all configurations. We only discuss the sensitivity of the OBRD configuration in Section 3.3, since the sensitivity experiments in all model configurations do not arrest our main conclusion that fixed-N ~~usage by diazotrophs.~~ inventory can be stabilized at non-zero levels in the ETSP OMZ only if the remineralization rate via denitrification is slower than that via aerobic respiration. The model behaviour is very similar in all sensitivity experiments, with two exceptions. When μ_{NF} is raised to $1/2\mu$ and remineralization fractions in different boxes are rearranged to f_U=f_S=60% combined with f_{UM}=f_I=30%, the VDRD and VIDRD configurations reach a steady state only in combination with facultative N_2-fixation.

Acknowledgements. The authors wish to acknowledge funding from CSC (Chinese Scholarship Council), Sonderforschungsbereich 754 "Climate-Biogeochemistry Interaction in the Tropical Ocean" (www.sfb754.de) supported by the Deutsche Forschungsgemeinschaft, the EU FP7 Carbochange Project, and the Cluster of Excellence "The Future Ocean", Kiel, Germany. The authors also wish to thank Ivonne Montes and Christopher Somes for the many helpful and inspiring discussions~~.~~, and Christopher Somes and Tim DeVries for providing their model results for the ETSP.

~~The service charges for this open access publicationhave been covered by the Max Planck Society.~~

References

Anderson, L. A. and Sarmiento, J. L.: Redfield ratios of remineralization determined by nutrient data analysis, Global Biogeochem. Cy., 8, 65–80, doi:10.1029/93GB03318, 1994.

Bethoux, J. P.: Oxygen consumption, new production, vertical advection and environmental evolution in the Mediterranean Sea, Deep-Sea Res., 36, 769–781, doi:10.1016/0198-0149(89)90150-7, 1989.

Bianchi, D, Dunne,J. P., Sarmiento, J. L. and Galbraith,E. D.: Data-based estimates of suboxia, denitrification, and N_2O production in the ocean and their sensitivities to dissolved O_2, Global Biogeochem. Cy., 26,1–13, doi:10.1029/2011GB004209, 2012.

Breitbarth, E, Oschlies, A. and LaRoche, J.: Physiological constrains on the global distribution of *Trichodesmium*-effect of temperature on diazotropy, Biogeosciences, 4, 53–61, doi:10.5194/bg-4-53-2007, 2007.

Bulow, S. E., Rich, J. J., Naik, H. S., Pratihary, A. K., and Ward, B. B.: Denitrification exceeds anammox as a nitrogen loss pathway in the Arabian Sea oxygen minimum zone, Deep-Sea Res. Pt. I, 57, 384–393, doi:10.1016/j.dsr.2009.10.014, 2010.

Canfield, D.: Models of oxic respiration, denitrification and sulfate reduction in zones of coastal upwelling, Geochim. Cosmochim. Ac., 70, 5753–5765, doi:10.1016/j.gca.2006.07.023, 2006.

Capone, D. G. and Knapp, A. N.: A marine nitrogen cycle fix?, Nature, 445, 159–160, doi:10.1038/445159a, 2007.

Capone, D. G., Zehr, J. P., Paerl, H. W., Bergman, B., and Carpenter, E. J.: *Trichodesmium*, a globally significant marine cyanobacterium, Science, 276, 1221–1229, doi:10.1126/science.276.5316.1221, 1997.

Caron, D. A. and Dennett, M. R.: Phytoplankton growth and mortality during the 1995 Northeast Monsoon and Spring Intermonsoon in the Arabian Sea, Deep-Sea Res. Pt. II, 46, 1665–1690, doi:10.1016/S0967-0645(99)00039-9, 1999.

Chu, S. P.: The utilization of organic phosphorus by phytoplankton, J. Mar. Biol. Assoc. U. K., 26, 285–295, 1946.

Cline, J. D. and Richards, F. A.: Oxygen deficient conditions and nitrate reduction in the Eastern Tropical North Pacific Ocean, Limnol. Oceanogr., 17, 885–900, 1972.

Codispoti, L. A.: Is the ocean losing nitrate?, Nature, 376, 724, doi:10.1038/376724a0, 1995.

Codispoti, L. A.: An oceanic fixed nitrogen sink exceeding 400 $\mathrm{Tg\,N\,a^{-1}}$ vs the concept of homeostasis in the fixed-nitrogen inventory, Biogeosciences, 4, 233–253, doi:10.5194/bg-4-233-2007, 2007.

Codispoti, L. A. and Christensen, J.: Nitrification, denitrification and nitrous oxide cycling in the Eastern Tropical South Pacific Ocean, Mar. Chem., 16, 277–300, doi:10.1016/0304-4203(85)90051-9, 1985.

Codispoti, L. A. and Packard, T.: Denitrification rates in the eastern tropical South Pacific, J. Mar. Res., 38, 453–477, 1980.

Codispoti, L. A. and Richards, F.: An analysis of the horizontal regime of denitrification in the eastern tropical North Pacific, Limnol. Oceanogr., 21, 379–388, 1976.

Codispoti, L. A., Brandes, J., Christensen, J., Devol, A., Naqvi, S., Paerl, H., and Yoshinari, T.: The oceanic fixed nitrogen and nitrous oxide budgets: moving targets as we enter the anthropocene?, Sci. Mar., 65, doi:10.3989/scimar.2001.65s285, 2001.

Cotner, Jr., J. B. and Wetzel, R. G: Uptake of dissolved inorganic and organic bphosphorus compounds by phytoplankton and bacterioplankton, Limnol. Oceanogr., 37, 232–243, doi:10.4319/lo.1992.37.2.0232, 1992.

Dalsgaard, T., Thamdrup, B., and Canfield, D. E.: Anaerobic ammonium oxidation (anammox) in the marine environment, Res. Microbiol., 156, 457–464, doi:10.1016/j.resmic.2005.01.011, 2005.

Deutsch, C., Sigman, D. M., Thunell, R. C., Meckler, A. N., and Haug, G. H.: Isotopic constraints on glacial/interglacial changes in the oceanic nitrogen budget, Global Biogeochem. Cy., 18, doi:10.1029/2003GB002189, 2004.

Deutsch, C., Sarmiento, J. L., Sigman, D. M., Gruber, N., and Dunne, J. P. Spatial coupling of nitrogen inputs and losses in the ocean, Nature, 445, 163–167, doi:10.1038/nature05392, 2007.

DeVries, T., Deutsch, C., Primeau, F., Chang, B., and Devol, A.: Global rates of water-column denitrification derived from nitrogen gas measurements, Nature, 5, 547–550, doi:10.1038/NGEO1515, 2012.

DeVries, T., Deutsch, C. Rafter, P. A. and Primeau., F.:Marine denitrification rates determined from a global 3-d inverse model, *Biogeosciences*, 10, 2481–2496, doi:10.5194/bg-10-2481-2013, 2013.

Devol, A. H. and Hartnett, H. E.: Role of the oxygen-deficient zone in transfer of organic carbon to the deep ocean, Limnol. Oceanogr., 46, 1684–1690, doi:10.4319/lo.2001.46.7.1684, 2001.

Eppley, R. W., Rogers, J. N., and McCarthy, J. J.: Half-saturation constants for uptake of nitrate and ammonium by marine phytoplankton, Limnol. Oceanogr., 14, 912–920, doi:10.4319/lo.1969.14.6.0912, 1969.

Eugster, O. and Gruber, N.: A probabilistic estimate of global marine N-fixation and denitrification, Global Biogeochem. Cy., 26, 1–15, doi:10.1029/2012GB004300, 2012.

Franz, J. M. S., Hauss, H., Sommer, U., Dittmar, T., and Riebesell, U.: Production, partitioning and stoichiometry of organic matter under variable nutrient supply during mesocosm experiments in the tropical Pacific and Atlantic Ocean, Biogeosciences, 9, 4629–4643, doi:10.5194/bg-9-4629-2012, 2012.

Fernandez, C., Farías, L., and Ulloa, O.: Nitrogen fixation in denitrified marine waters, PLoS ONE, 6, e20539, doi:10.1371/journal.pone.0020539, 2011.

Furnas, M. J.: In situ growth rates of marine phytoplankton: approaches to measurement, community and species growth rates, J. Plankton Res., 12, 1117–1151, doi:10.1093/plankt/12.6.1117, 1990.

Galloway, J. N., Dentener, F. J., Capone, D. G., Boyer, E. W., Howarth, R. W., Seitzinger, S. P., Asner, G. P., Cleveland, C. C., Green, P. A., Holland, E. A., Karl, D. M., Michaels, A. F. Porter, J. H., Townsend, A. R., and Vörösmarty, C. J.: Nitrogen cycles: past, present and future, Biogeochemistry, 70, 153–226, doi:10.1007/s10533-004-0370-0, 2004.

Ganachaud, A. and Wunsch, C.: Oceanic nutrients and oxygen transports and bounds on export production during the World Ocean Circulation Experiment, Global Biogeochem. Cy., 16, 1–14, doi:10.1029/2000GB001333, 2002.

Garcia, H. E., Locarnini, R. A., Boyer, T. P., Antonov, J. I., Baranova, O. K., Zweng, M. M., and Johnson, D. R.: Volume 3: dissolved oxygen, apparent oxygen utilization, and oxygen saturation, in: World Ocean Atlas 2009, edited by: Levitus, S., NOAA Atlas NESDIS 70, US Government Printing Office, Washington, D. C., p. 344, 2010a.

Garcia, H. E., Locarnini, R. A., Boyer, T. P., Antonov, J. I., Zweng, M. M., Baranova, O. K., and Johnson, D. R.: Volume 4: nutrients (phosphate, nitrate, silicate), in: World Ocean Atlas 2009, NOAA Atlas NESDIS 71, US Government Printing Office, Washington, D. C., p. 398, 2010b.

Gruber, N.: The dynamics of the marine nitrogen cycle and its influence on atmospheric CO_2 variations, in: The Ocean Carbon Cycle and Climate, edited by: Follows, M. and Oguz, T., vol. 40 of NATO Science Series, Kluwer Academic, Dordrecht, the Netherlands, chap. 4, 97–148, 2004.

Gruber, N. and Sarmiento, J. L.: Global patterns of marine nitrogen fixation and denitrification, Global Biogeochem. Cy., 11, 235–266, doi:10.1029/97GB00077, 1997.

Hamersley, M. R., Lavik, G., Woebken, D., Rattray, J. E., Lam, P., Hopmans, E. C., Damsté, J. S. S., Krüger, S., Graco, M., Gutiérrez, D., and Kuypers, M. M. M.: Anaerobic ammonium oxidation in the Peruvian oxygen minimum zone, Limnol. Oceanogr., 52, 923–933, doi:10.4319/lo.2007.52.3.0923, 2007.

Holl, C. M. and Montoya, J. P.: Interactions between nitrate uptake and nitrogen fixation in continuous cultures of the marine diazotroph *Trichodesmium* (cyanobacteria), J. Phycol., 41, 1178–1183, doi:10.1111/j.1529-8817.2005.00146.x, 2005.

Houlton, B. Z., Wang,Y.-P., Vitousek, P. M and Field., C., B.: A unifying framework for dinitrogen fixation in the terrestrial biosphere, Nature, 454, 327–331, doi:doi:10.1038/nature07028, 2008.

Kalvelage, T., Lavik, G., Lam, P., Contreras, S., Arteaga, L., Löscher, C. R., Oschlies, A., Paulmier, A., Stramma, L., and Kuypers, M. M. M.: Nitrogen cycling driven by organic matter export in the South Pacific oxygen minimum zone, Nat. Geosci., 6, 228–234, doi:10.1038/NGEO1739, 2013.

Key, R. M., Kozyr, A., Sabine, C. L., Lee, K., Wanninkhof, R., Bullister, J. L., Feely, R. A., Millero, F. J., Mordy, C., and Peng, T.-H.: A global ocean carbon climatology: results from Global Data Analysis Project (GLODAP), Global Biogeochem. Cy., 18, 1–23, doi:10.1029/2004GB002247, 2004.

Kuypers, M. M. M., Lavik, G., Woebken, D., Schmid, M., Fuchs, B. M., Amann, R., Jørgensen, B. B., and Jetten, M. S. M.: Massive nitrogen loss from the Benguela upwelling system through anaero-

bic ammonium oxidation, P. Natl. Acad. Sci. USA, 102, 6478–6483, doi:10.1073/pnas.0502088102, 2005.

La Roche, J. and Breitbarth, E.: Importance of the diazotrophs as a source of new nitrogen in the ocean, J. Sea Res., 53, 67–91, doi:10.1016/j.seares.2004.05.005, 2005.

Landolfi, A., Dietze, H., Koeve, W., and Oschlies, A.: Overlooked runaway feedback in the marine nitrogen cycle: the vicious cycle, Biogeosciences, 10, 1351–1363, doi:10.5194/bg-10-1351-2013, 2013.

Lenton, T. M. and Watson, A. J.: Redfield revisited 1. Regulation of nitrate, phosphate, and oxygen in the ocean, Global Biogeochem. Cy., 14, 225–248, doi:10.1029/1999GB900065, 2000.

Libby, W. F.: Radiocarbon dating, Am. Sci., 44, 98–112, 1956.

Liu, K.-K. and Kaplan, I. R.: Denitrification rates and availability of organic matter in marine environments, Earth Planet. Sc. Lett., 68, 88–100, doi:10.1016/0012-821X(84)90142-0, 1984.

Martin, J. H., Knauer, G. A., Karl, D. M., and Broenkow, W. W.: VERTEX: carbon cycling in the northeast Pacific, Deep-Sea Res., 34, 267–285, 1987.

McAllister, C. D., Shah, N., and Strickland, J. D. H.: Marine phytoplankton photosynthesis as a function of light intensity: a comparison of methods, J. Fish. Res. Board Can., 21, 159–181, doi:10.1139/f64-010, 1964.

Mills, M. M. and Arrigo, K. R.: Magnitude of oceanic nitrogen fixation influenced by the nutrient uptake ratio of phytoplankton, Nat. Geosci., 3, 412–416, doi:10.1038/NGEO856, 2010.

Mills, M. M., Ridame, C., Davey, M., La Roche, J., and Geider, R. J.: Iron and phosphorus co-limit nitrogen fixation in the eastern tropical North Atlantic, Nature, 429, 292–232, doi:10.1038/nature02550, 2004.

Molina, V. and Farías, L.: Aerobic ammonium oxidation in the oxycline and oxygen minimum zone of the eastern tropical South Pacific off northern Chile ($\sim 20^\circ$ S), Deep-Sea Res. Pt. II, 56, 1032–1041, doi:10.1016/j.dsr2.2008.09.006, 2009.

Monteiro, F. M., Follows, M. J., and Dutkiewicz, S.: Distribution of diverse nitrogen fixers in the global ocean, Global Biogeochem. Cy., 24, 1–16, doi:10.1029/2009GB003731, 2010.

Moore, J. K. and Doney, S. C.: Iron availability limits the ocean nitrogen inventory stabilizing feedbacks between marine denitrification and nitrogen fixation, Global Biogeochem. Cy., 21, 1–12, doi:10.1029/2006GB002762, 2007.

Morrison, J., Codispoti, L., Gaurin, S., Jones, B., Manghnani, V., and Zheng, Z.: Seasonal variation of hydrographic and nutrient fields during the US JGOFS Arabian Sea Process Study, Deep-Sea Res. Pt. II, 45, 2053–2101, doi:10.1016/S0967-0645(98)00063-0, 1998.

Palmer, J. and Totterdell, I.: Production and export in a global ocean ecosystem model, Deep-Sea Res. Pt. I, 48, 1169–1198, doi:10.1016/S0967-0637(00)00080-7, 2001.

Paulmier, A. and Ruiz-Pino, D.: Oxygen minimum zones (OMZs) in the modern ocean, Prog. Oceanogr., 80, 113–128, doi:10.1016/j.pocean.2008.08.001, 2009.

Redfield, A. C., Ketchum, B. H., and Richards, F. A.: The influence of organisms on the composition of sea-water, in: The Sea, 26–77, 1963.

Robarts, R. D. and Zohary, T.: Temperature effects on photosynthetic capacity, respiration, and growth rates of bloom forming cyanobacteria, New Zeal. J. Mar. Fresh., 21, 391–399, doi:10.1080/00288330.1987.9516235, 1987.

Schmittner, A., Oschlies, A., Matthews, H. D., and Galbraith, E. D.: Future changes in climate, ocean circulation, ecosystems, and biogeochemical cycling simulated for a business-as-usual CO_2 emission scenario until year 4000 AD, Global Biogeochem. Cy., 21, doi:10.1029/2007GB002953, 2008.

Shaffer, G. and Sarmiento, J. L.: Biogeochemical cycling in the global ocean 1. A new, analytical model with continuous vertical resolution and high-latitude dynamics, J. Geophys. Res., 100, 2659–2672, doi:10.1029/94JC01167, 1995.

Somes, C. J., Schmittner, A., Galbraith, E. D., Lehmann, M. F., Altabet, M. A., Montoya, J. P., Letelier, R. M., Mix, A. C., Bourbonnais, A. and Eby, M.: Simulating the global distribution of nitrogen isotopes in the ocean, Global Biogeochem. Cy., 24,1–16, doi:10.1029/2009GB003767, 2010.

Suess, E.: Particulate organic carbon flux in the ocean surface productivity and oxygen utilization, Nature, 288, 260–263, doi:10.1038/288260a0, 1980.

Toggweiler, J. R., Dixon, K., and Bryan, K.: Simulations of radiocarbon in a coarse-resolution world ocean model 1. Steady state prebomb distributions, J. Geophys. Res., 94, 8217–8242, doi:10.1029/JC094iC06p08217, 1989.

Tyrrell, T.: The relative influences of nitrogen and phosphorus on oceanic primary production, Nature, 400, 525–531, 1999.

Van Mooy, B. A. S., Keil, R. G., and Devol, A. H.: Impact of suboxia on sinking particulate organic carbon: enhanced carbon flux and preferential degradation of amino acids via denitrification, Geochim. Cosmochim. Ac., 66, 457–467, doi:10.1016/S0016-7037(01)00787-6, 2002.

Voss, M., Dippner, J. W., and Montoya, J. P.: Nitrogen isotope patterns in the oxygen-deficient waters of the Eastern Tropical North Pacidic Ocean, Deep-Sea Res. Pt. I, 48, 1905–1921, doi:10.1016/S0967-0637(00)00110-2, 2001.

Ward, B. B., Devol, A. H., Rich, J. J., Chang, B. X., Bulow, S. E., Naik, H., Pratihary, A., and Jayakumar, A.: Denitrification as the dominant nitrogen loss process in the Arabian Sea, Nature, 461, 78–81, doi:10.1038/nature08276, 2009.

Ye, Y., Völker, C, Bracher, A, Taylor, B. and Wolf-Gladrow., D. A.: Environmental controls on N_2 fixation by Trichodesmium in thetropical eastern North Atlantic Ocean—A model-based study, Deep-Sea Res. I, 64, 104–117, doi:10.1016/j.dsr.2012.01.004, 2012.

Table 1. Model variables.

Variables	Units	Description	Equation
Phy_i	$\mu\mathrm{mol\,N\,kg^{-1}}$	Ordinary phytoplankton in box i	Eq. (2)
NF_i	$\mu\mathrm{mol\,N\,kg^{-1}}$	Nitrogen fixers in box i	Eq. (3)
N_i	$\mu\mathrm{mol\,N\,kg^{-1}}$	Nitrate concentration in box i	Eq. (7)
$\mathrm{N_{avg}}$	$\mu\mathrm{mol\,N\,kg^{-1}}$	Average nitrogen concentration	[a]
P_i	$\mu\mathrm{mol\,P\,kg^{-1}}$	Phosphate concentration in box i	Eq. (8)
$\mathrm{P_{avg}}$	$\mu\mathrm{mol\,P\,kg^{-1}}$	Average phosphorus concentration	[b]
O_{2i}	$\mu\mathrm{mol\,kg^{-1}}$	Oxygen concentration in box i	Eq. (9)

[a] $\mathrm{N_{avg}} = \frac{(\mathrm{N_U}+\mathrm{Phy_U}+\mathrm{NF_U})\cdot V_\mathrm{U}+\mathrm{N_{UM}}\cdot V_\mathrm{UM}+(\mathrm{N_S}+\mathrm{Phy_S}+\mathrm{NF_S})\cdot V_\mathrm{S}+\mathrm{N_I}\cdot V_\mathrm{I}+\mathrm{N_D}\cdot V_\mathrm{D}}{V_\mathrm{U}+V_\mathrm{UM}+V_\mathrm{S}+V_\mathrm{I}+V_\mathrm{D}}$

[b] $\mathrm{P_{avg}} = \frac{\left(\mathrm{P_U}+\frac{\mathrm{Phy_U}+\mathrm{NF_U}}{r_\mathrm{P}}\right)\cdot V_\mathrm{U}+\mathrm{P_{UM}}\cdot V_\mathrm{UM}+\left(\mathrm{P_S}+\frac{\mathrm{Phy_S}+\mathrm{NF_S}}{r_\mathrm{P}}\right)\cdot V_\mathrm{S}+\mathrm{P_I}\cdot V_\mathrm{I}+\mathrm{P_D}\cdot V_\mathrm{D}}{V_\mathrm{U}+V_\mathrm{UM}+V_\mathrm{S}+V_\mathrm{I}+V_\mathrm{D}}$

Table 2. Parameters of the physical model configurations. The detailed explanations for these parameters are given in Table 3.

Parameter \ Configuration	**STD** **RD**	VD VDRD	VID **VIDRD** OB **OBRD**	Units
K_{US}	8.44	3.37	3.41	$\mathrm{m\,yr^{-1}}$
K_{UM}	1.59	0.40	0.58	$\mathrm{m\,yr^{-1}}$
K_{H}	47 799	50 475	42 938	$\mathrm{m\,yr^{-1}}$
A	7.20	7.30	7.22	$\mathrm{m\,yr^{-1}}$
B	18.01	19.60	23.07	$\mathrm{m\,yr^{-1}}$
g_{U}	9.87	8.89	9.88	$\mathrm{m\,yr^{-1}}$
g_{S}	2.94	1.42	1.46	$\mathrm{m\,yr^{-1}}$

Configurations in bold are the main configurations.

Table 3. Model parameters.

Parameter	Description	Units	Value	Range[(reference)]
r_{a}	O_2-used/NO_3-produced during organic carbon(OC) oxidation	–	10.6	8.6–10.6[a]
r_{c}	C/N ratio of OC oxidation	–	6.63	6.63–7.31[a]
f_{U}	Remineralization ratio in U	–	20 %	[b]
f_{S}	Remineralization ratio in S	–	20 %	[b]
f_{UM}	Remineralization ratio in UM	–	70 %	[b]
f_{I}	Remineralization ratio in I	–	70 %	[b]
r_{den}	OC/NO_3^- in denitrification	–	1.02	1.02[a]
r_{p}	N/P released in OC oxidation	–	16	15–16[a]
μ	Maximum growth rate of Phy	yr^{-1}	91.5	36.5–1861.5[c]
μ_{NF}	Maximum growth rate of NF	yr^{-1}	30.5[e]	65.7–438[d]
M_{q}	Quadratic mortality	$\mathrm{yr}^{-1}\,(\mu\mathrm{mol\,N\,kg}^{-1})^{-1}$	18.25	3.65–18.25[f]
$\mathrm{N_h}$	Nitrate half saturation constant	$\mu\mathrm{mol\,N\,kg}^{-1}$	0.5	0.5[g]
$\mathrm{P_h}$	Phosphate half saturation constant	$\mu\mathrm{mol\,P\,kg}^{-1}$	0.03125	0.03[h]
L_x	Length of box x	m	see Fig. 1	–
H_x	Depth of box x	m	see Fig. 1	–
K_H	Horizontal exchange	$\mathrm{m\,yr}^{-1}$	[n]	157.68–56 765[a]
K_{US}	Vertical mixing between surface and intermediate depth	$\mathrm{m\,yr}^{-1}$	[n]	0.79–31.54[a]
K_{UM}	Vertical mixing between intermediate depth and deep ocean	$\mathrm{m\,yr}^{-1}$	[n]	0.21–7.88[a]
$A+B$	Upwelling rates	$\mathrm{m\,yr}^{-1}$	[n]	23.7–630.7[a]
$\mathrm{O_{2U}}$	Oxygen concentration in U	$\mu\mathrm{mol\,kg}^{-1}$	159.54[i]	–
$\mathrm{O_{2S}}$	Oxygen concentration in S	$\mu\mathrm{mol\,kg}^{-1}$	198.11[i]	–
g_{U}	Gas exchange coefficient for U	$\mathrm{m\,yr}^{-1}$	[l]	–
g_{S}	Gas exchange coefficient for S	$\mathrm{m\,yr}^{-1}$	[l]	–
λ	Radioactive decay rate for ^{14}C	yr^{-1}	1.21×10^{-4}	1.21×10^{-4} [j]
$\mathrm{N_{SD}}$	Southern boundary nitrate concentration at depth of D	$\mu\mathrm{mol\,kg}^{-1}$	32.65	[k]
$\mathrm{N_{SI}}$	Southern boundary nitrate concentration at depth of I	$\mu\mathrm{mol\,kg}^{-1}$	10.93	[k]
$\mathrm{P_{SD}}$	Southern boundary phosphate concentration at depth of D	$\mu\mathrm{mol\,kg}^{-1}$	2.30	[k]
$\mathrm{P_{SI}}$	Southern boundary phosphate concentration at depth of I	$\mu\mathrm{mol\,kg}^{-1}$	0.84	[k]
$\mathrm{O_{2SD}}$	Southern boundary oxygen concentration at depth of D	$\mu\mathrm{mol\,kg}^{-1}$	181.37	[k]
$\mathrm{O_{2SI}}$	Southern boundary oxygen concentration at depth of I	$\mu\mathrm{mol\,kg}^{-1}$	217.98	[k]

[a] Ranges for r_{a}, r_{c}, r_{den}, K_{US}, K_{UM},K_{H}, A and B are the same as in Canfield (2006) .
[b] The fraction of regeneration above 500 m has been estimated between 92 % (Suess, 1980) and 97 % (Martin et al., 1987) . According to Canfield (2006) , most likely 60–70 % of the primary production is remineralised in the OMZ. Thus, we define 20 % and 70 % of export production remineralised in the surface boxes and intermediate boxes respectively.
[c] Furnas (1990)
[d] Robarts and Zohary (1987); Capone et al. (1997)
[e] Temperature-corrected maximum growth rate of NF (Breitbarth et al., 2007) .
[f] Palmer and Totterdell (2001); Schmittner et al. (2008)
[g] Eppley et al. (1969)
[h] McAllister et al. (1964)
[i] Average 0–100 m O_2 concentrations of the corresponding areas from World Ocean Atlas (2009).
[j] Libby (1956)
[k] Averages of the corresponding areas from World Ocean Atlas (2009).
[l] These parameter values are defined in Table 2.

Table 4. $\Delta^{14}C$ (in ‰) data from GLODAP used for calibration of the model physical parameters.

Box	Lat (S)	Lon (W)	Depth (m)	Data[a]
U	5–15	80–90	0–100	−72.39
UM	5–15	80–90	100–500	−93.28
S	0–20	90–190	0–100	−62.21
I	0–20	90–190	100–500	−81.02
D	0–20	80–190	500–2000	−160.30
SI[b]	20–40	90–190	100–500	−71.02
SD[b]	20–40	80–190	500–2000	−134.4

[a] GLODAP natural ^{14}C data averaged over the respective regions.
[b] SI and SD represent the southern boundary outside the I and D boxes, respectively.

Table 5. Summary of model configurations.

~~Parameters of the physical model configurations.~~

Configuration	Abbreviation	Reduced denitrification rate	O_2, ^{14}C ventilation of D	O_2, ^{14}C ventilation of I	NO_3^-, PO_4^{3-} exchange of D and I
Standard	**STD**				
Reduced-denitrification	**RD**	+			
Ventilation-D	VD		+		
Ventilation-D+Reduced-denitrification	VDRD	+	+		
Ventilation-ID	VID		+	+	
Ventilation-ID+Reduced-denitrification	**VIDRD**	+	+	+	
Open-boundary	OB		+	+	+
Open-boundary+ Reduced-denitrification	**OBRD**	+	+	+	+

~~VID~~

+ means that the modification applies to this configuration. The configurations in bold are the main configurations in the text, while the others are the sensitivity configurations described in Appendix E. STD is defined in Sections 2.2 and 2.3; in RD, a reduced denitrification rate is applied; VD indicates that the southern boundary of the model domain is partially opened to allow ventilation of O_2 and ^{14}C (but not NO_3^- and PO_4^{3-}) to the D box; VDRD is the configuration when a reduced denitrification rate is applied in VD; VID differs from VD only in that the partially open southern boundary is extended to allow ventilation of O_2 and ^{14}C also into the I box; VIDRD is the configuration when a reduced denitrification rate is applied in VID; in OB, nutrient (NO_3^- and PO_4^{3-}) mixing is added to VID; OBRD is the configuration in which the reduced denitrification rate is added to OB.

~~VIDRDOBOBRD K_{US} 8.44 3.37 3.41 K_{UM} 1.59 0.40 0.58 K_H 47799 50475 42938 A 7.20 7.30 7.22 B 18.01 19.60 23.07 g_U 9.87 8.89 9.88 g_S 2.94 1.42 1.46~~

~~Model parameters.~~

Table 6. ~~Fluxes~~ Denitrification comparison with ~~other models~~model-based and observational estimates.~~Export production is the export production sinking into the OMZ; aerobic and anaerobic remineralization represent organic matter remineralization under oxic and anoxic conditions respectively; fixed-N loss defines the fixed-N removal from OMZ via denitrification/anammox; input via transport denotes the fixed-N influx into the OMZ from adjacent regions.~~

Data/Models	Denitrification ($\mathrm{Tg\,N\,yr^{-1}}$)
OBRD configuration	5.0[c]
Kalvelage et al. (2013) [a]	10.2[c]
DeVries et al. (2013, pers. comm.) [b]	7.0±2.0[c]
Bianchi et al. (2012) [a]	17.6[d]
Somes et al. (2010, pers. comm.) [b]	5.8[c]
Mills and Arrigo (2010) [b]	1.9[c,*]

[a]observational estimate; [b]model results; [c]ETSP; [d]entire South Pacific; [*]OMZ value extrapolated to UM box of our model.

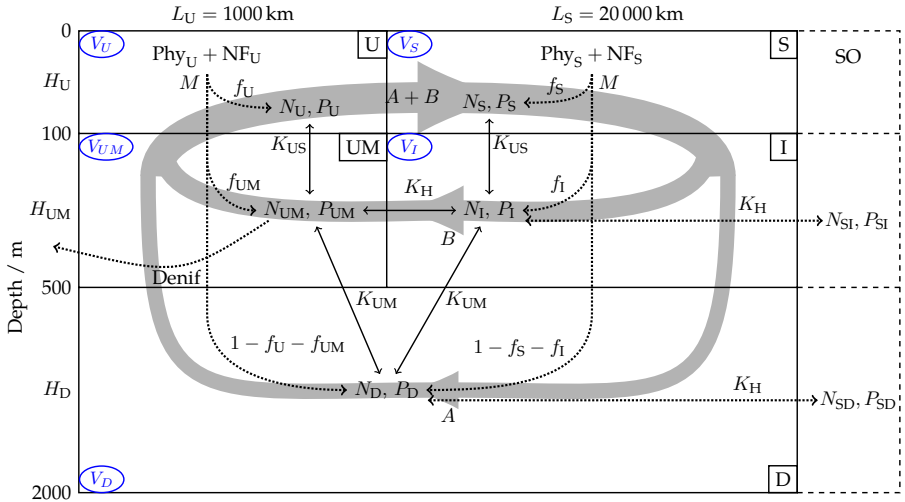

Fig. 1. Model structure and configurations. The model domain comprises five active boxes representing the top 100 m of an upwelling region (U), the underlying oxygen minimum zone (UM), and an adjacent open-ocean basin divided into a surface (S) and an intermediate-depth box (I). A deep box (D) underlies both the upwelling region and the open ocean. The large-scale circulation is represented by deep (A) and shallow (B) convection (thick grey lines). Mixing between boxes is implemented via mixing coefficients (K). Remineralization derived from net primary production by ordinary (Phy) and diazotrophic (NF) phytoplankton in the surface boxes consumes oxygen. Under anoxic conditions remineralization is fueled by anaerobic remineralization (Denif). The model can be configured to exchange nutrients and oxygen with the southern subtropical ocean (right, denoted as "SO"). See Table 3 for symbol definitions and text for details.

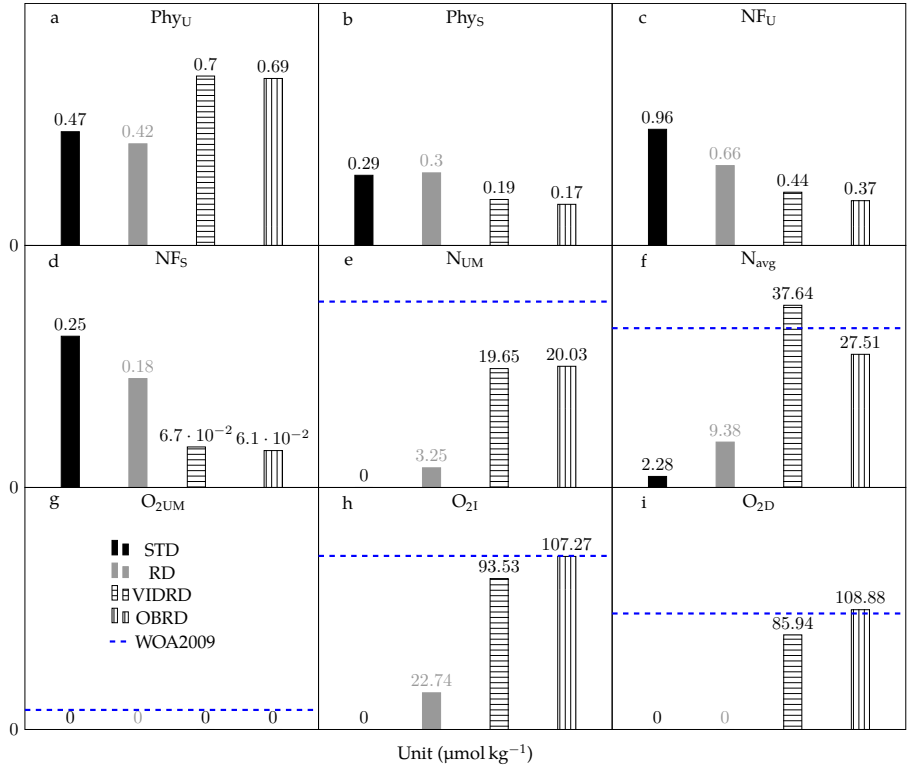

Fig. 2. Simulated steady-state phytoplankton, nutrient and oxygen concentrations for the main model configurations defined in Tables 5 and 2. Each panel uses linear scale of the y-axis starting at zero. ~~Gridded panels~~ Dashed blue lines represent the average of the WOA2009 data of the corresponding boxes, however, there are no data for $\mathrm{Phy_U}$, $\mathrm{Phy_S}$, $\mathrm{NF_U}$ and $\mathrm{NF_S}$.

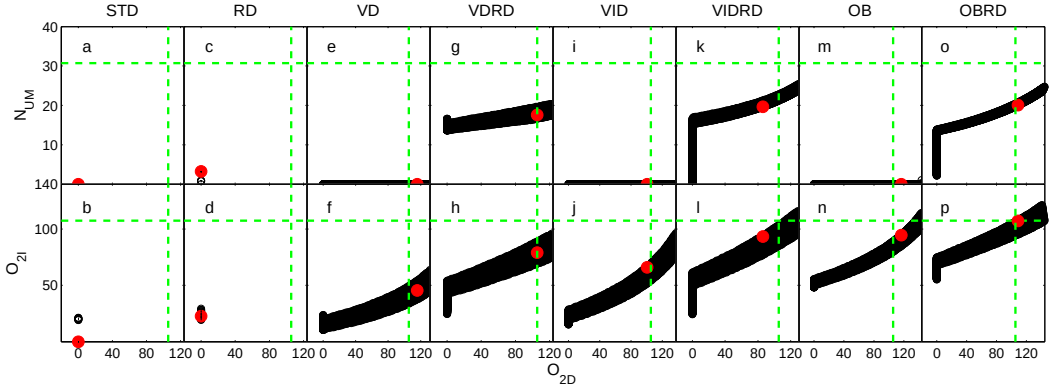

Fig. 3. ~~Simulated steady-state biogeochemical fluxes for the model configurations defined~~ NO_3^- concentration in ~~Tables 5 and 2. NPP_{PhyU}, NPP_{PhyS}, NPP_{NFU} and NPP_{NFS} represent~~ the ~~net primary production rates of Phy_U, Phy_S, NF_U~~ OMZ and ~~NF_S respectively. $Denif_{UM}$ indicates the nitrogen loss rate by anaerobic remineralization~~ O_2 concentrations in the ~~UM~~ I box ~~. $Export_U$ and $Export_S$ represent the export production rate out~~ for all combinations of ~~U~~ g_U and ~~S~~g_S resulting in all transport parameters being inside the literature range as given in Table 3. ~~$Respiration_{UM}$ represents aerobic respiration rate~~ The x-axis is the O_2 concentration in the ~~UM~~ D box. ~~Note that all panels are~~ Red dot in ~~units~~ each panel is the selected suite of ~~nitrogen except (H),~~ physical transport parameters which ~~is~~ fit the biogeochemical data best in ~~units of~~ each model configuration. ~~Each panel uses a different linear scale~~ The horizontal green dashed lines represent the average of WOA2009 data for N_{UM} and O_{2I}, and the ~~y-axis starting at zero~~vertical green dashed lines denote the average of WOA2009 data for O_{2D}.

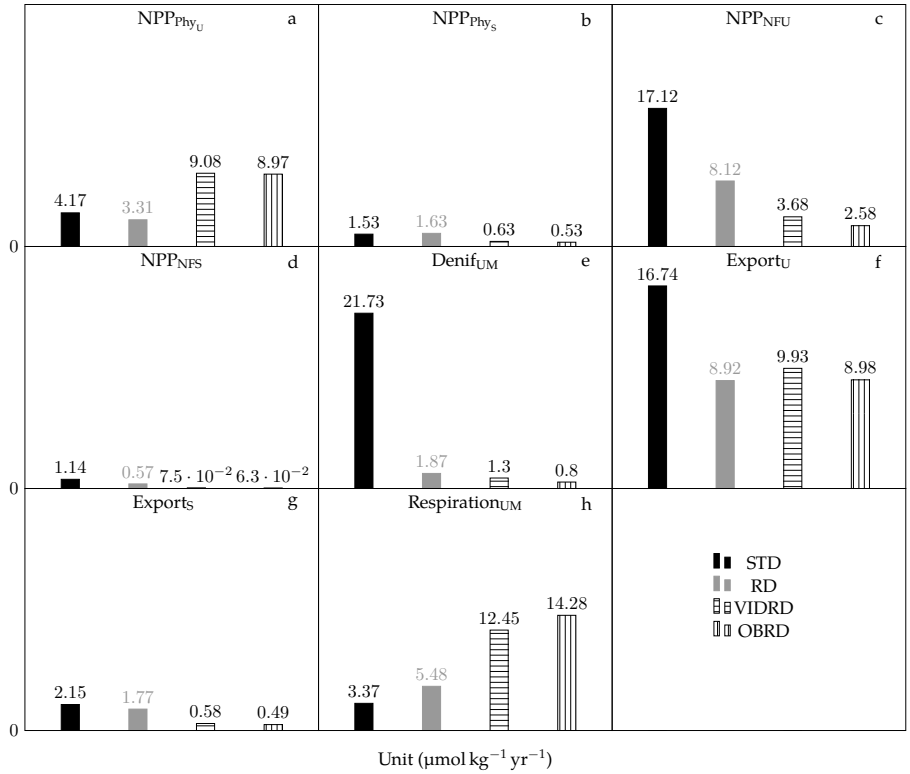

Fig. 4. Simulated steady-state biogeochemical fluxes for the main model configurations defined in Tables 5 and 2. NPP_{PhyU}, NPP_{PhyS}, NPP_{NFU} and NPP_{NFS} represent the net primary production rates of Phy_U, Phy_S, NF_U and NF_S respectively. $Denif_{UM}$ indicates the nitrogen loss rate by anaerobic remineralization in the UM box. $Export_U$ and $Export_S$ represent the export production rate out of U and S. $Respiration_{UM}$ represents aerobic respiration rate in the UM box. Note that all panels are in units of nitrogen except **(h)**, which is in units of O_2. Each panel uses a different linear scale for the y-axis starting at zero.

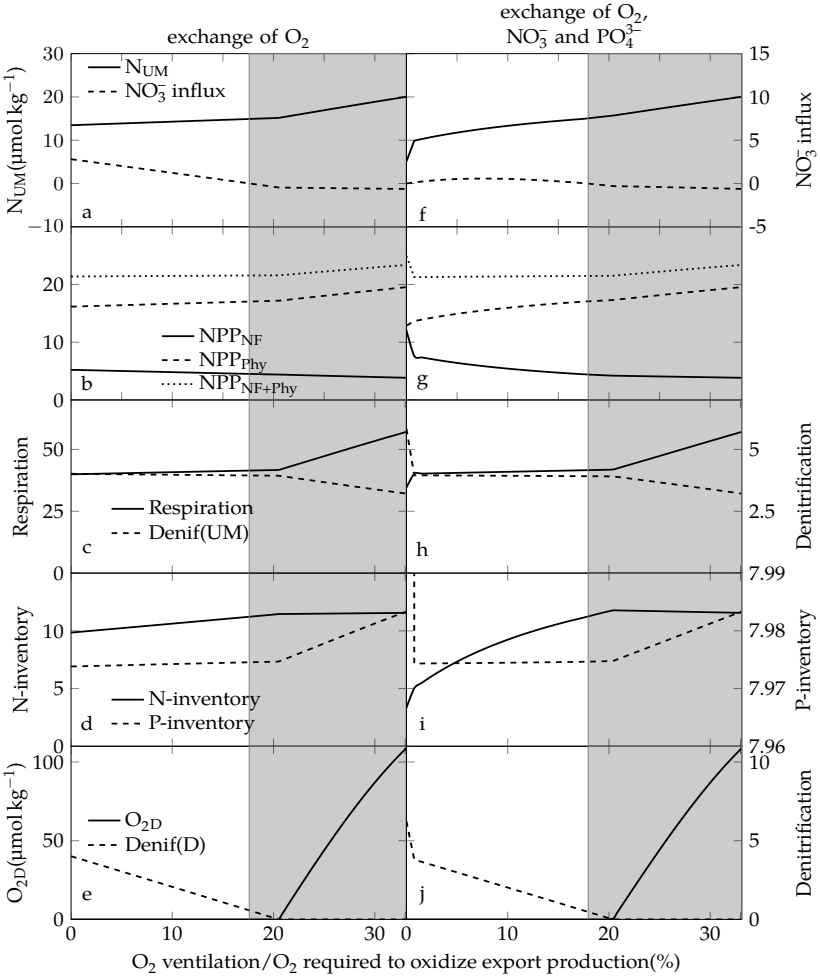
exchange of O_2
exchange of O_2, NO_3^- and PO_4^{3-}
N_{UM}
NO_3^- influx
$N_{UM}(\mu mol\,kg^{-1})$
NO_3^- influx
a
f
NPP_{NF}
NPP_{Phy}
NPP_{NF+Phy}
b
g
Respiration
Denif(UM)
Respiration
Denitrification
c
h
N-inventory
P-inventory
N-inventory
P-inventory
d
i
O_{2D}
Denif(D)
$O_{2D}(\mu mol\,kg^{-1})$
Denitrification
e
j
O_2 ventilation/O_2 required to oxidize export production(%)

Fig. 5. Dependence of ~~the~~ biogeochemical processes on the ~~ratio~~ exchange of O_2 ~~supply from~~ , NO_3^-, and PO_4^{3-} with the subtropical ocean through the southern boundaries of the I and D boxes. The x-axes indicate the contribution of O_2 supplied from the subtropical ocean relative to that required to oxidize all export production from the surface ocean (boxes U and S). ~~N_{UM}~~ (a–e) only O_2 exchanged through the southern boundaries is reduced; (f–j) exchange of O_2, NO_3^-, and PO_4^{3-} is reduced. N_{UM} is NO_3^- ~~influx represent~~ concentration in the UM box and NO_3^- influx is the NO_3^- flux ~~from~~ through the southern boundary (positive into model domain). ~~NPP_{Phy}~~ NPP_{Phy}, ~~NPP_{NF}~~ NPP_{NF} and ~~NPP_{NF+Phy}~~ NPP_{NF+Phy} are net primary production by ordinary phytoplankton, nitrogen fixers, and the sum of ~~ordinary phytoplankton and nitrogen fixers~~ both in the surface ocean. Respiration and ~~denitrification~~ Denif (UM) represent O_2 consumption by aerobic remineralization and NO_3^- removal by anaerobic remineralization, respectively, in the UM box. N-inventory and P-inventory are the total nitrogen and phosphorus inventories in the model domain, including all ~~the related~~ organic and inorganic species. ~~O_{2D}~~ O_{2D} and ~~denitrification~~ Denif (D) represent O_2 concentration and NO_3^- removal by anaerobic remineralization in the D box. Units of all ~~the~~ variables ~~in this figure~~ are 10^{11} μmol yr^{-1} m^{-1} except for ~~N_{UM}~~ N_{UM} and ~~O_{2D}~~O_{2D}, which are given in μmol kg^{-1}, and N-inventory and P-inventory, which are 10^{11} μmol m^{-1}. The shaded area denotes the parameter range for which the model domain is a ~~-~~net source of ~~fixed-N~~NO_3^-.

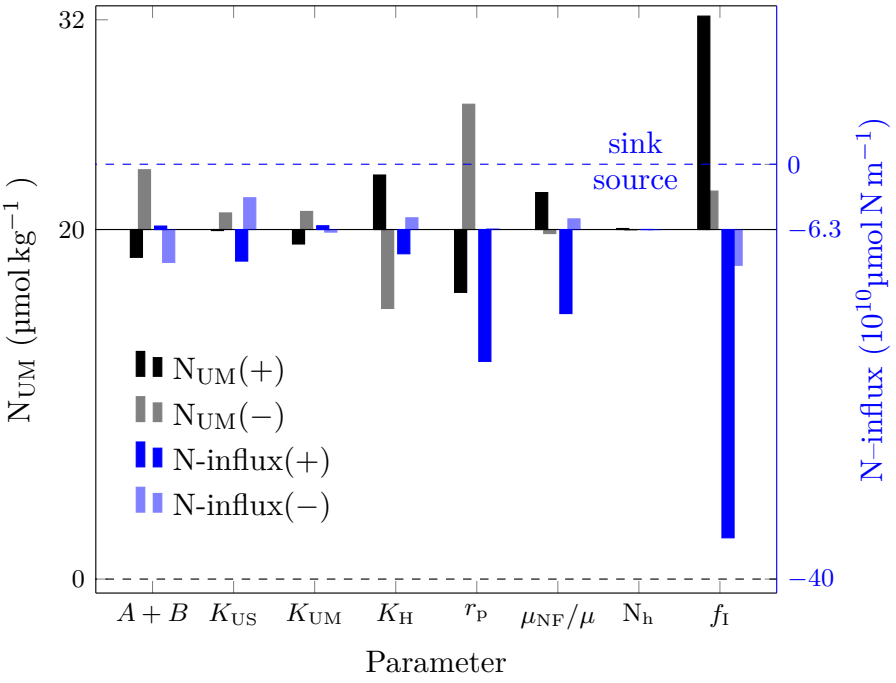

Fig. 6. Sensitivity of NO_3^- concentration in the ~~strength of~~ OMZ (N_{UM}) and the net NO_3^- flux out of the model domain ~~for different~~ to variations of the individual parameters describing ocean transport and biogeochemical processes (see ~~Table~~Tables 2, 3 and Fig. 1 for a description of the parameters). ~~The flux is normalized by~~ Black and blue bars represent changes in N_{UM} and N-influx, respectively. + and − indicate the ~~flux simulated~~ response to increased and decreased parameters. Physical circulation parameters are varied by ~~the OBRD model configuration~~ ±50 %. r_P is varied between 12 and 20. μ_{NF}/μ is varied between 1/4 and 1/2. N_h varies between 0.3 and 0.9 μmol kg^{-1}. For f_i, "+" indicates f_U=f_S=60 % and f_{UM}=f_I=30 %, and "−" means 40 % and 50 %, respectively.

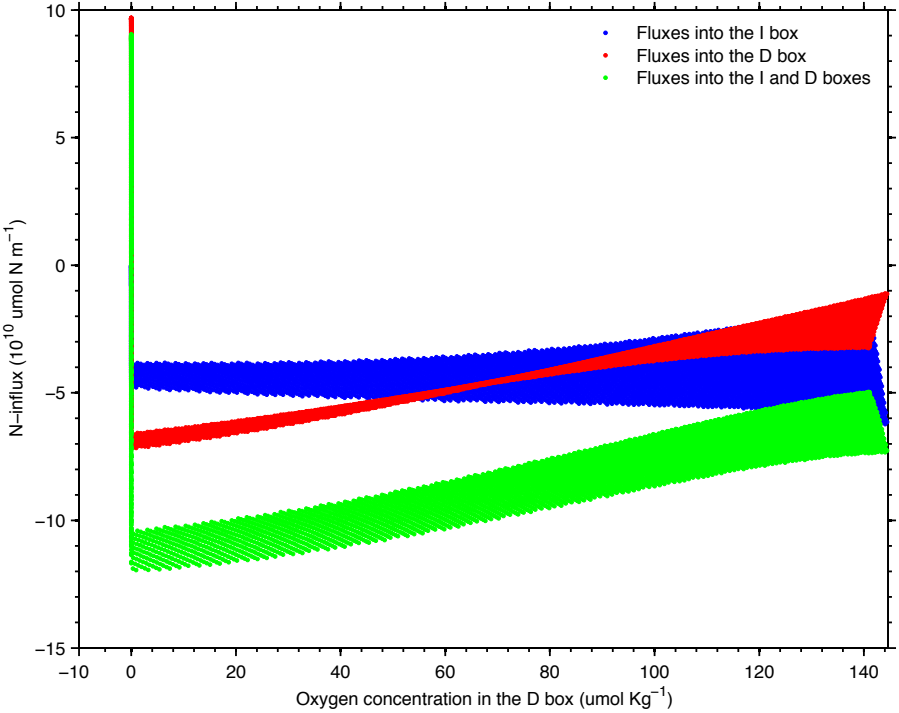

Fig. 7. Lateral NO_3^- input into the model domain of the OBRD configuration as a function of the oxygen concentration in the D box. "Fluxes into the I box" represents lateral NO_3^- input into the I box; "fluxes into the D box" represents lateral NO_3^- input into the D box; "fluxes into the I and D boxes" is the sum of the above two processes. Note that only the I and D boxes can exchange O_2 or nutrients with the region outside of the model domain. In this figure, negative values indicate that the model is a NO_3^- source, and positive values that the model is a NO_3^- sink instead.

~~concentration in the OMZ and concentrations in the I box for all combinations of physical transport parameters in the literature range. The x-axis is the concentration in the D box. Red dot in each panel is the selected suite of physical transport parameters which fit the biogeochemical data best in each model configuration. The horizontal green dashed lines represent the average of WOA2009 data for N_{UM} and O_{2I}, and the vertical green dashed lines denote the average of WOA2009 data for O_{2D}.~~

~~Same as Fig. 2 but with diazotrophs utilising also nitrate when available (Eqs. E1 and E1). Again, each panel uses a different linear scale for the y-axis starting at zero. Gridded panels represent the average of the WOA2009 data of the corresponding boxes, however, there are no data for Phy_U, Phy_S, NF_U and NF_S.~~

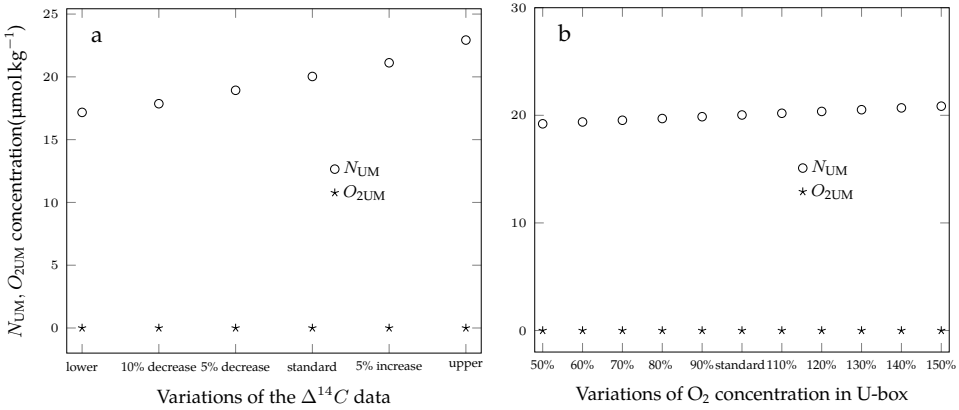

Fig. 8. NO_3^- and O_2 concentrations in the OBRD configuration for different physical parameters derived from variations of the Δ^{14}C data **(a)** and O_2 concentration in U-box **(b)**. **(a)** Decrease and increase mean that Δ^{14}C values in all boxes are reduced or increased simultaneously. **(b)** Values of the x-axis denote the variations of O_2 concentration in the U-box relative to the standard. Standard run in each figure is the OBRD configuration with physical parameters defined in Table 2.